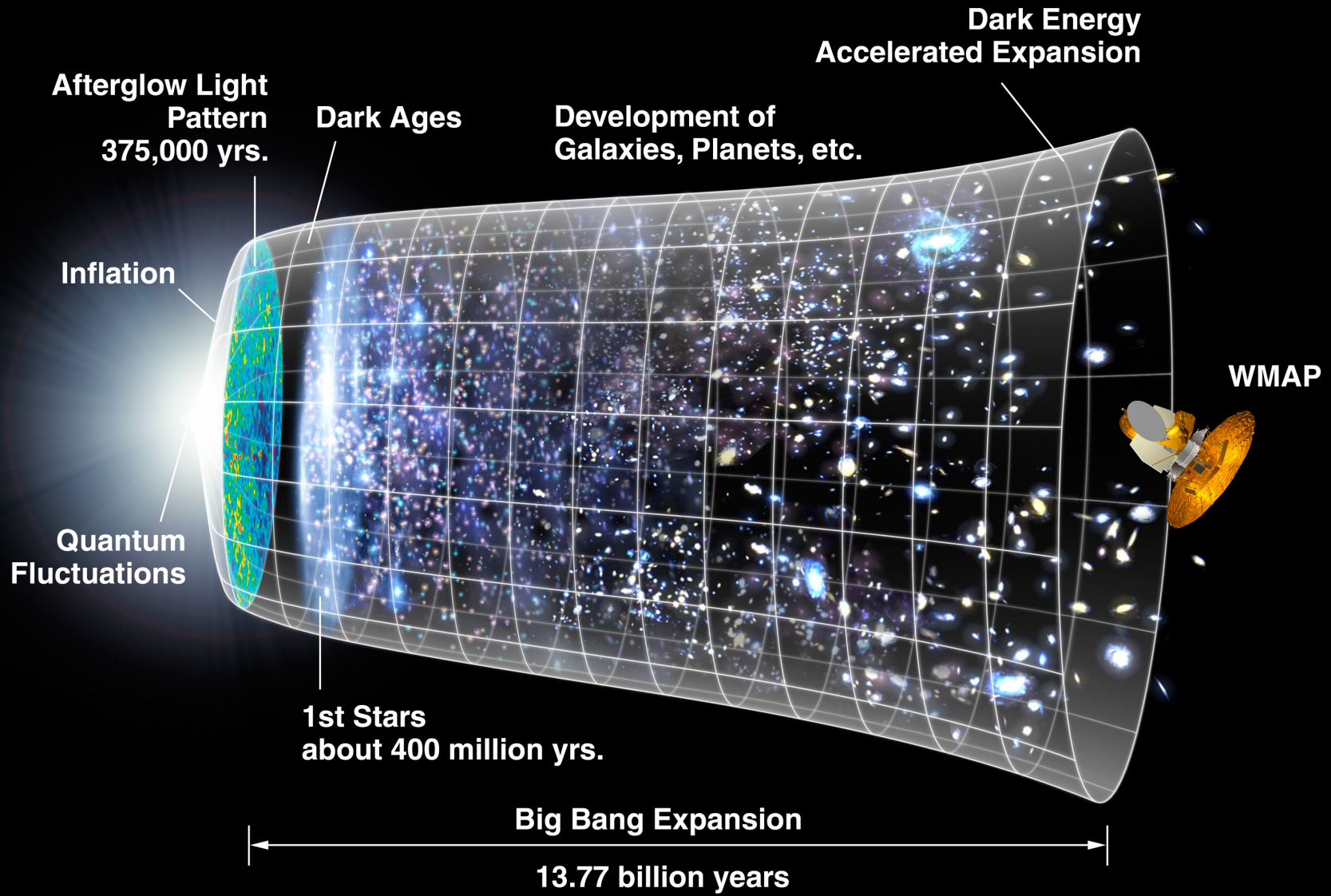


# Clusters of galaxies and large scale structure

A. Montaña (& I. Aretxaga)  
2020

Following the notes from Claudia Mendes de Oliveira



# Large Scale Structure (LSS)

- How is matter distributed in the Universe?
- How does it evolve?
- How do structures and sub-structures form, interact and evolve?
- How does the underlying cosmological model affect all these?
- How does the velocity field behave?
- etc....

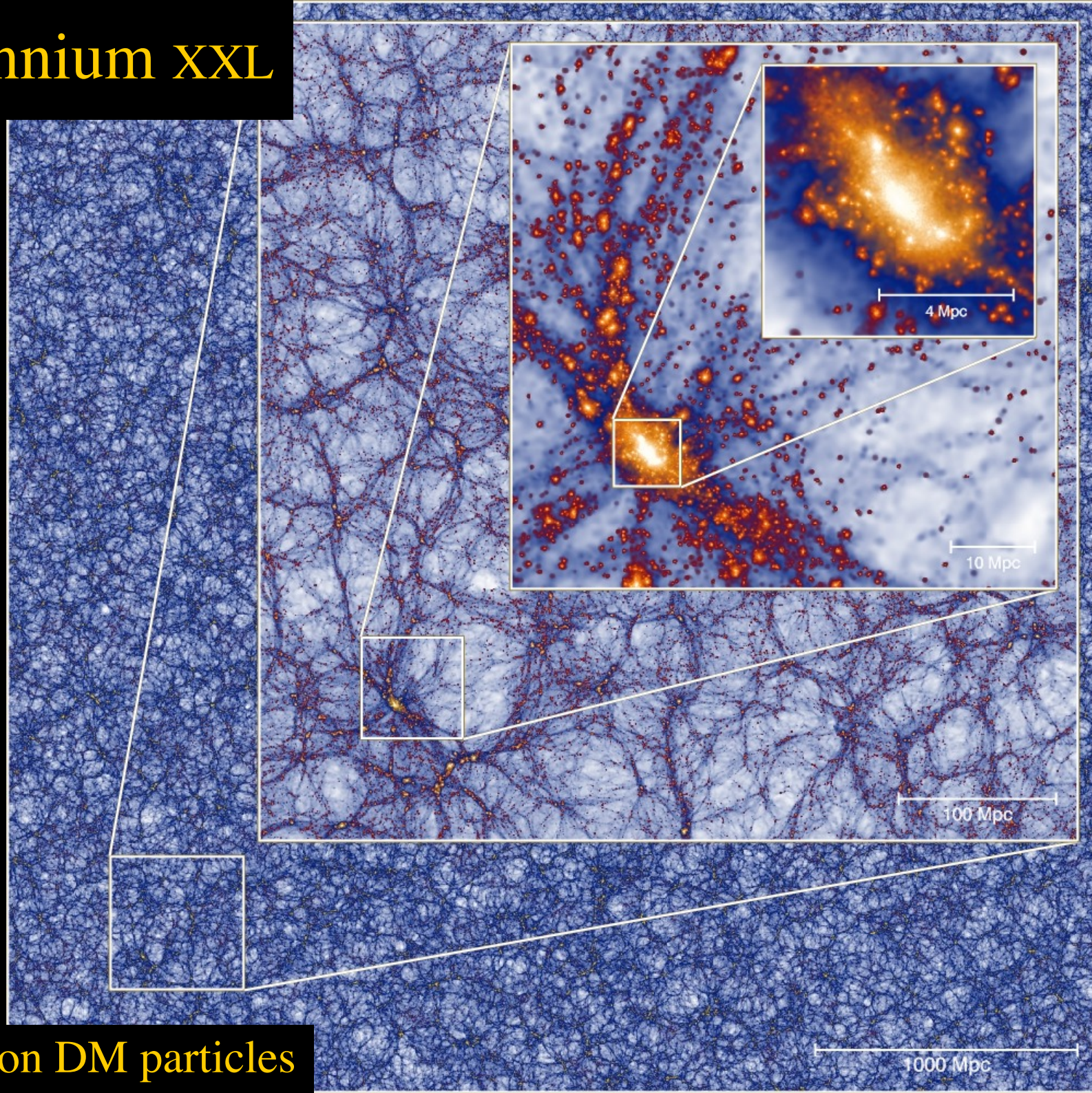
Relatively modern field

Large/deep surveys

Redshift information

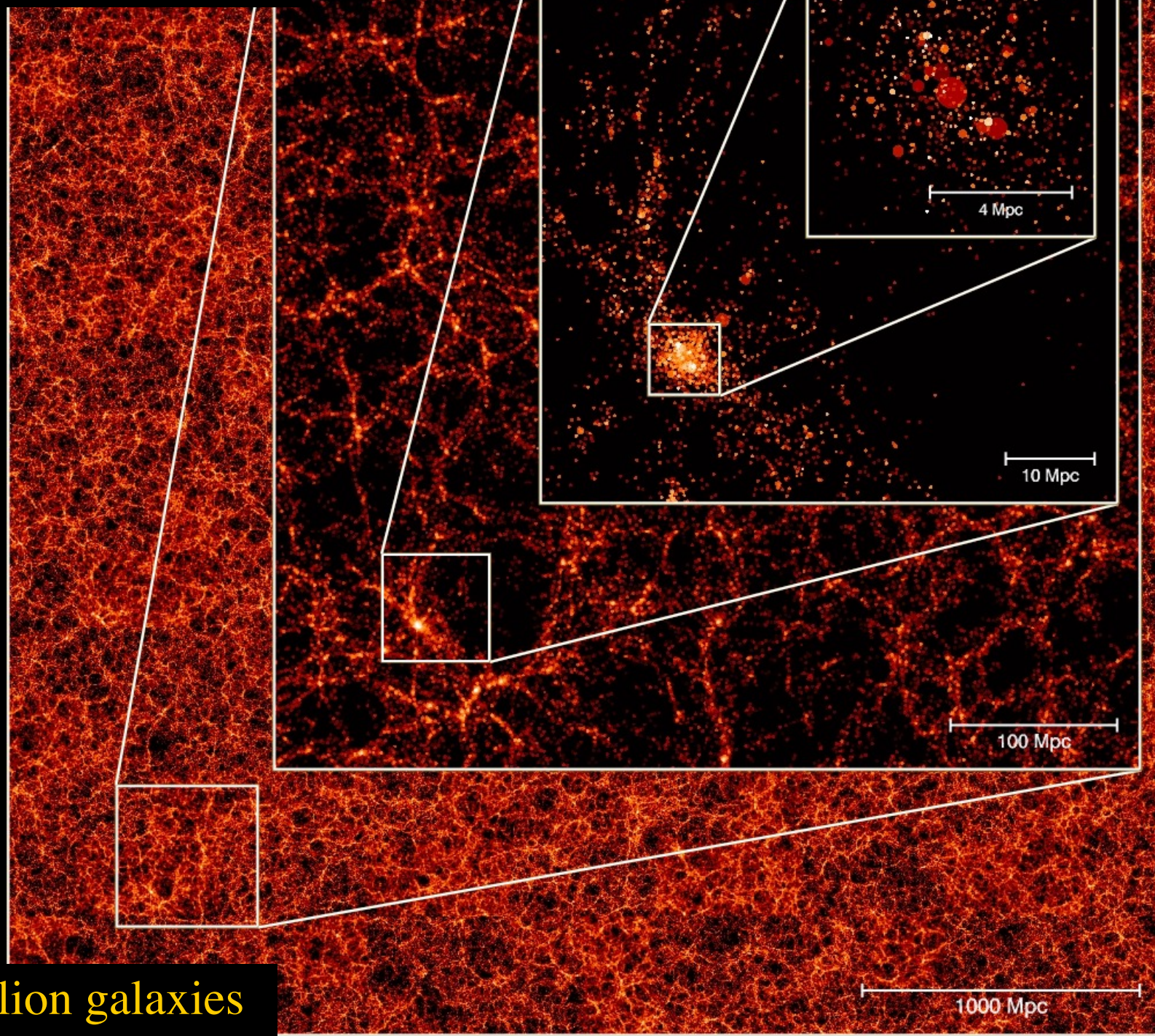
Computing power

# Millennium XXL



300 billion DM particles

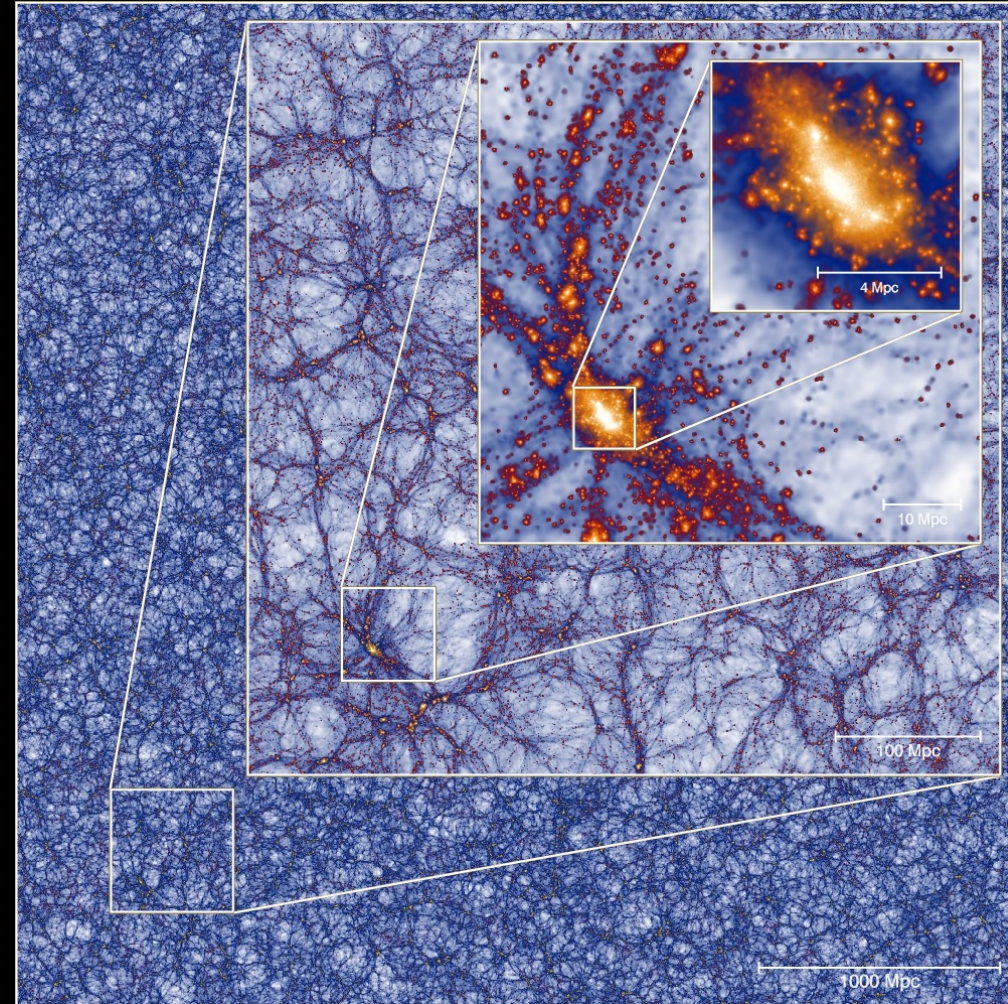
# Millennium XXL



700 million galaxies

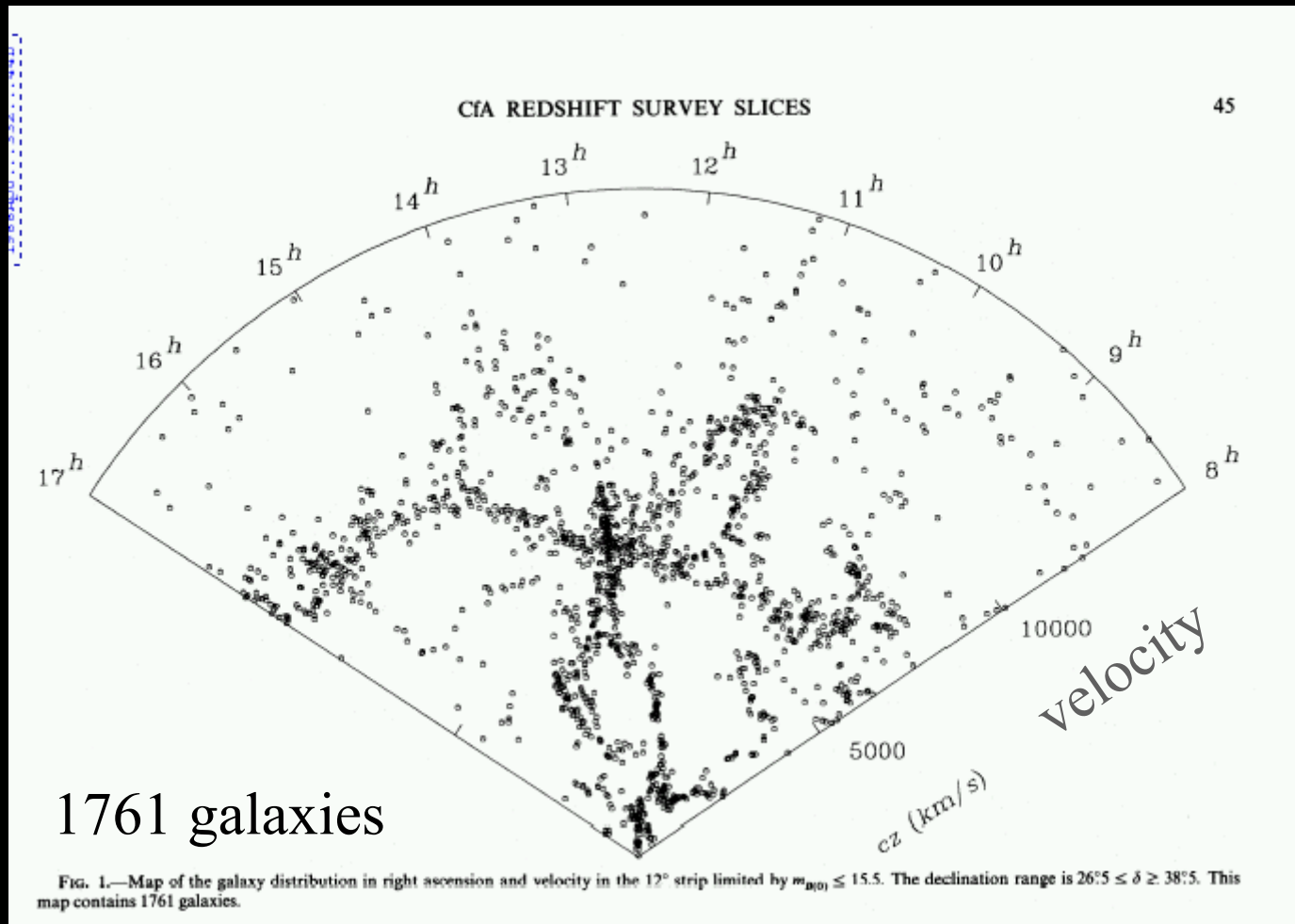
# Structures

- Voids: 100 – 200 Mpc.
- Sheets (or walls): boundaries of voids.
- Filaments: intersection between sheets.
- Clusters: 100's-1000's of galaxies,  $10^{14} - 10^{15} M_{\odot}$ ,  $\sim 5$  Mpc
- Groups: 10's of galaxies,  $M < 10^{14} M_{\odot}$ , scale  $< 1$  Mpc
- Super-clusters:  $>1000$ 's of galaxies, scales  $\sim 50$  Mpc



# The CfA redshift survey

Harvard-Smithsonian Center for Astrophysics

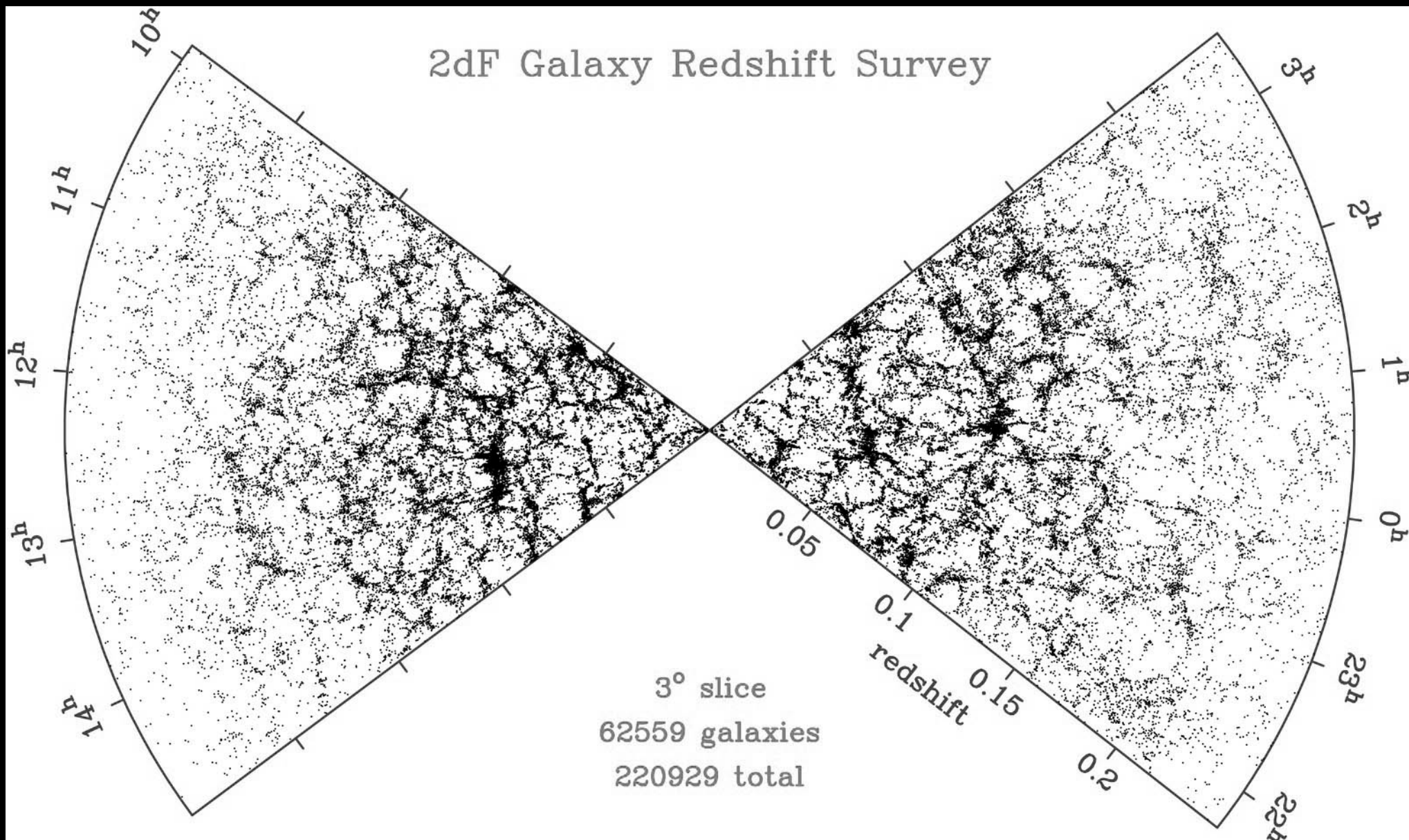


Hubble's  
law  
 $d=v/H_0$

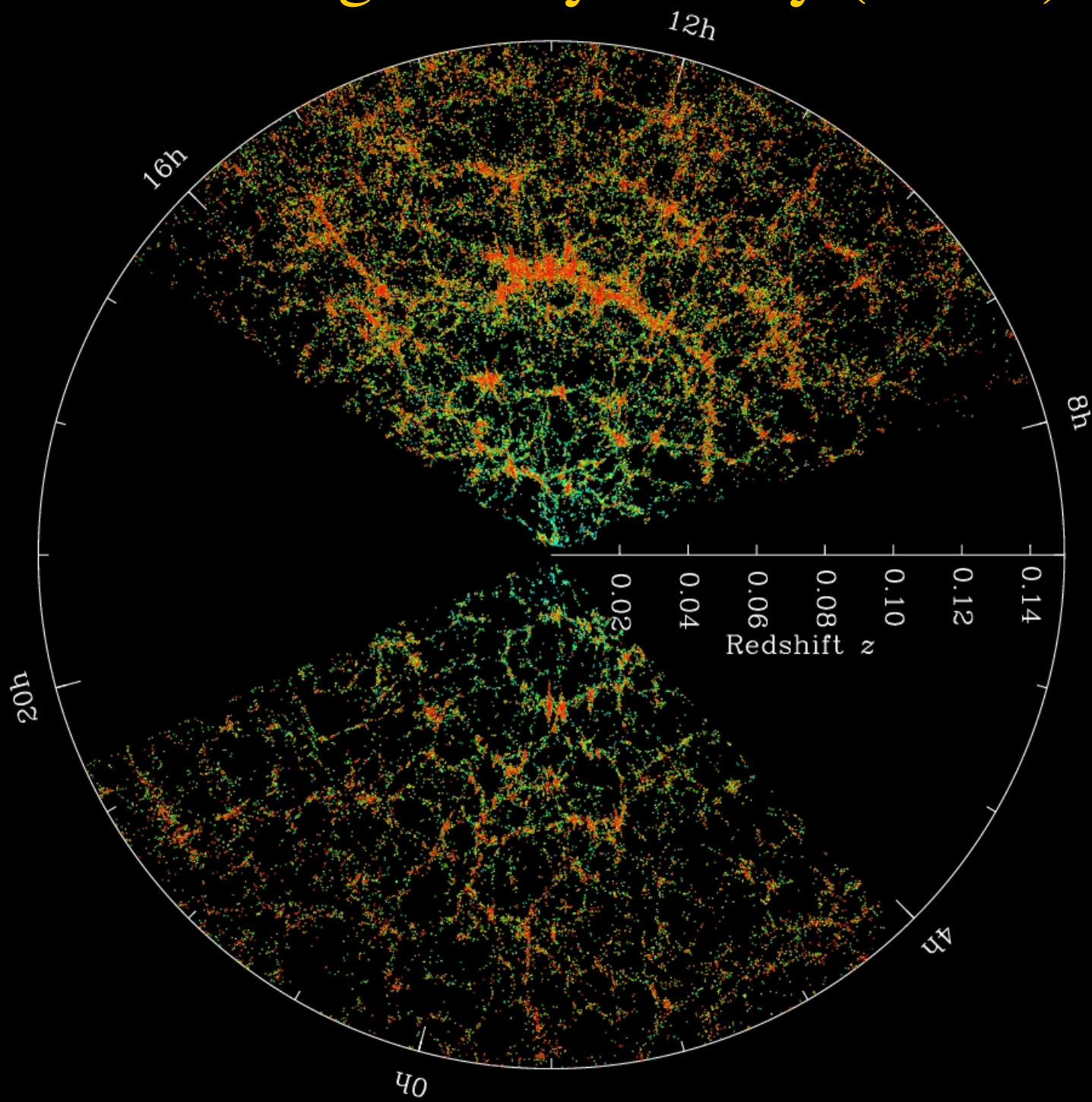
De Lapparent et al. (1988)  
Smithsonian Astrophysical Observatory

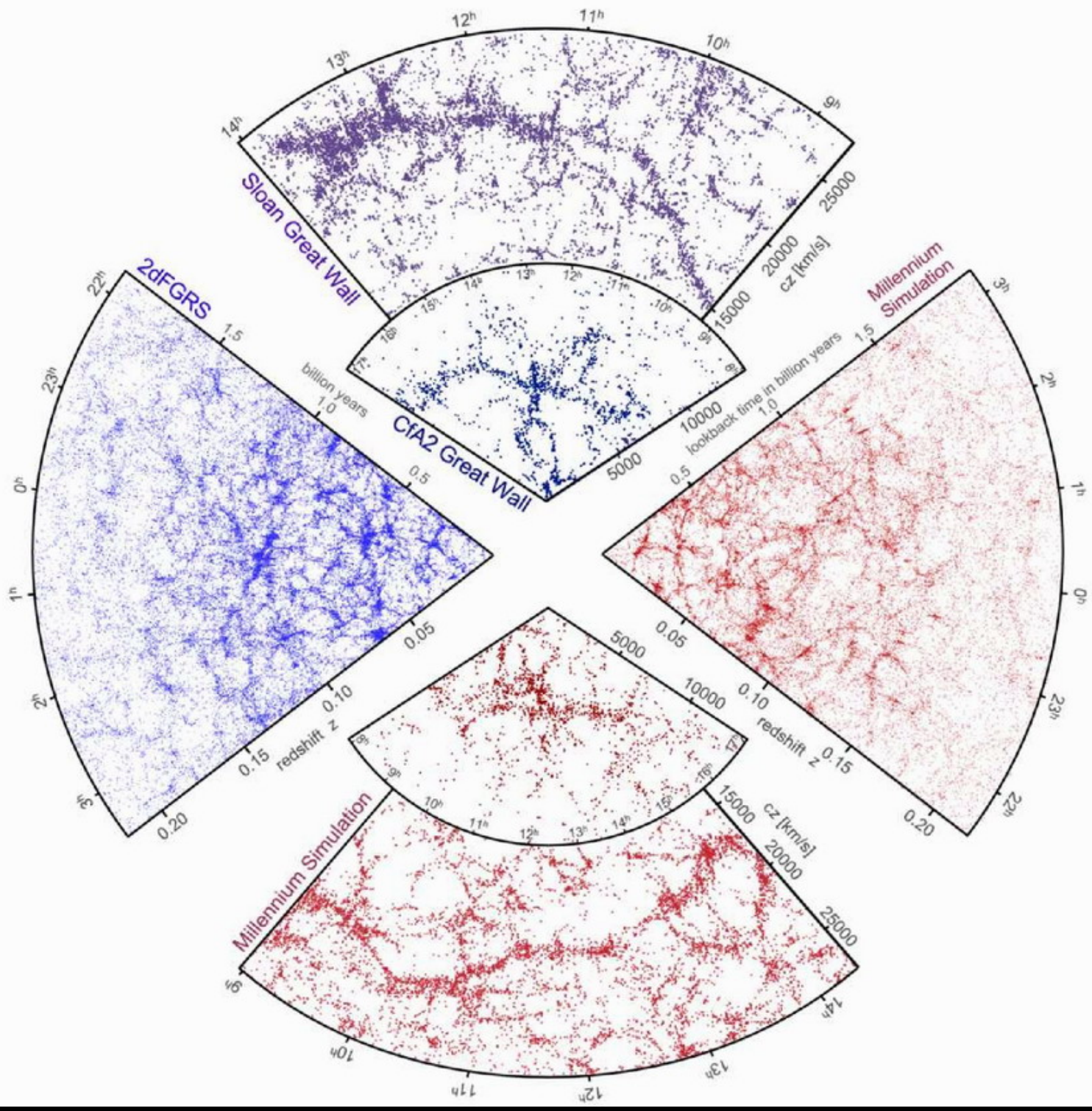
# Two-degree-Field Galaxy Redshift Survey (2dF)

Anglo-Australian Observatory (AAO)



# Sloan Digital Sky Survey (SDSS)





# Dark Matter N-body simulations ( $\Lambda$ CDM)

31.25 Mpc/h

31.25 Mpc/h

$z = 18.3$  ( $t = 0.21$  Gyr)

$z = 5.7$  ( $t = 1$  Gyr)

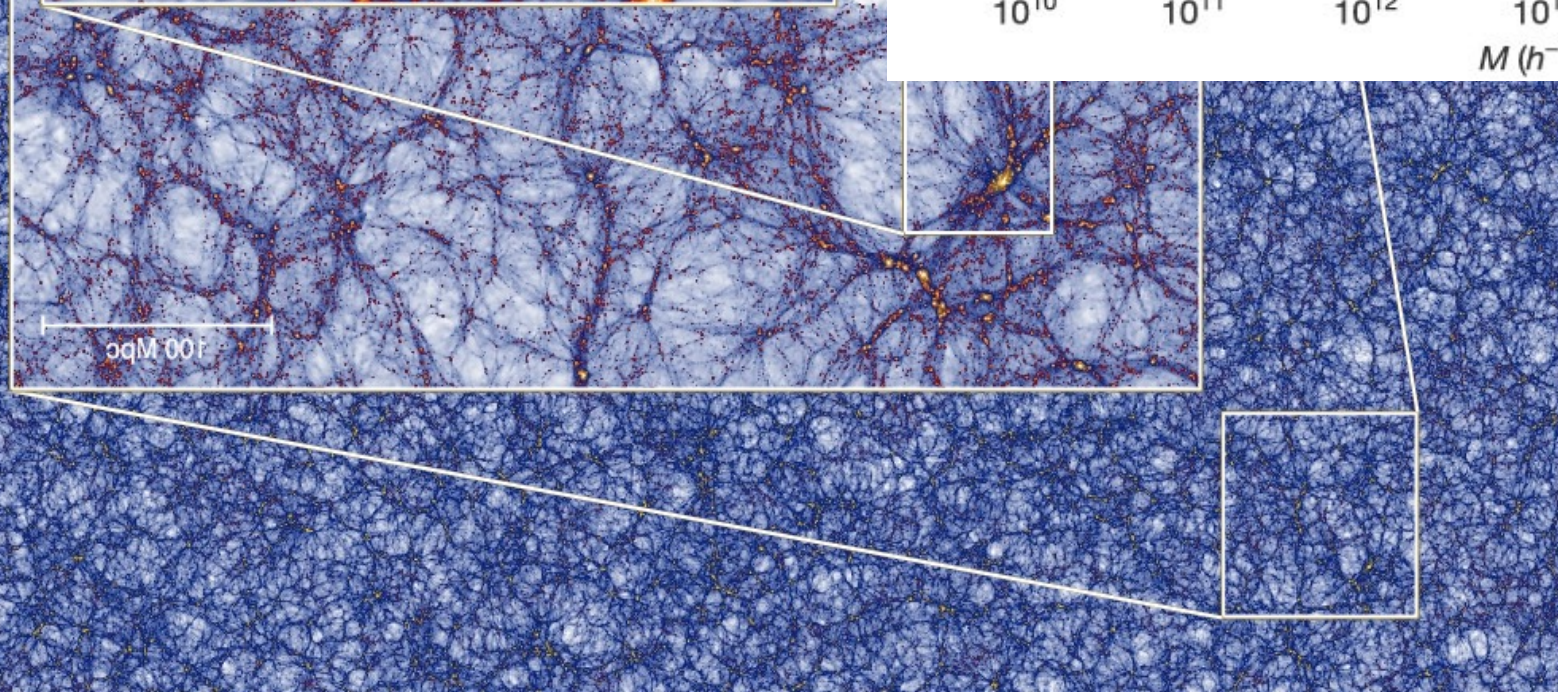
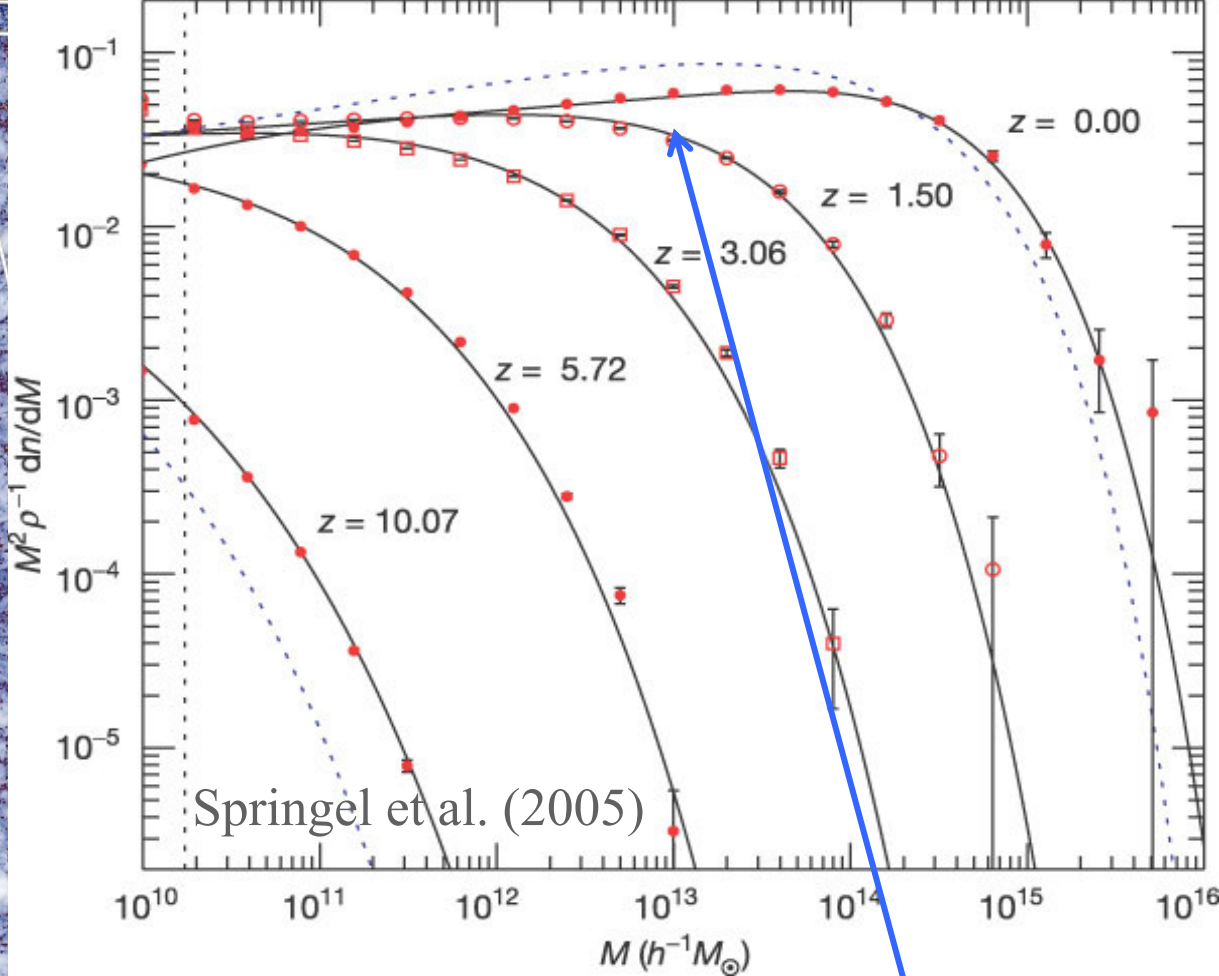
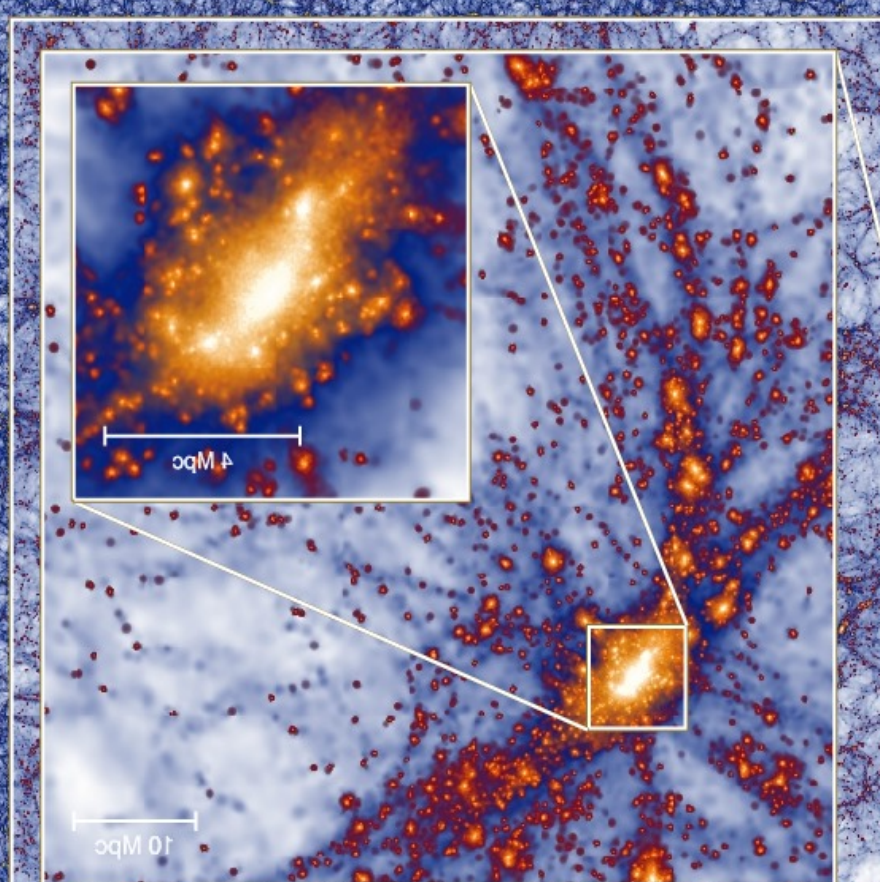
Hierarchical clustering.  
Clusters are still growing  
today! Many of them may  
therefore not be virialized.

31.25 Mpc/h

31.25 Mpc/h

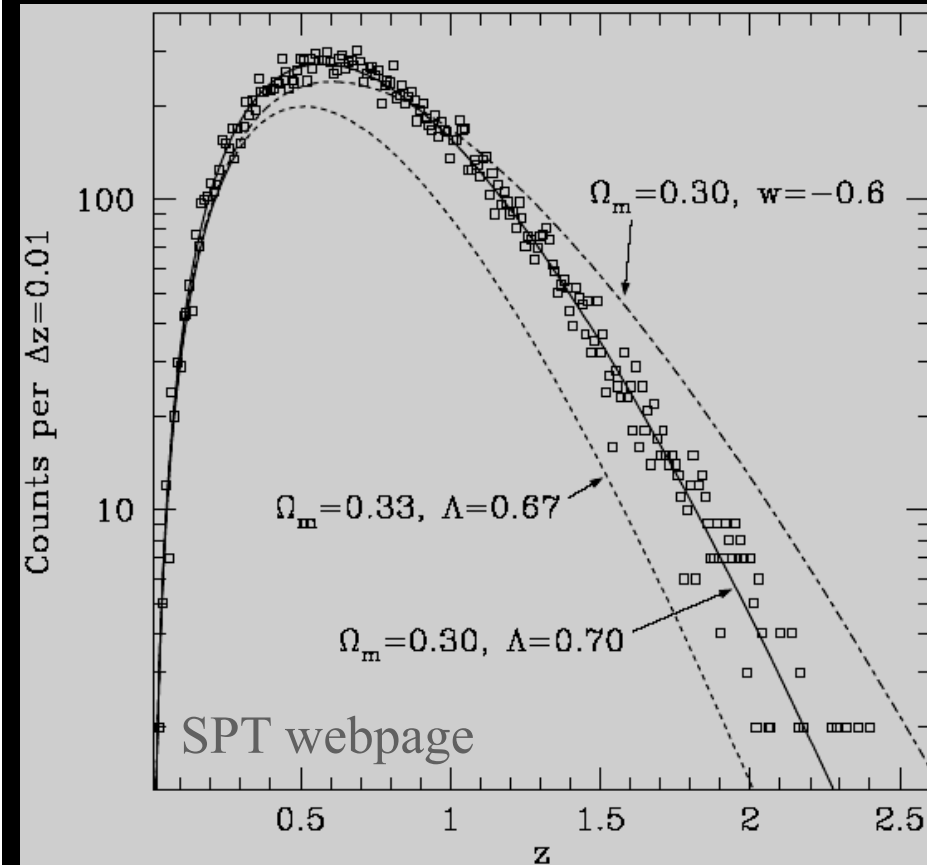
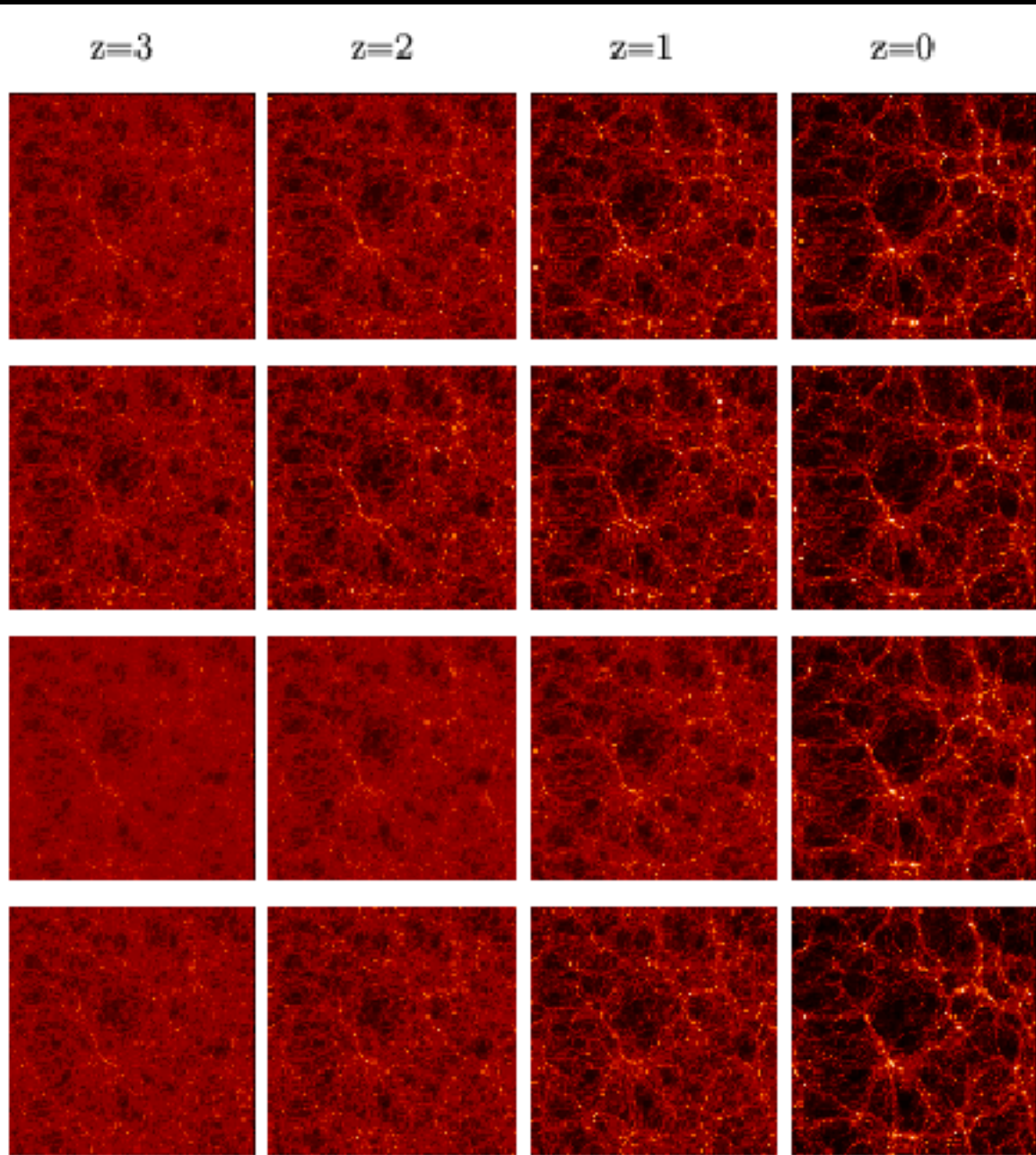
$z = 1.4$  ( $t = 4.7$  Gyr)

$z = 0$  ( $t = 13.6$  Gyr)

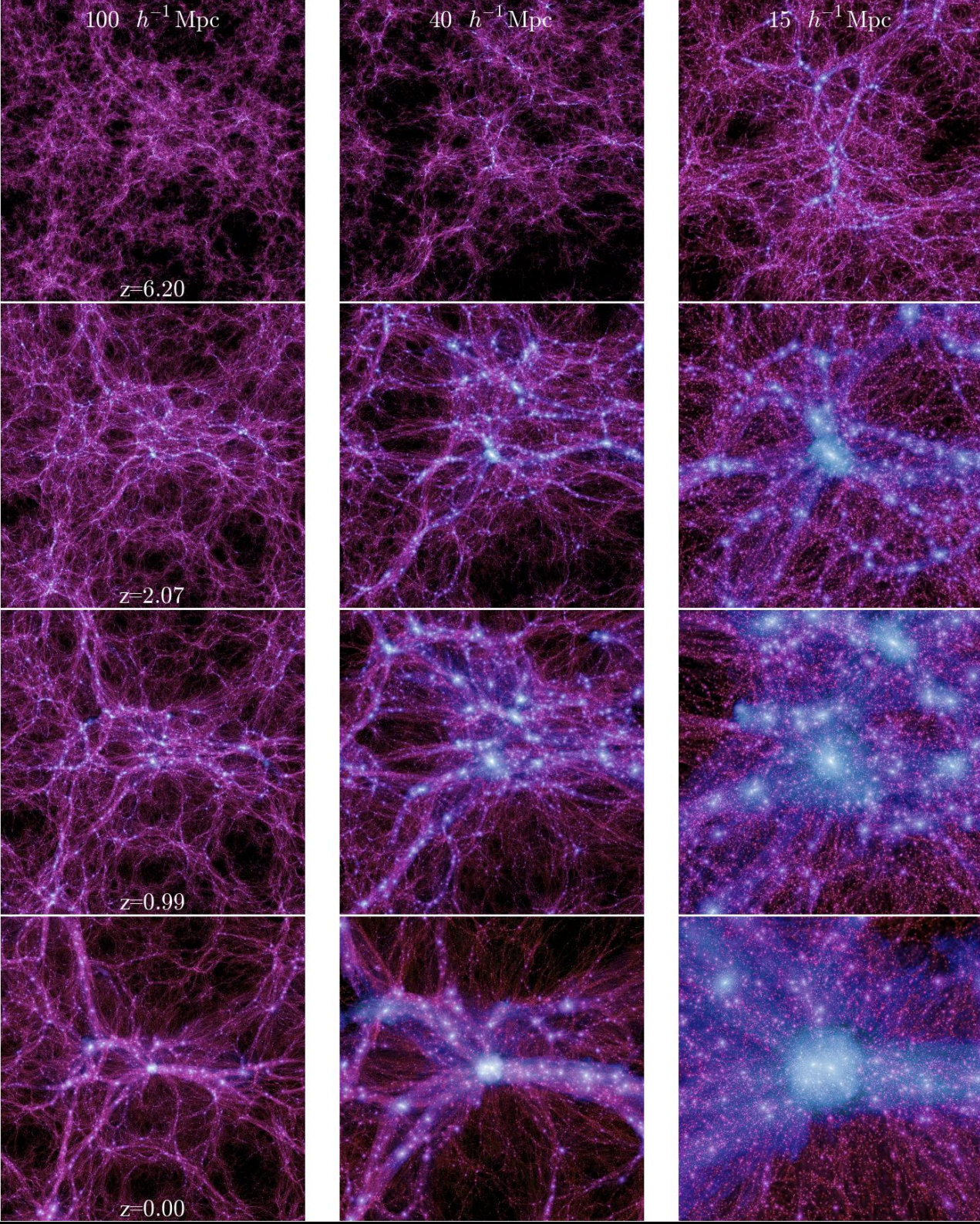


Hierarchical clustering.  
Clusters are still forming today!

# Model-dependent cluster-density evolution



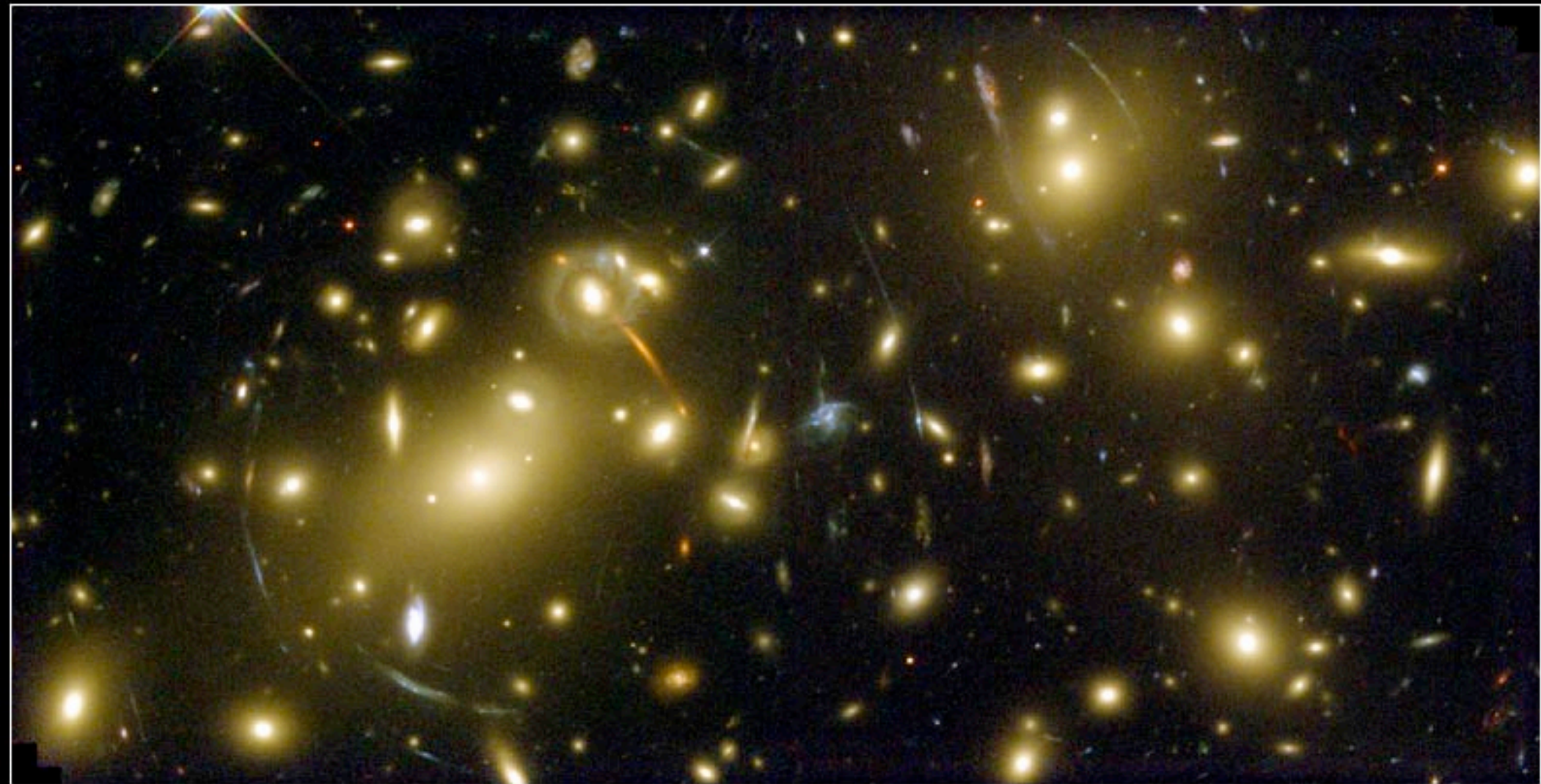
Simulation of an SPT/SZE mass-limited ( $M > 2 \times 10^{14} M_{\odot}$ ) galaxy cluster survey.



# Remember!

- Galaxy clustering is a continuous hierarchy
- Any attempt to identify individual clusters requires rather arbitrary and subjective boundaries to be drawn.
- There is no unique and unambiguous definition of what constitutes a cluster of galaxies, and thus no single method of identifying them.
- For this reason, studies of clusters and their properties depend on the methods used to identify and catalogue them.

# Clusters of galaxies



**Galaxy Cluster Abell 2218**

**HST • WFPC2**

NASA, A. Fruchter and the ERO Team (STScI) • STScI-PRC00-08

# Why study clusters of galaxies?

- Clusters are the largest objects in the universe to have reached a quasi-equilibrium state.
- Clusters provide excellent laboratories to study galaxy formation, evolution and interactions.
- Clusters provided the first and best evidence of vast quantities of dark matter in the universe.
- Clusters have provided important insights into a wide range of topics, such as high-energy astrophysics, particle physics, cosmology, etc...
- Clusters can be used to map and trace the large-scale structure of the universe.

# A bit of history

- Charles Messier published his famous catalogue of nebulae in 1784 (~103 objects). He noted that: “The constellation of Virgo... is one of the constellations that contains the greatest number of nebulae” .
- Other similar concentrations of nebulae were found in the 18<sup>th</sup> and 19<sup>th</sup> centuries by the Herschels (~2500 objects). William Herschel (1785) commented on the many hundreds of nebulae which can be seen in Coma Berenices” .
- Other clusters of nebulae were discovered by: Wolf (1902, 1906), Lundmark (1927), Baade (1928), Christie (1929), Hubble and Humason (1931), Shapley (1934).
- ~1920's-30's some of those nebulae are really other galaxies ... far far away (Shapley, Curtis, Slipher, Hubble, etc).

# Clusters of galaxies

Hundreds to thousands of galaxies

Masses  $\sim 10^{14} - 10^{15} M_{\odot}$

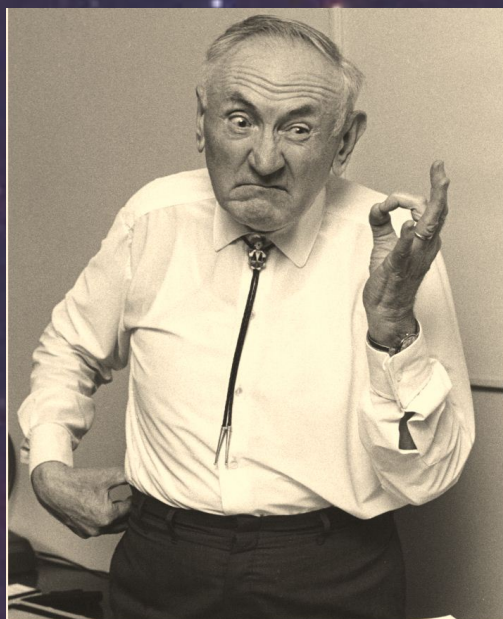
Scales  $\sim 5$  Mpc

Only  $\sim 15\%$  of their total mass is visible

**5% in galaxies (gas and stars)**

**10% in the intra-cluster medium (ICM)**

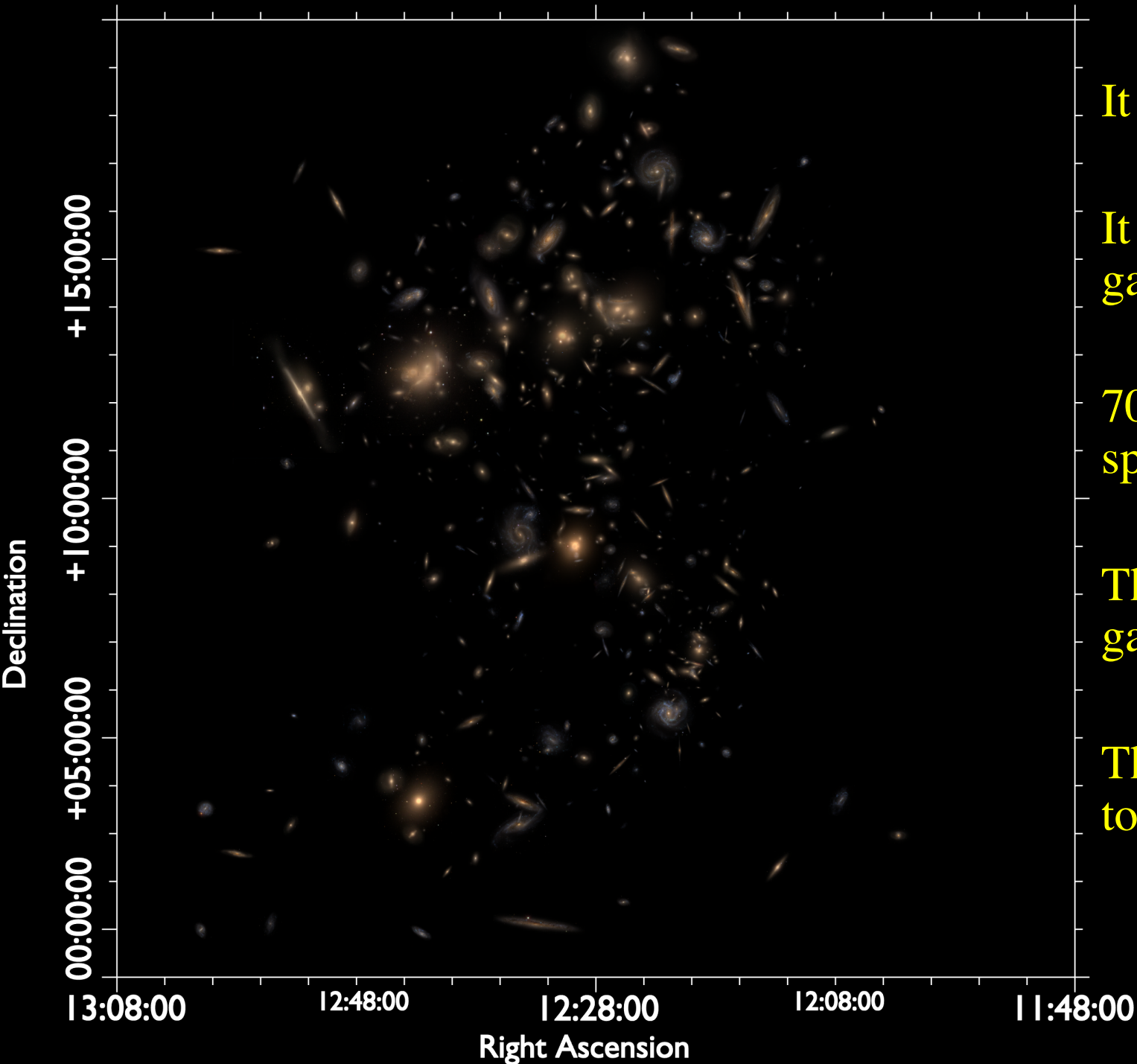
Therefore  $\sim 85\%$  must be dark matter



Fritz Zwicky  
(1933)

The Coma Cluster

# The Virgo cluster



It is 18 Mpc from Earth

It has a few thousand galaxies

70% of galaxies are spirals

The distribution of galaxies is clumpy

The LG is infalling towards Virgo

# The Coma cluster



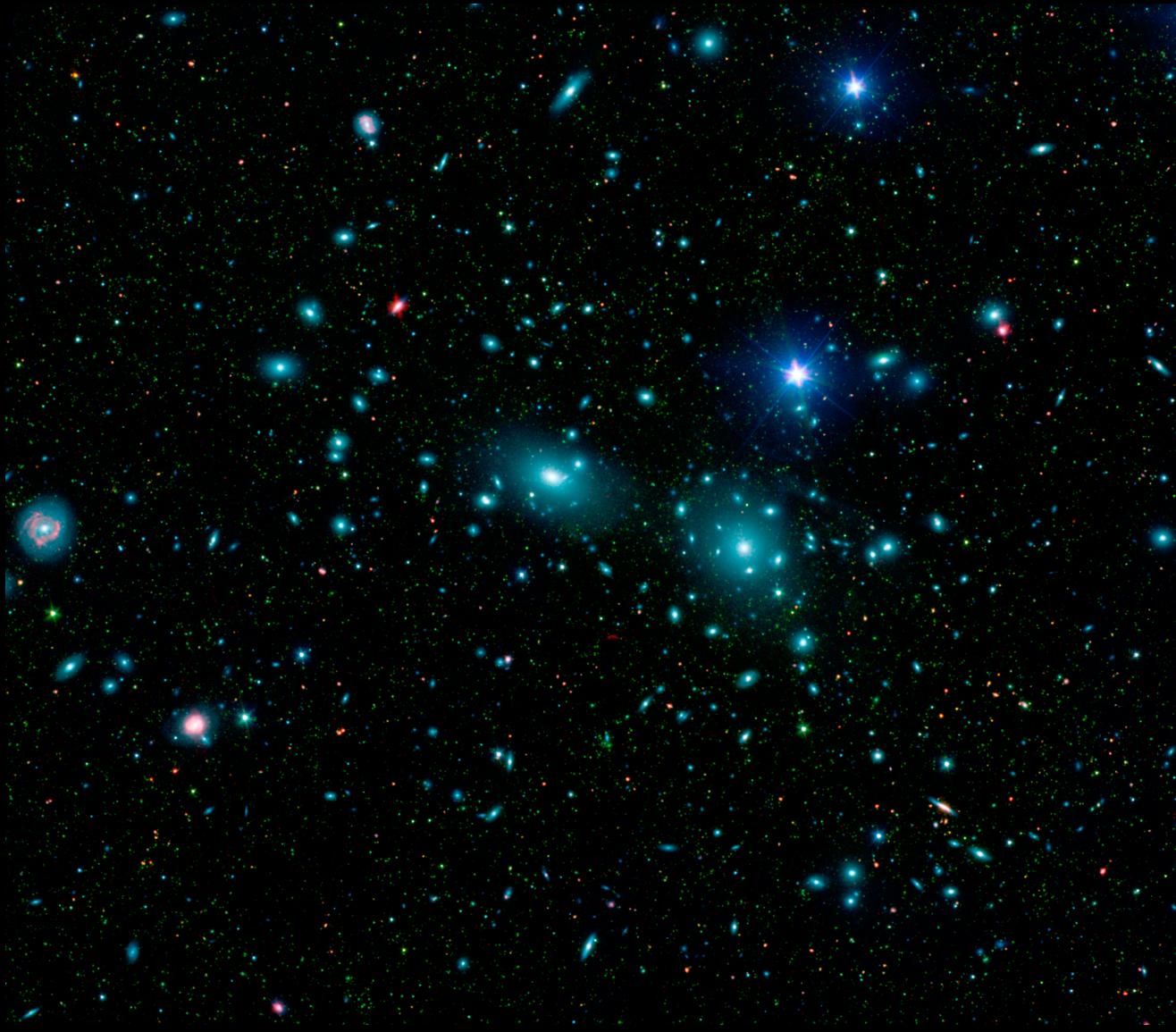
Distance:  $\sim 98$  Mpc  
( $z=0.023$ )

Brightest members are  
ellipticals

$\sim$  up to 1,000 members

Best-studied of all  
clusters

# The Coma cluster



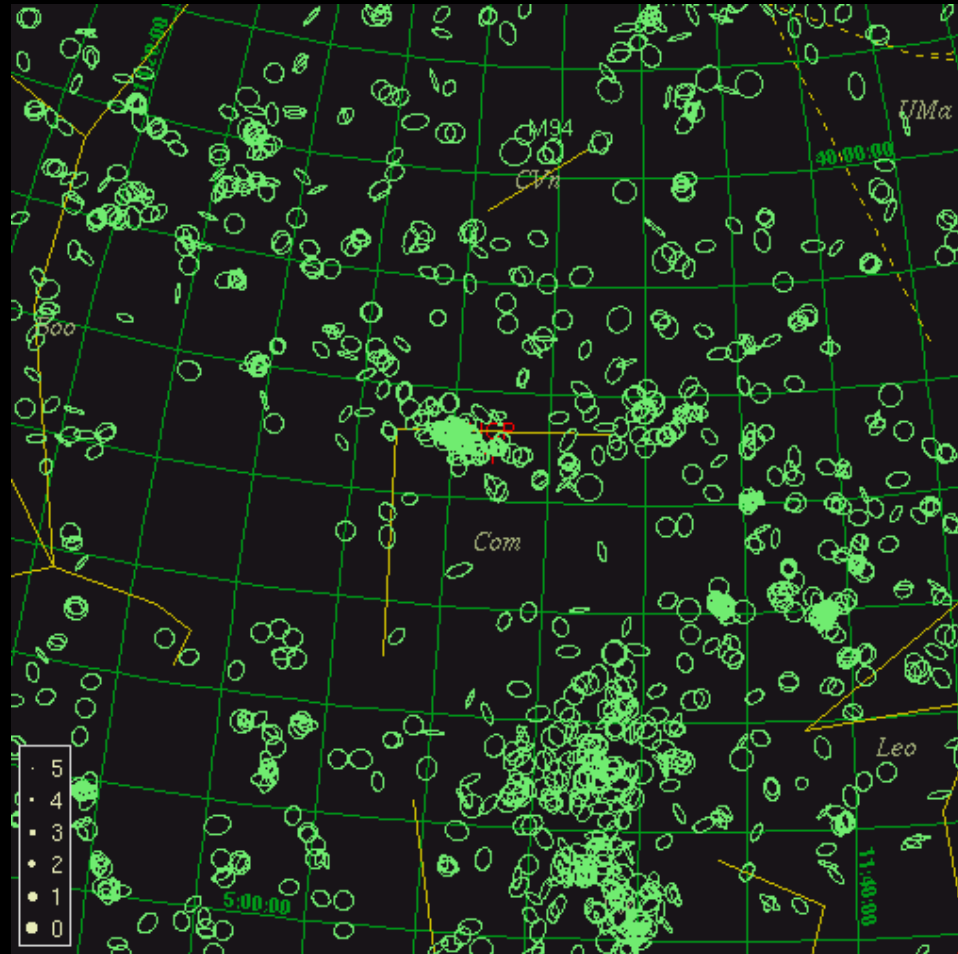
Distance:  $\sim 98$  Mpc  
( $z=0.023$ )

Brightest members are  
ellipticals

$\sim$  up to 1,000 members

Best-studied of all  
clusters

# The Coma cluster



# Nearby massive clusters

Name	Distance from earth (Mpc)
Virgo	15.5
Pisces-Perseus	
Abell 262	70
Abell 426	77
Coma	98
Hercules	156
Hydra	234

# Cluster catalogues

## 19.1 Selection Criteria for Clusters and Groups

### 19.1.1 Abell's Catalog of Rich Clusters (1958)

Abell's criteria:

- $> 50$  cluster members in the magnitude range  $[m_3, m_3 + 2]$  (with the magnitude  $m_3$  of the 3rd brightest galaxy) and within the radius  $R_{\text{Abell}} = \frac{1.7}{(1+z)} \simeq 3h_{50} \text{Mpc}$ .  
*1.5h Mpc*
- Redshift range:  $0.02 < z < 0.20$
- Sorted into 'richness classes' according to number of galaxies  $N$  and density.
- The redshift was usually not measured, but determined from the apparent magnitude of the brightest cluster galaxies.
- The clusters were found using the Palomar Sky Survey

Richness class  
(R)

$N_{gal}$

Clusters in the complete  
northern sample

0	30-49	$\geq 10^3$
1	50-79	1224
2	80-129	383
3	130-199	68
4	200-299	6
5	$\geq 300$	1

## Zwicky et al. (1961-1968)

Zwicky catalogued about 10,000 clusters by eye. Because a less rigorous cluster definition was used, this catalogue is not as complete or homogeneous as Abell's.

## Shectman (1985)

Used an automated computer procedure to identify 646 clusters from the Lick galaxy survey.

## Edinburgh-Durham Cluster Catalog

(Lumsden et al. 1992)

An automated procedure based on Abell's cluster definition was used (737 clusters identified in the southern sky).

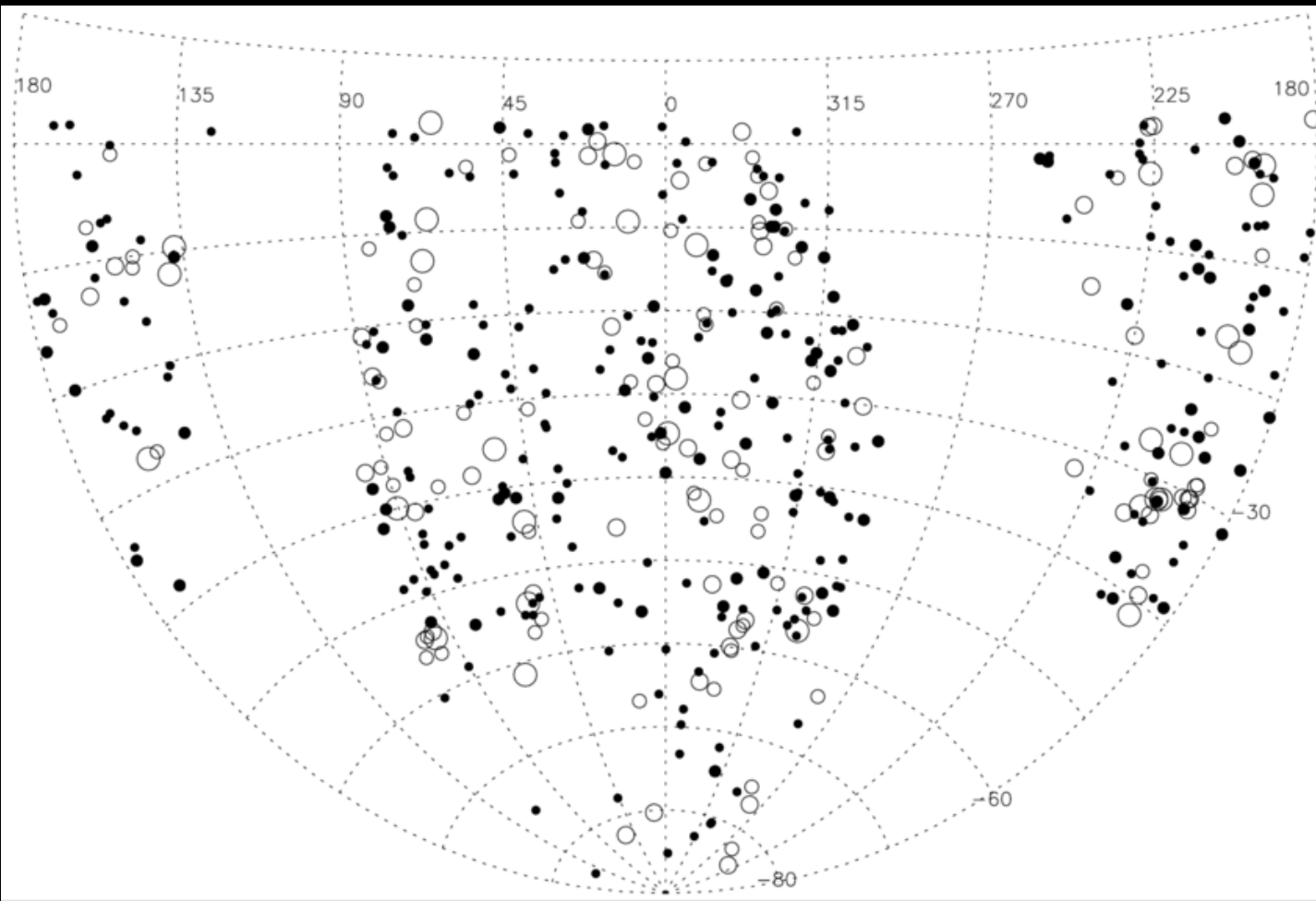
## APM Cluster Catalog (Dalton et al. 1992)

A different automated procedure (220 clusters). Galaxies were counted within  $r=0.075 h^{-1}$  Mpc. Different magnitude range.

## 2dF and SDSS cluster surveys - several

# X-ray galaxy cluster surveys

RASS, XMM-BCS, REFLEX, EMSS, SHARC, WARPS, MACS



Sky distribution in  $\alpha$  and  $\delta$  of the galaxy clusters in the REFLEX sample. The symbols give an indication of the cluster flux. The clusters are sorted into five flux bins:  $3-5 \times 10^{-12}$ ,  $5-7 \times 10^{-12}$ ,  $7-10 \times 10^{-12}$ ,  $1-2 \times 10^{-11}$ , and  $\geq 2 \cdot \times 10^{-11} \text{ erg s}^{-1} \text{ cm}^{-2}$  and indicated by increasing symbol size, respectively.

Böhringer et al. 2004

Flux limited surveys

# SZE cluster surveys (mm)

SPT, ACT, *Planck*

Planck Collaboration: *Planck* catalogue of Sunyaev–Zeldovich sources

**Planck 2013 results**

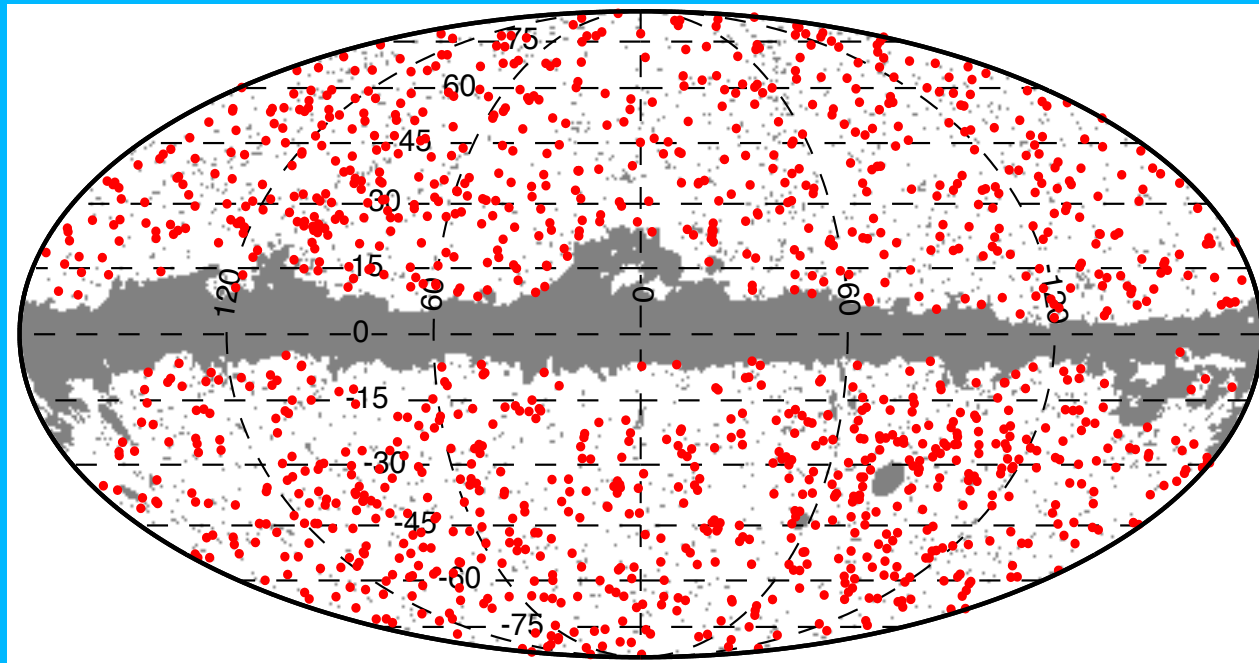
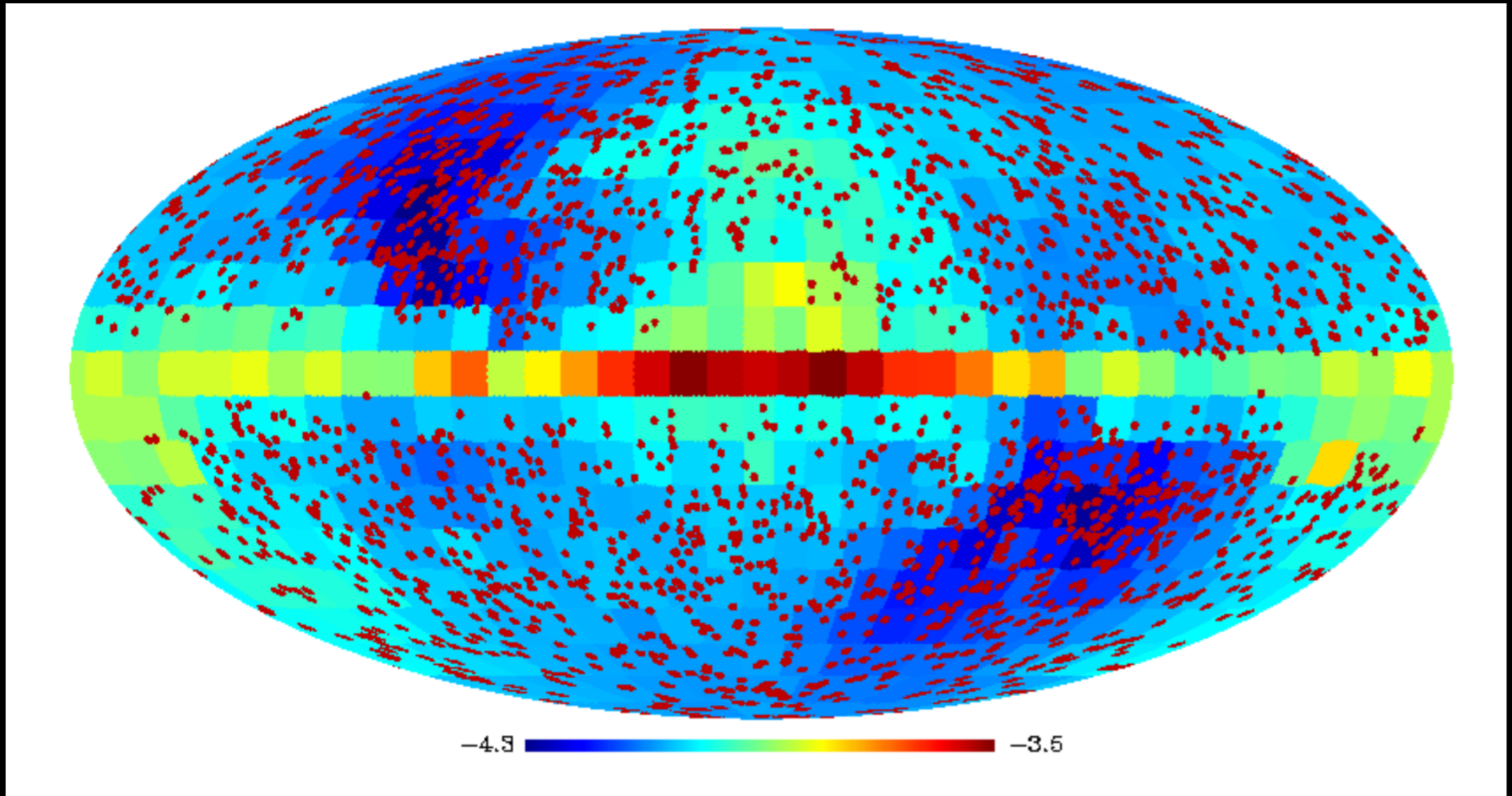


Fig. 2: Sky distribution of the 1227 *Planck* clusters and candidates (red dots), in a Mollweide projection with the Galactic plane horizontal and centred at longitude zero. Small grey dots show the positions of masked point sources, and grey shading shows the mask used to exclude the Magellanic clouds and the Galactic plane mask. The mask covers 16.3% of the sky.

Mass limited surveys

# X-ray + SZE

ROSAT all-sky survey (RASS) + *Planck*



Tarrió-Alonso et al. (2019). The all-sky catalogue of galaxy clusters and cluster candidates obtained from joint X-ray-SZ detections contains 2323 objects: 1597 candidates correspond to already known clusters, 212 coincide with other cluster candidates still to be confirmed, and the remaining 514 are completely new detections.

# Galaxies in clusters

# Observations of galaxies in clusters - Richness

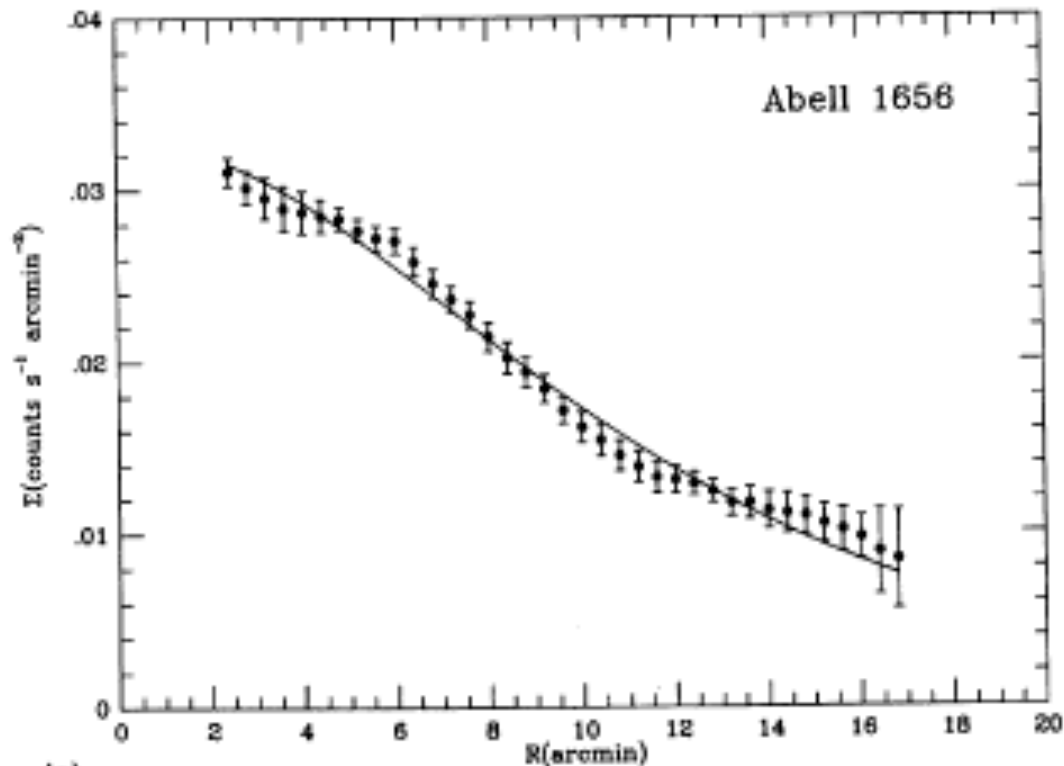
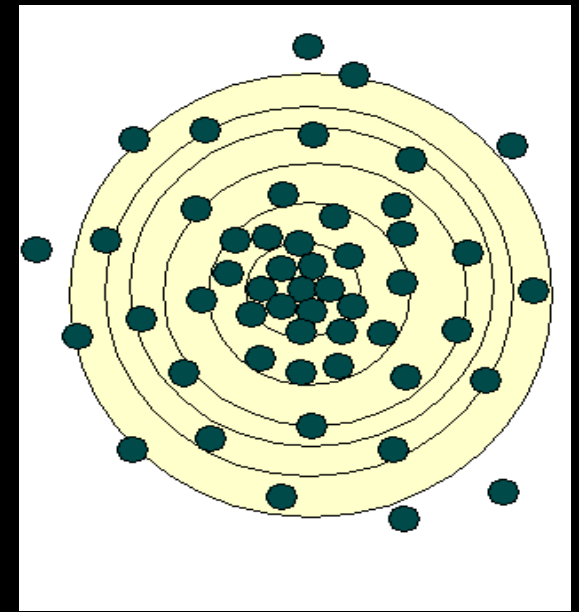
Richness is a measure of the total number of galaxies that belong to a cluster.

It is very difficult to determine the total galaxy populations of a cluster because:

- 1) it depends on the mag limit to which one counts
- 2) clusters do not have clear (sharp) boundaries
- 3) there is contamination from foreground and background galaxies

# Density Profiles

Density profiles provide information on the radial mass distribution, which can be related to theories of cluster formation.



**Regulars:** spherical & centrally concentrated

**Irregulars:** wiggles in the profile suggest substructure is present.

# Density Profiles

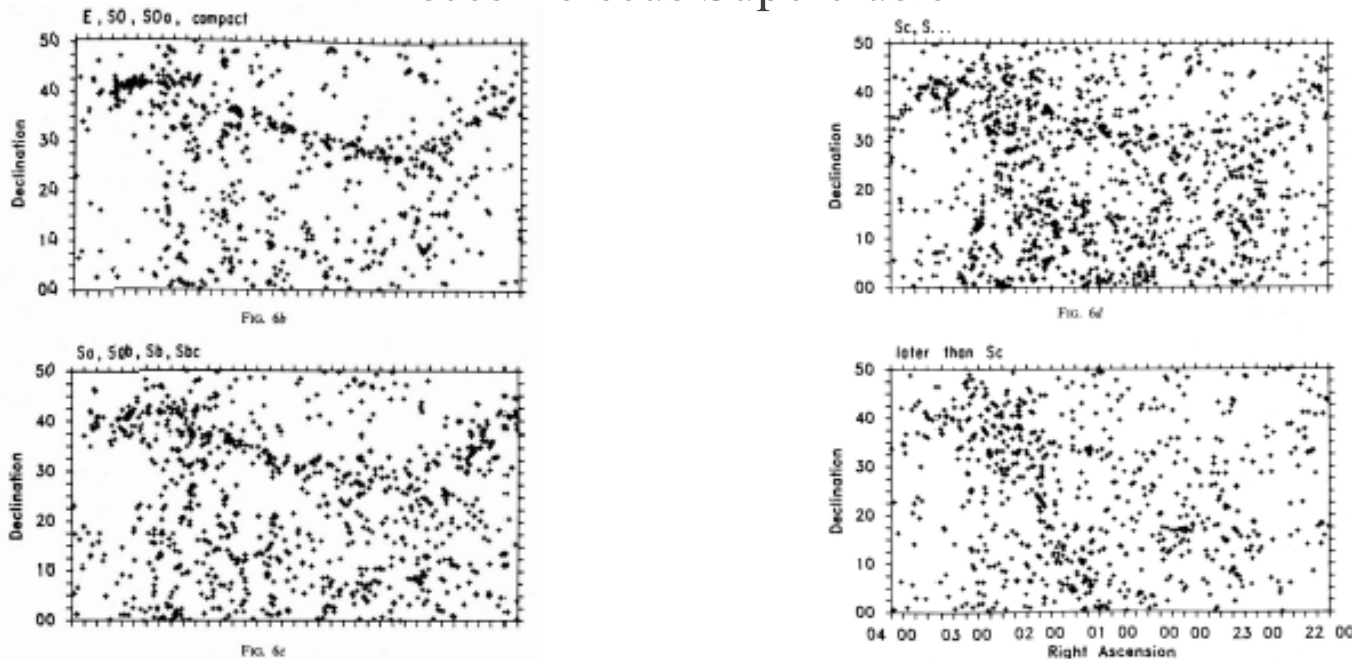
Several different functional forms have been proposed to describe density profiles. Often more than one can fit the data.

- $\sigma(r) = \sigma_0 r^{-\alpha}$  (power – law)
- $\sigma(r) = \sigma_0 \exp [-7.67(r/r_e)^{1/4}]$  (de Vaucouleurs)
- $\sigma(r) = \sigma_0 [1+(r/r_c)]^{-2}$  (Hubble profile)
- $\sigma(r) = \sigma_0 [1+(r/r_c)^2]^{-1}$  (King profile)

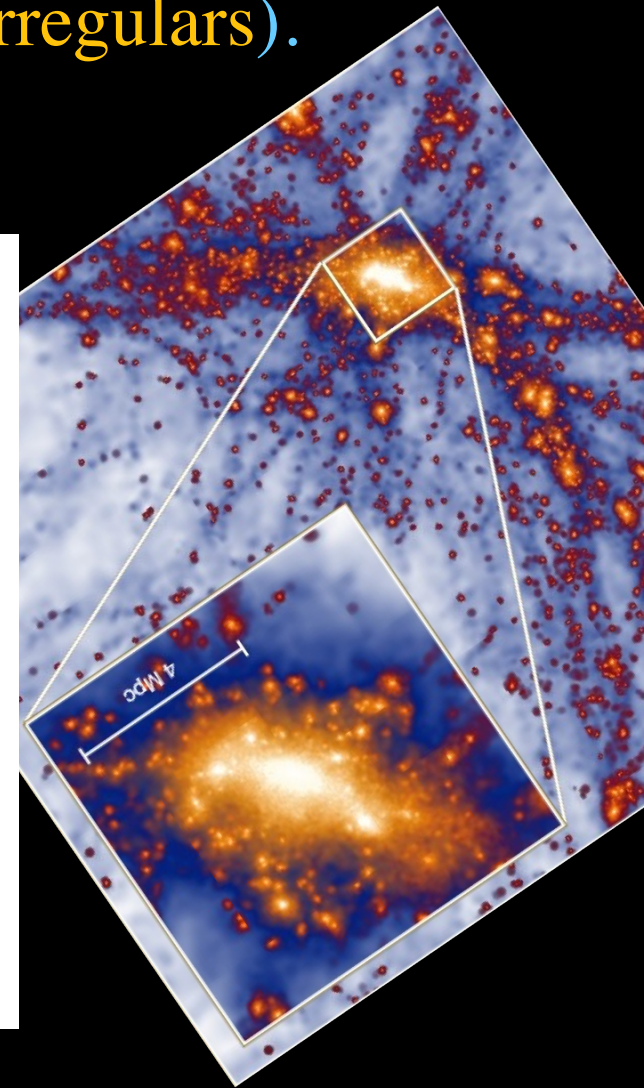
# Observations of galaxies in clusters – galaxy distribution

- Galaxy distributions in clusters show a wide range of morphologies, from smooth centrally-condensed (**regulars**) to clumpy with no well-defined centroid (**irregulars**).
- Many clusters are very elongated.

## Pisces-Perseus Supercluster

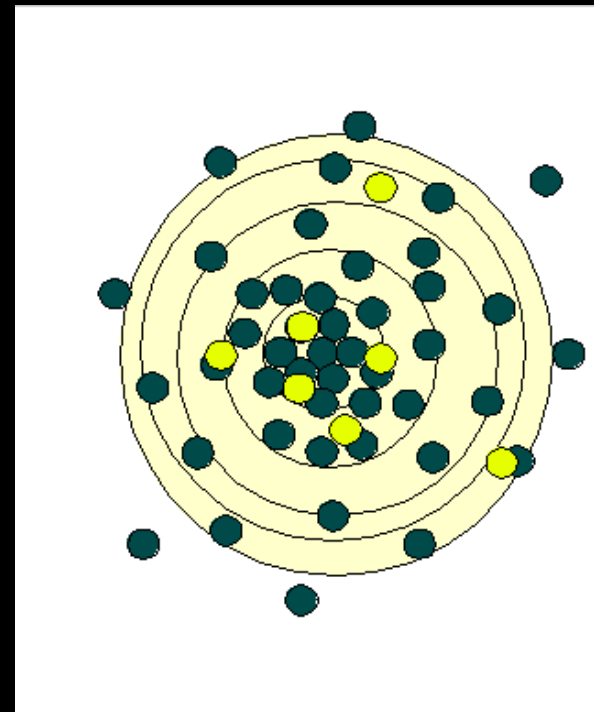
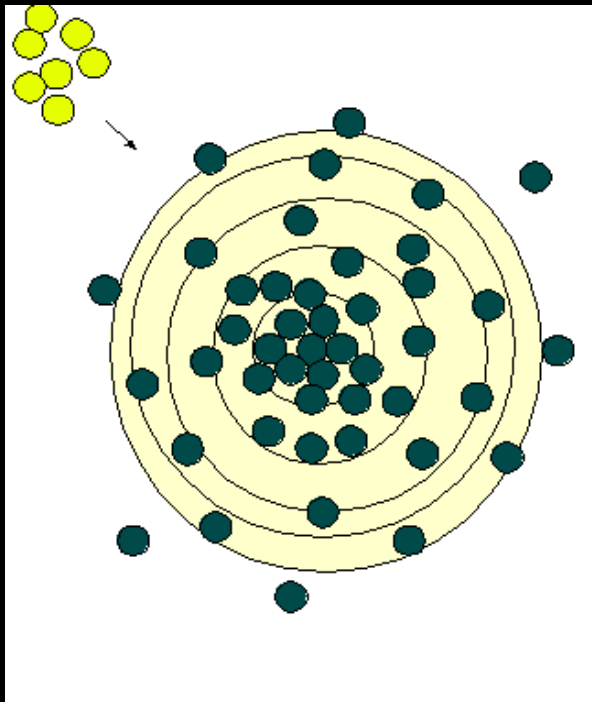


see: Giovanelli et al. (1986) *ApJ*, 300, 77



# Substructures

- Many clusters (about 50% or more) show substructure
- Dynamical evolution will rapidly erase substructure. Therefore its prevalence indicates that many clusters have “formed” fairly recently.
- If clusters are dynamically young, they may still carry clues about their initial conditions at the time of formation.

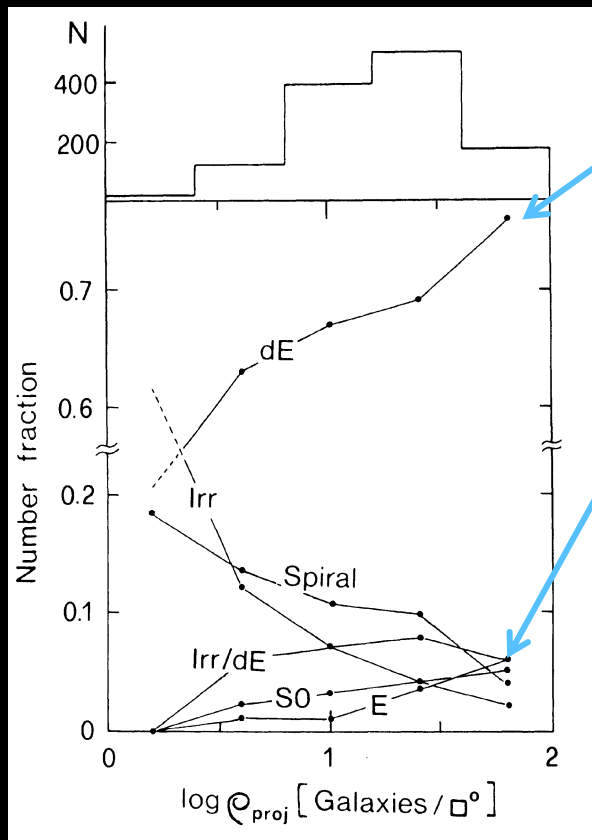


# Observations of galaxies in clusters – galaxy distribution

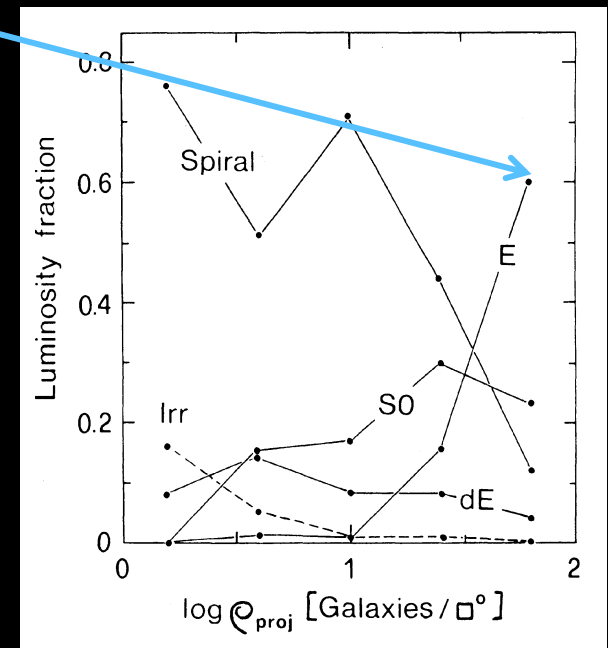
- The mixture of different galaxy types varies widely from cluster to cluster.
- Poor clusters have a greater fraction of S and Irr.
- Rich clusters have a greater percentage of elliptical galaxies (because they are older? More massive? Both? how do ellipticals form?).

# Morphology – density relation

Galaxy type correlates with density; ellipticals are found preferentially in high-density regions.



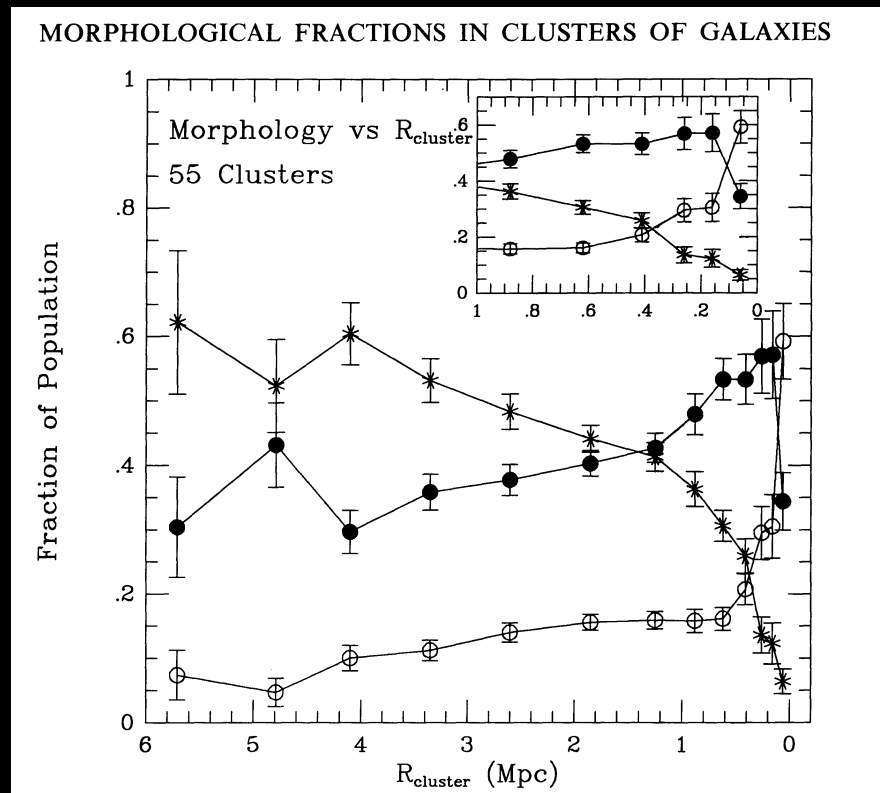
Virgo cluster



Binggeli et al. 1987  
(Astronomical Journal, Vol. 94)

# Morphology clustercentric-distance relation

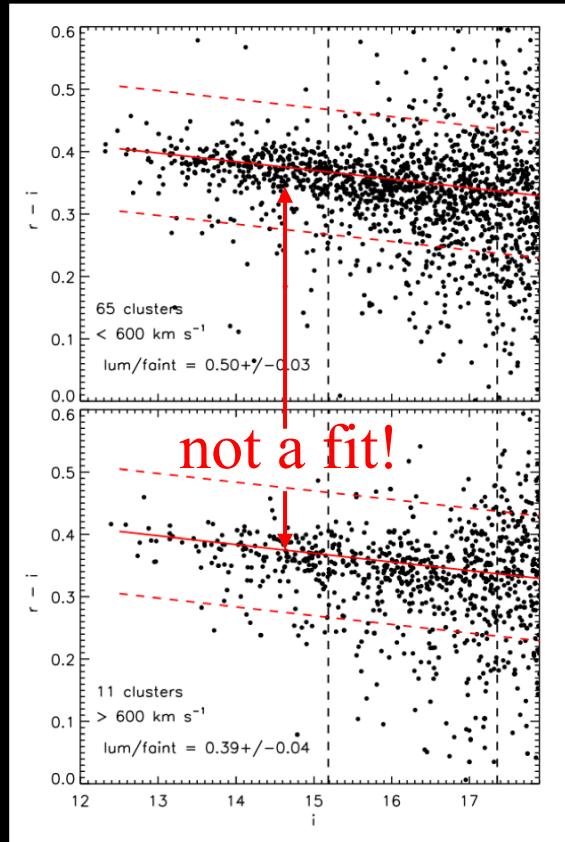
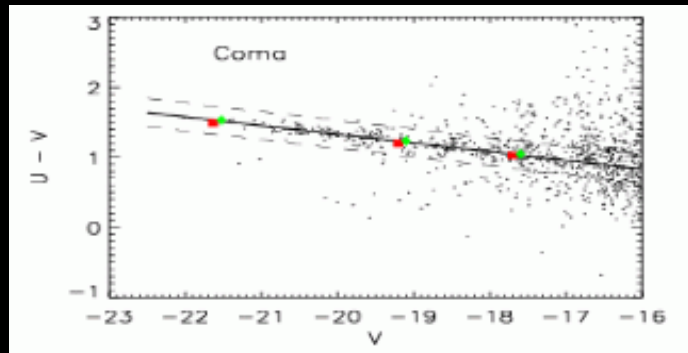
Galaxy type correlates with position; ellipticals are found preferentially near the cluster centre.



Whitmore et al. 1993 (ApJ 407)

# The colour-magnitude diagram

Clusters present the red-sequence, at low and intermediate redshifts



(De Lucia et al. 2007)

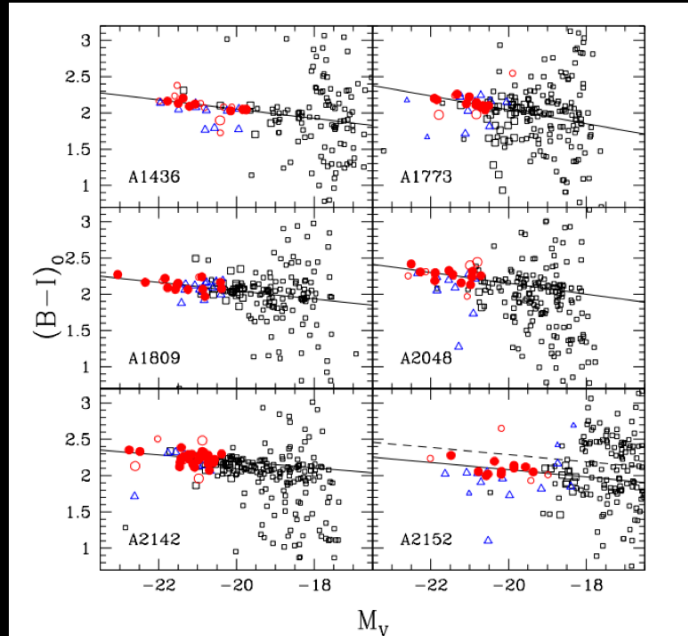
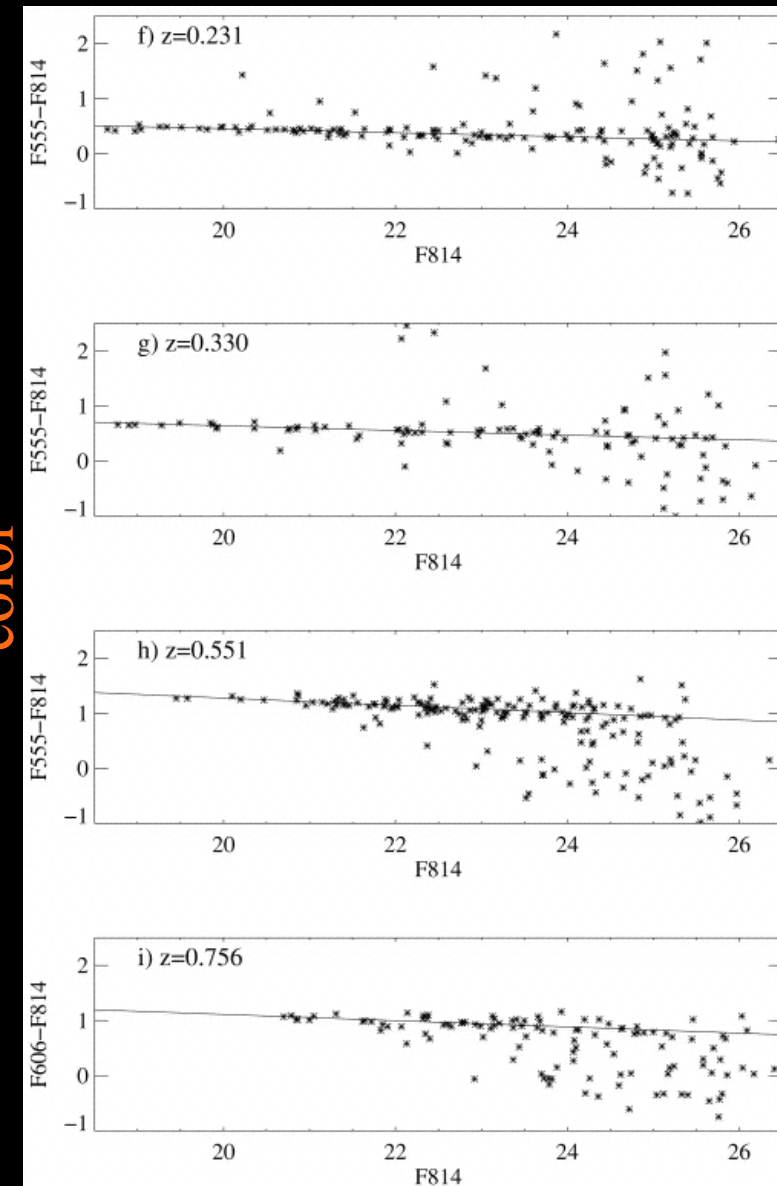


**Fig. 3** —  $M_V - (B - I)_0$  color-magnitude diagrams of the galaxies in six clusters (circles : early-type galaxies, squares : unclassified galaxies, and triangles : late-type galaxies). Large symbols and small symbols represent confirmed members and uncertain members, respectively. Large filled circles represent the data used for a linear fit of the CMR that is plotted by the straight line, while large open circles represent the data not used for fitting. The dashed line in the color-magnitude diagram of A2152 indicates a boundary for separating galaxies in A2152 from background cluster galaxies.

(Jong et al. 2008)



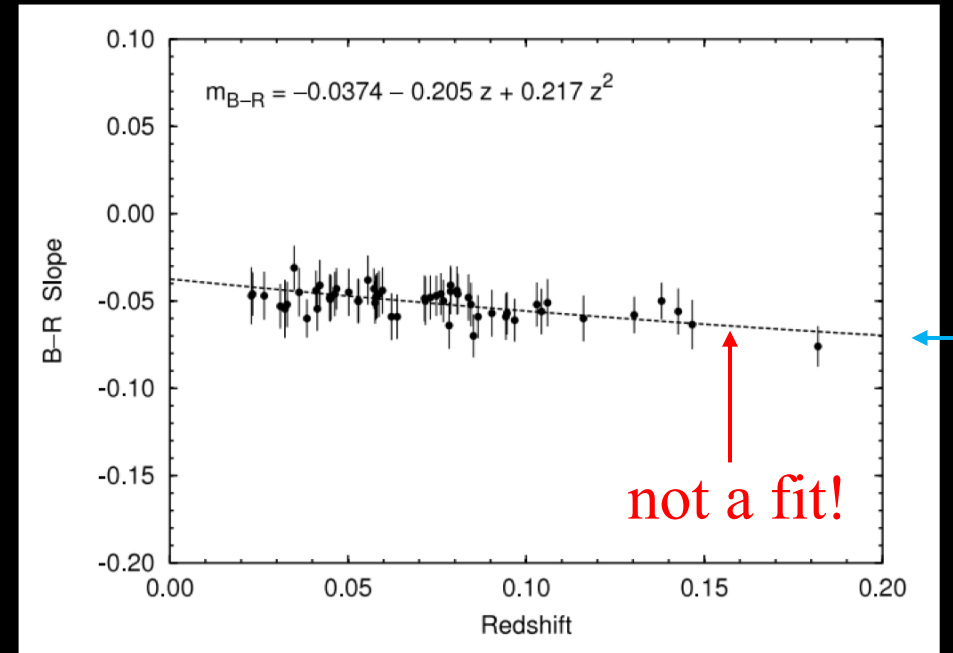
(Ellis et al; Kodama et al; Gladders et al)

# Implications of the Colour-magnitude relation of clusters

Lopez-Cruz et al. (2004) studied the CMR for 57 X-ray detected Abell clusters.

## Universality of the CMR

- “Models that explain the CMR in terms of metallicity and passive evolution can naturally reproduce the observed behaviour of the CMRs studied”
- “The observed properties of the CMR are consistent with models in which the last episode of strong star formation [...] occurred significantly more than  $\sim 3$  Gyr ago ( $z \sim 0.26$ ) [...] early-type galaxies in clusters were formed more than 7 Gyr ago ( $z \sim 0.82$ )”



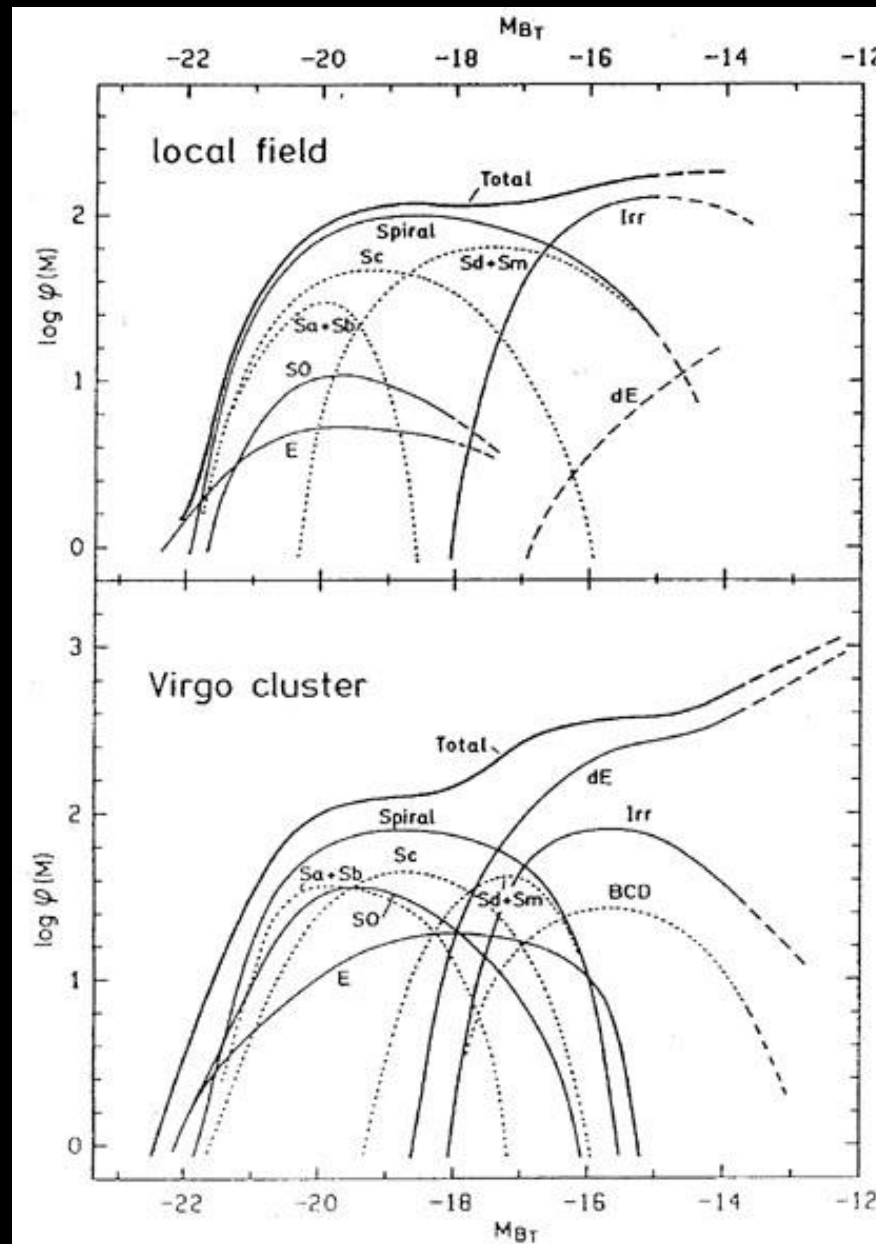
# The luminosity function of galaxies in clusters



Count number of  
galaxies in each  
bin of magnitud

# The luminosity function of galaxies in clusters

Binggeli, Sandage,  
and Tammann 1988



# The luminosity function of galaxies in clusters

The LF ( $n$ ,  $\Phi$ ,  $\phi$ ) is usually well-described by a Schechter form:

$$n(L) dL = \phi^* \left( \frac{L}{L^*} \right)^\alpha e^{-L/L^*} \frac{dL}{L^*}$$

Where  $n(L)$  = the number of galaxies with luminosities  $L$  to  $L+dL$

$$L_* = 1 \times 10^{10} h^{-2} L_\odot$$

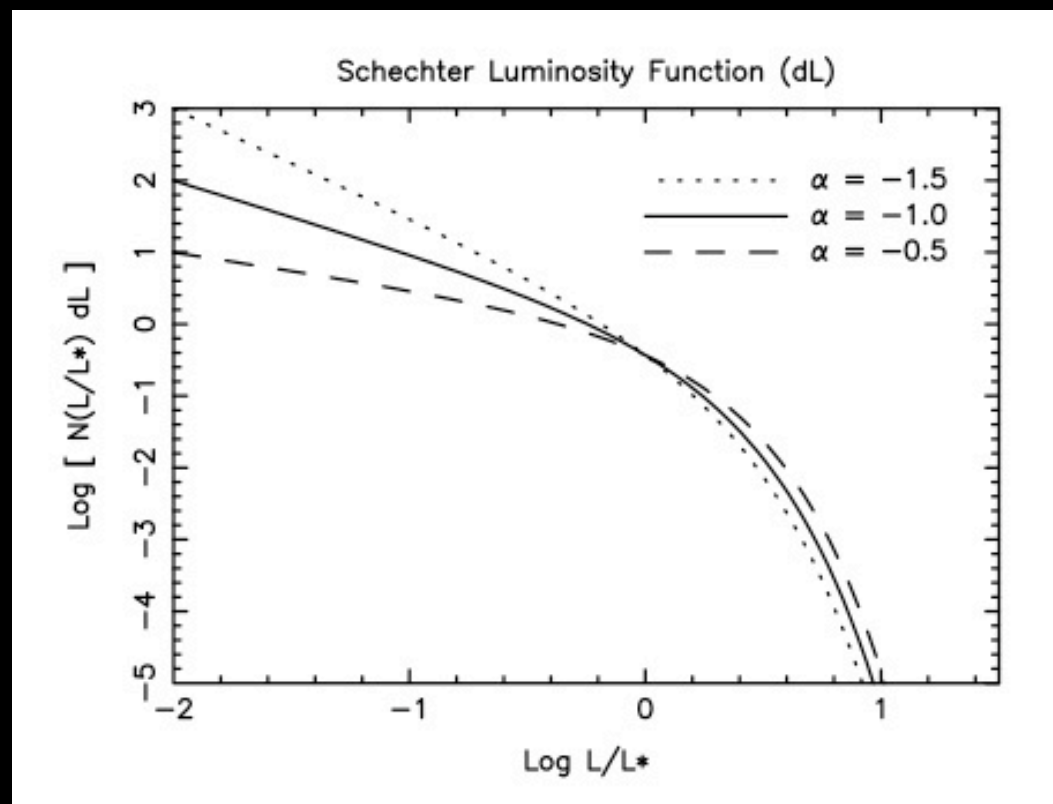
$$\alpha = -1.0 \text{ to } -1.5$$

$$\phi^* = 0.03 h^3 \text{ Mpc}^{-3}$$

$$n(M) dM = 0.4 \ln 10 \phi^* [10^{0.4(M^* - M)}]^\alpha \exp[-10^{0.4(M^* - M)}] dM$$

# Luminosity function: What are $L_*$ and $\alpha$ ?

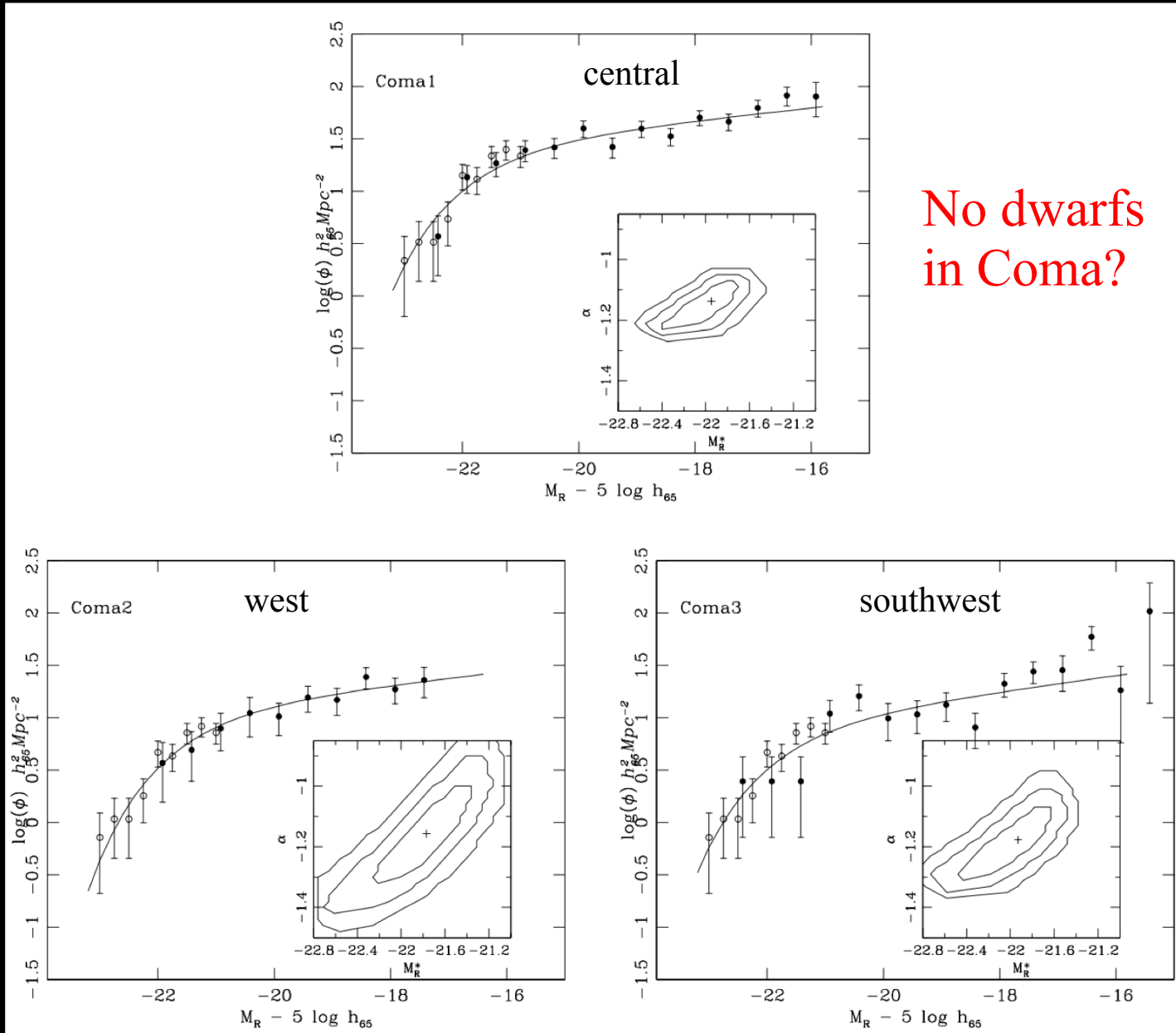
- The value of  $\alpha$  indicates the dwarf content of the cluster
- For steep faint-end,  $\alpha < -1$ , the system is rich in dwarfs
- For a declining faint-end  $\alpha > -1$ , few dwarfs
- $L_*$  is the knee of the function at the bright end



# Coma Luminosity Function (Mobasher et al. 2003)

Over 700 galaxies with measured redshifts down to  $M_B = -16$

They find a flat luminosity function with  $\alpha \approx -1.18$



# cD galaxies

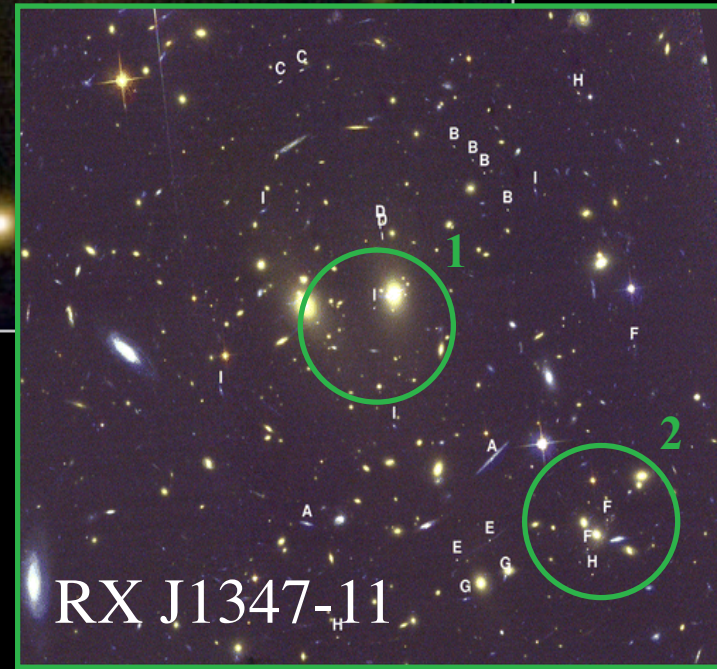
- cDs are the largest galaxies in the Universe, surrounded by faint envelopes which may extend for many hundreds of kpc.
- They are found in the centre of clusters and of a few groups.
- They may have formed by galaxy cannibalism or by accretion of tidally-stripped material from other galaxies.
- cD galaxies are often oriented in the same direction as the major axis of the cluster in which they reside.
- Originally studied to determine cosmological parameters (e.g. Sandage et al. 1972) and measure large-scale streaming motions (e.g. Lauer and Postman 1994).

# cD galaxies multi-nuclei clusters



**Galaxy Cluster Abell 2218**

NASA, A. Fruchter and the ERO Team (STScI) • STScI-PRC00-08



**RX J1347-11**

# Cluster kinematics – known long ago...

- In a cluster of galaxies the only important force acting between the galaxies is gravity. It is the pulling of the galaxies on each other that gives rise to their velocities. The more mass in the cluster, the greater the forces acting on each galaxy (the higher the relative velocities).
- If the velocity of a given galaxy is too large, it will be able to escape the cluster. Therefore, by knowing that all of the galaxies have velocities smaller than the escape velocity, one can estimate the total mass of a cluster.
- In the 30' s, Zwicky and Smith examined the individual galaxies making up two nearby clusters (Coma and Virgo). What they found is that the velocities of the galaxies were about a factor of ten to one hundred larger than they expected.

# Cluster kinematics

- Clusters are not static systems. Their galaxy populations are in constant motion.
- The speed of galaxies in clusters is characterised by the line-of-sight velocity dispersion

$$\sigma_{los} = \left[ \frac{1}{N} \sum_{i=1}^N (v_i - \langle v \rangle)^2 \right]^{1/2}$$

- If the galaxy orbits are isotropic, then:

$$\sigma_{3D} = (\sigma_x^2 + \sigma_y^2 + \sigma_z^2)^{1/2} = 3^{1/2} \sigma_{los}$$

# Cluster kinematics

- Velocity distribution in Coma 552 gals.
- Multi-Gaussian distribution results in better fit. Evidence of sub-structure and merging activity.

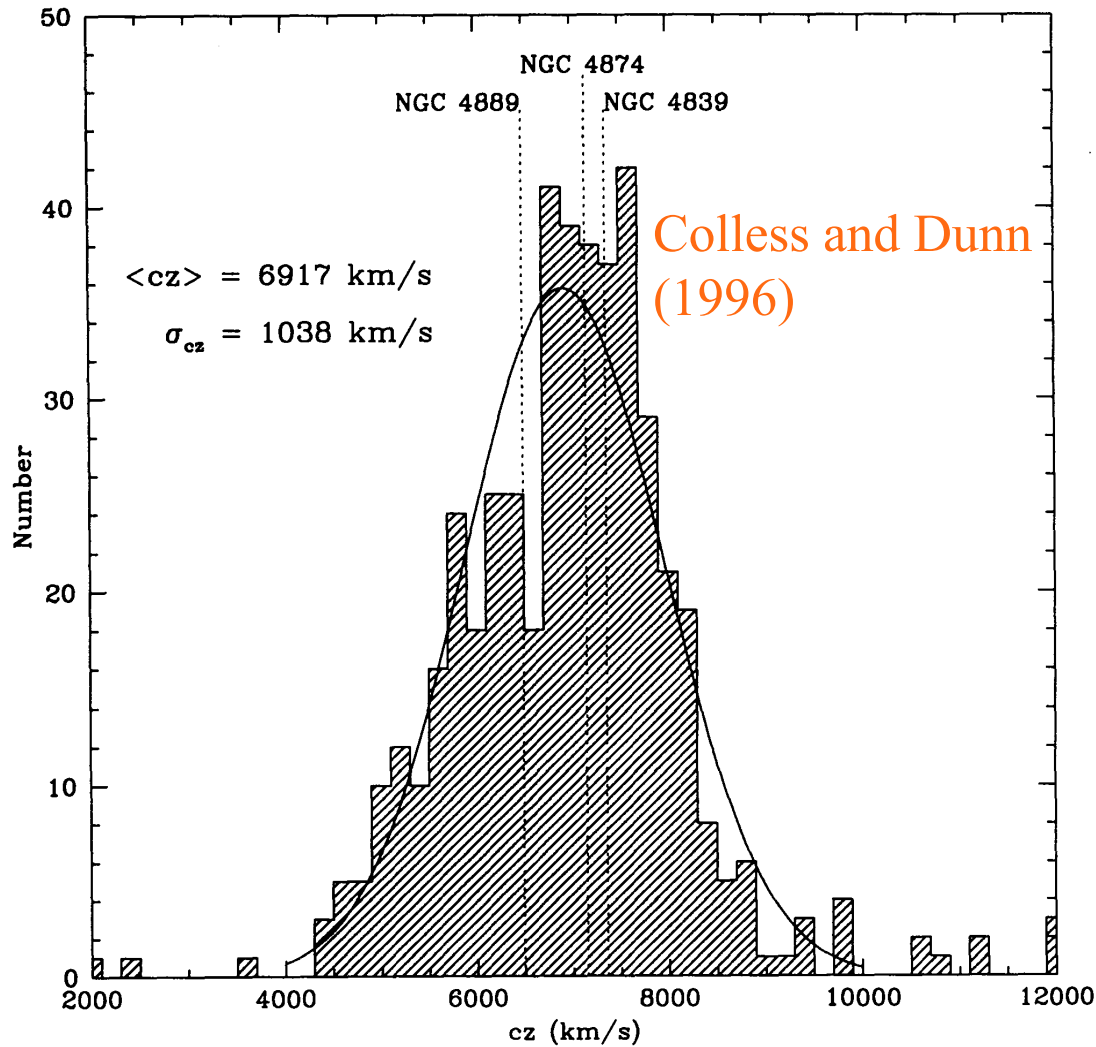
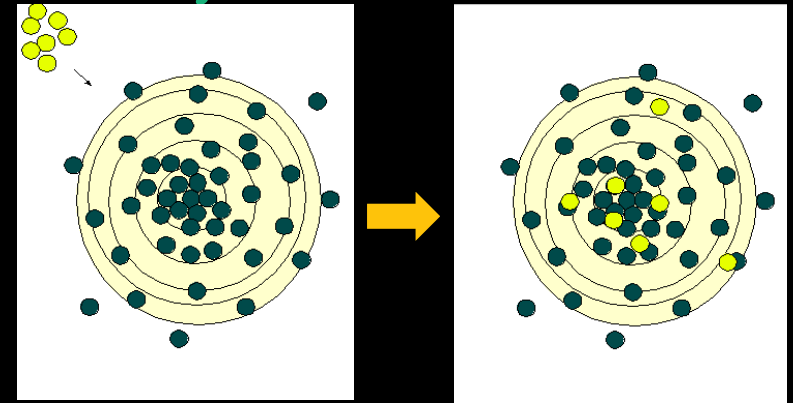
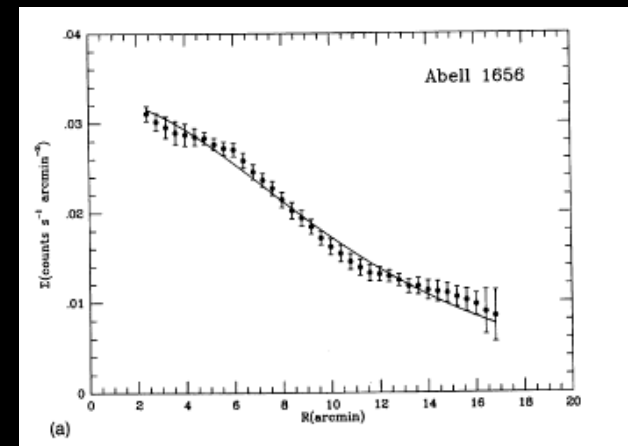


FIG. 5.—Distribution of radial velocities for galaxies in the Coma cluster. The curve is a Gaussian with mean  $6917 \text{ km s}^{-1}$  and standard deviation  $1038 \text{ km s}^{-1}$ . The velocities of the three dominant cluster galaxies are indicated.



wiggles in the radial profile?



# Cluster kinematics

- The shape of the velocity distribution gives information about the dynamical state of the cluster.
- Significant deviations from Gaussian may indicate non-isotropic orbits or sub-clustering.
- These can be measured from moments of the velocity distribution.
- 1<sup>st</sup> moment =  $\langle v \rangle$
- 2<sup>nd</sup> moment =  $\sigma$

- 3<sup>rd</sup> moment =  $Skewness = \frac{1}{N} \sum_{i=1}^N \left[ \frac{v_i - \langle v \rangle}{\sigma} \right]^3$
- 4<sup>th</sup> moment =  $Kurtosis = \frac{1}{N} \sum_{i=1}^N \left[ \frac{v_i - \langle v \rangle}{\sigma} \right]^4 - 3$

# How to weigh a cluster of galaxies: the Virial Theorem

A self-gravitating system in a steady-state will satisfy the virial theorem:  $2T+U=0$ , where  $T$ =kinetic energy and  $U$ =potential energy. Hence,

$$M_{cl}\sigma^2 - \frac{\alpha GM_{cl}^2}{R} = 0$$

where  $\alpha$  depends on the matter distribution

$\alpha = 3/5$  for a uniform sphere

$\alpha \sim 1$  for typical profiles

This yields,

$$M_{cl} \sim 10^{15} M_{\odot} \left( \frac{\sigma_{los}}{10^3 km/s} \right)^2 \left( \frac{R}{1 Mpc} \right)$$

- Virial estimates indicate total cluster masses  $M_{cl} \sim 10^{13}-10^{15} M_{\odot}$
- Visible galaxies account for only  $\sim 5 - 10\%$  of  $M_{cl}$

# Physical processes affecting cluster galaxies

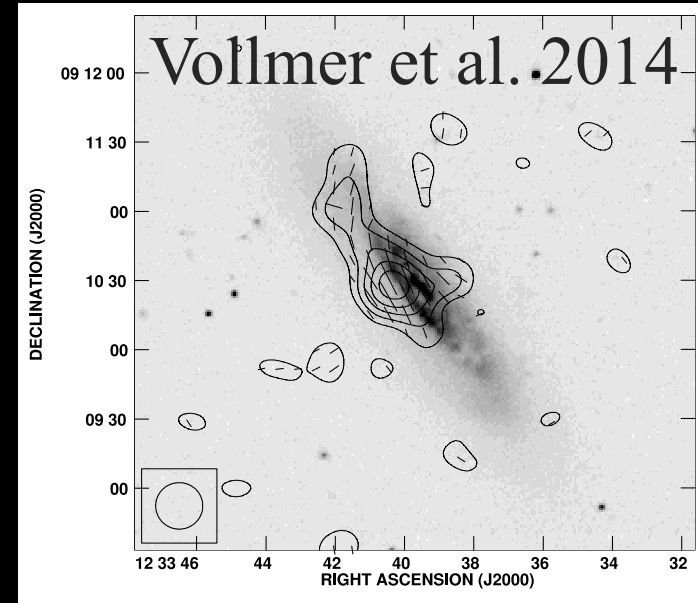
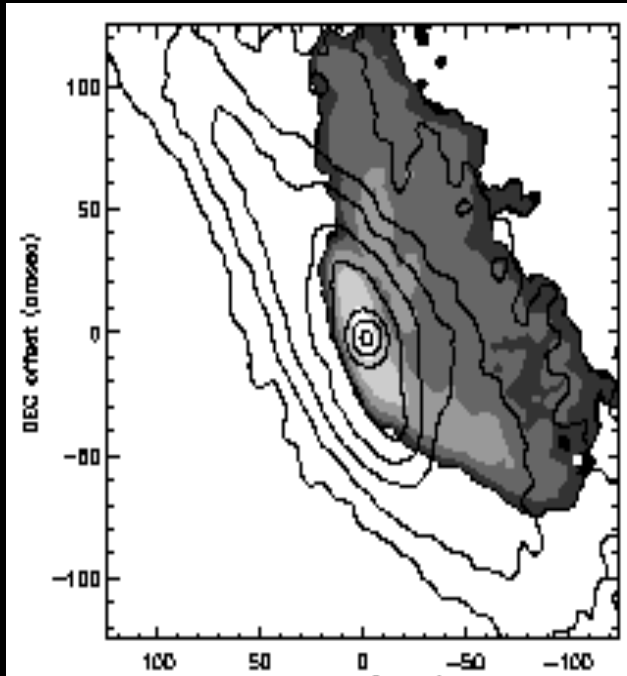
- **Ram pressure stripping** (Gunn and Gott 1972, Quilis et al. 2000)
- **Tidal effects, mergers and accretion** (Toomre and Toomre 1972, Bekki 2001, Aguerri et al. 2001)
- **Harassment** (Moore et al. 1996, Mastropietro et al. 2004)  
Transformation of a late-type spiral galaxy into a dwarf galaxy through interactions between cluster galaxies and the gravitational cluster potential.

NGC 4438

Grey: gas    Contours: stars

NGC 4522

Harassment  
Kenney et al. 1995



Ram pressure



Gas in X-rays

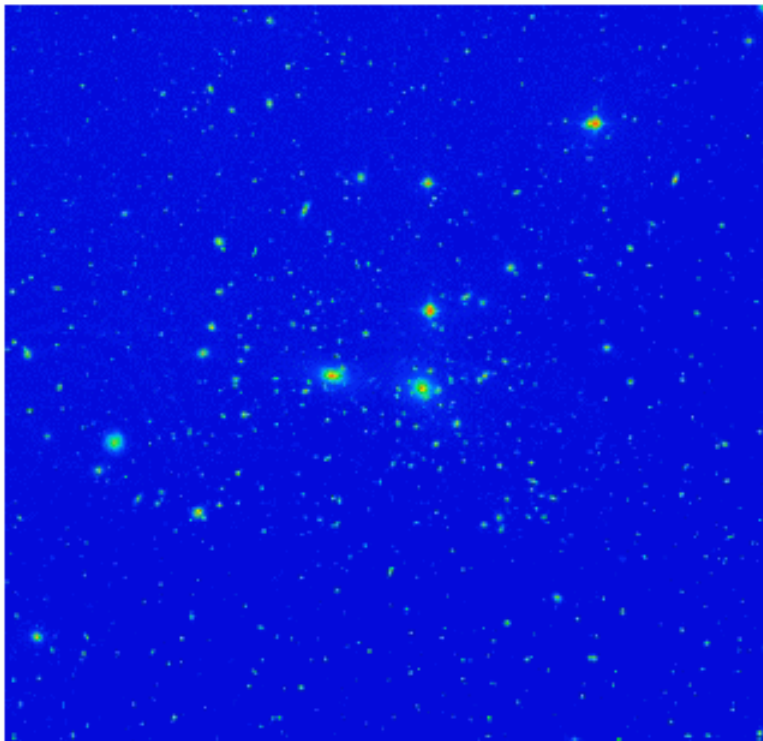
ESO 137-001 (Abell 3627, *HST*)

# Summary to remember!

- Clusters of galaxies are a very diverse class of objects.
- Many (50% or more) of clusters show significant substructure in their galaxy distributions.
- Member galaxies span an enormous range of luminosities and morphological mixtures. Elliptical galaxies prefer dense environments.
- The distribution of galaxy velocities can provide information on the dynamical state of a cluster.
- Cluster masses can be measured from the virial theorem.
- Cluster masses range from  $10^{13}$ - $10^{15} M_{\odot}$ . Galaxies account for only  $\sim 5\%$  of this mass, the ICM for  $\sim 10\%$ , and hence most of the cluster mass must be “dark”.

# The intracluster medium

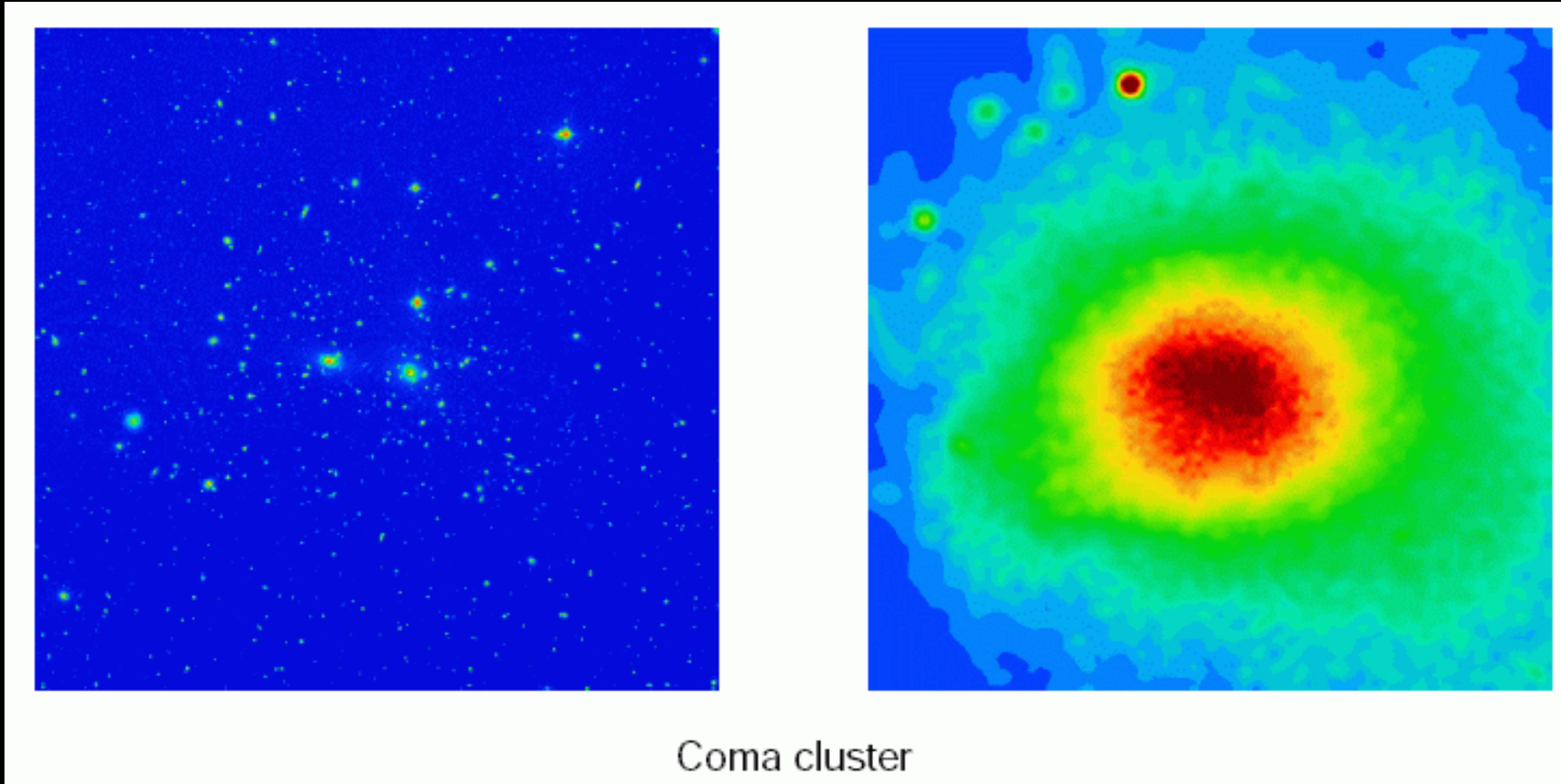
Clusters are among the most luminous X-ray sources in the sky. This X-ray emission comes from hot intracluster gas.



Coma cluster

X-ray observations provide information on the amount, distribution, temperature and chemical composition of the intra-cluster gas

Clusters are among the most luminous X-ray sources in the sky. This X-ray emission comes from hot intracluster gas.



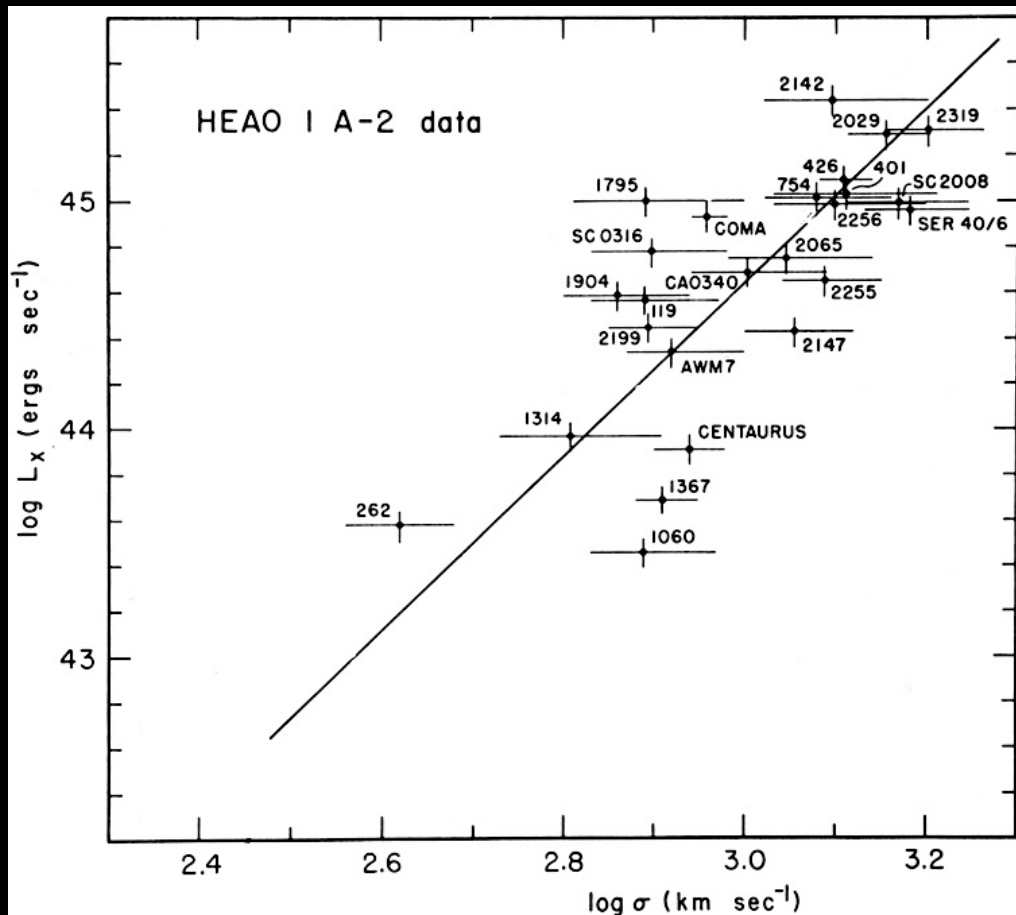
X-ray observations provide information on the amount, distribution, temperature and chemical composition of the intra-cluster gas

# For comparison ...

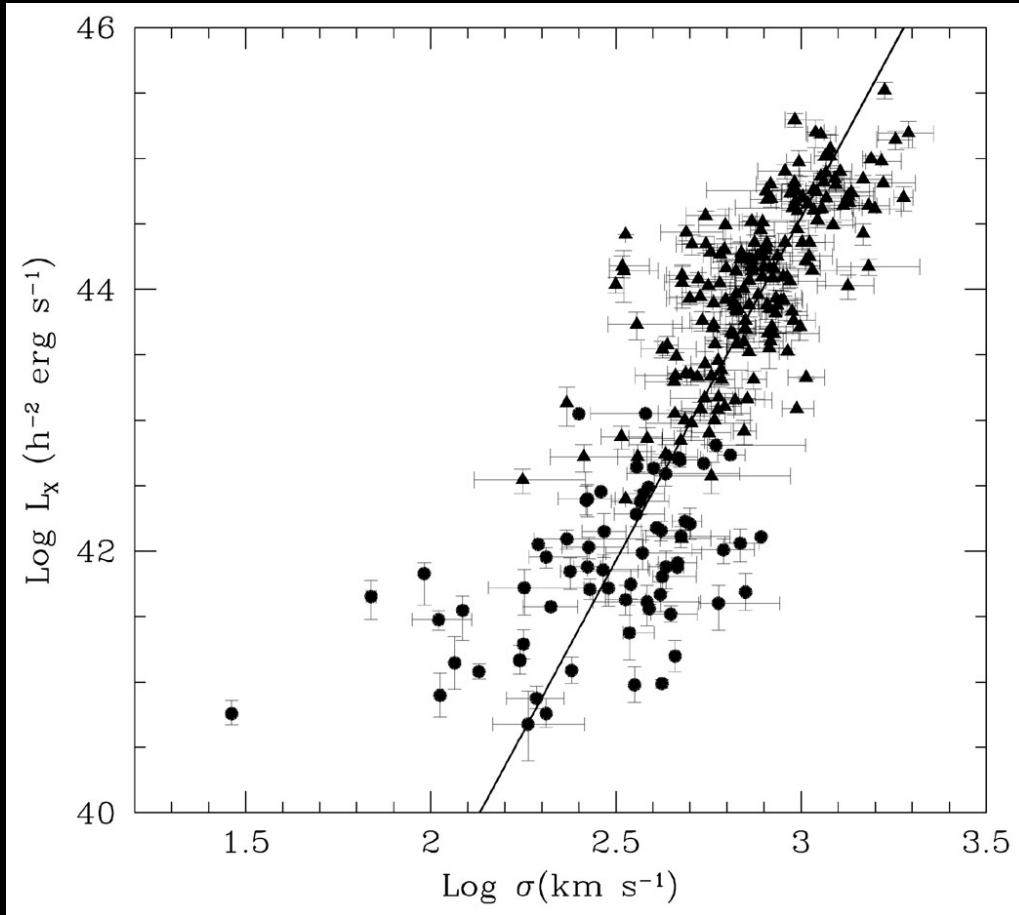
- Cataclysmic variables  $L_x = 10^{32} - 10^{38}$  erg/s
- Milky Way, M31  $L_x = 10^{39}$  erg/s
- Clusters of galaxies  $L_x = 10^{43} - 10^{45}$  erg/s
- Only Seyferts, QSOs, and other AGN rival clusters in X-ray output.
- Clusters may emit nearly as much energy at X-ray wavelengths as in the optical:

$$L_{\text{opt}} = 100 L_* \text{ galaxies} \sim 10^{45} \text{ erg/s}$$

# The $L_x - \sigma$ correlation



Quintana and Melnick (1982)



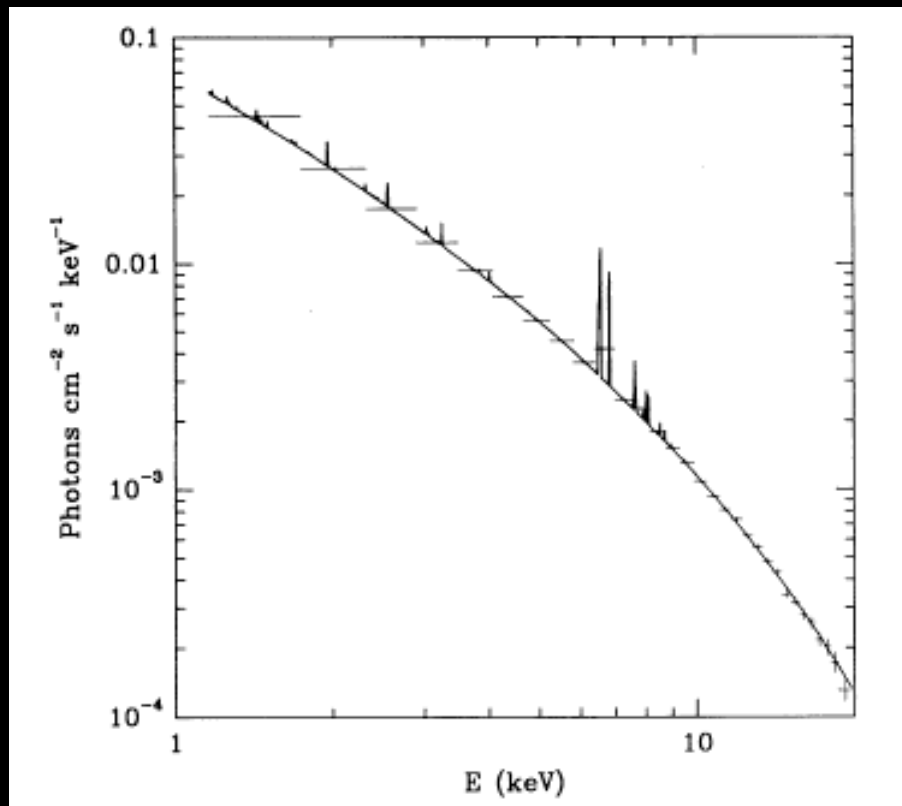
Groups (circles, Xue & Wu 2000 and Helsdon & Ponman 2000).  
Clusters (triangles, Wu et al. 1999)

# Origin of cluster X-ray emission

- Hot ( $10^7 - 10^8$  K) low-density ( $10^{-3} \text{ cm}^{-3}$ ) gas, mostly H and He, between galaxies. At these high temperatures the gas is fully ionized.
- Two emission mechanisms:
  - 1) Thermal Bremsstrahlung (dominant  $T > 3 \times 10^7$  K)  
free electrons may be rapidly accelerated by the attractive force of atomic nuclei, resulting in photon emission.  
X-ray luminosity is a function of gas density and temperature
$$L_x = \Lambda(T, \text{Abundances}) \int n_e n_p dV$$
  - 2) Recombination of electrons with ions (strong at  $T \lesssim 10^7$  K).  
Fe and Ni [ , C, N, O, Ne, Mg, Si, S, Ar, and Ca]

# X-ray spectra

- Spectroscopy of the intra-cluster gas provides information on its temperature and composition.
- Observed spectra show exponential decrease at high-frequencies that is characteristic of bremsstrahlung.



Coma Cluster  
(Hughes et al. 1993)

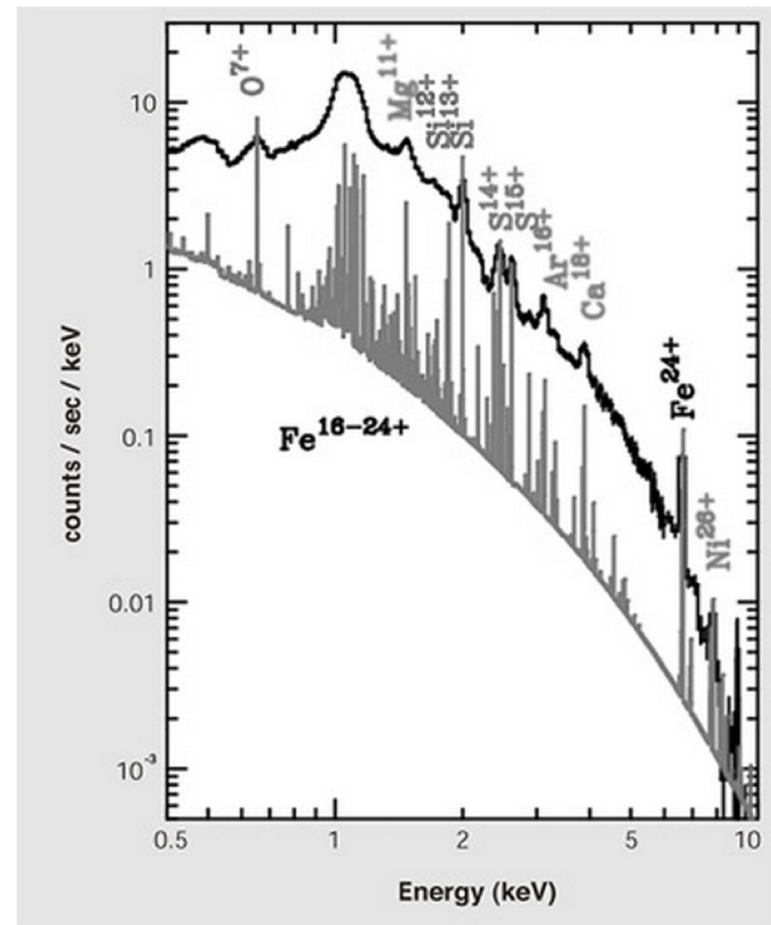


Fig. 1 X-ray spectrum of the Virgo Galaxy Cluster observed by XMM-Newton satellite

- Emission lines due to Fe, Ni and other heavy elements suggest that **much of the intra-cluster gas must have been processed through stars.**
- Chemical abundance of the intra-cluster gas can be measured from the equivalent widths of these emission lines. It is found to be about  **$0.3-0.4Z_{\odot}$**

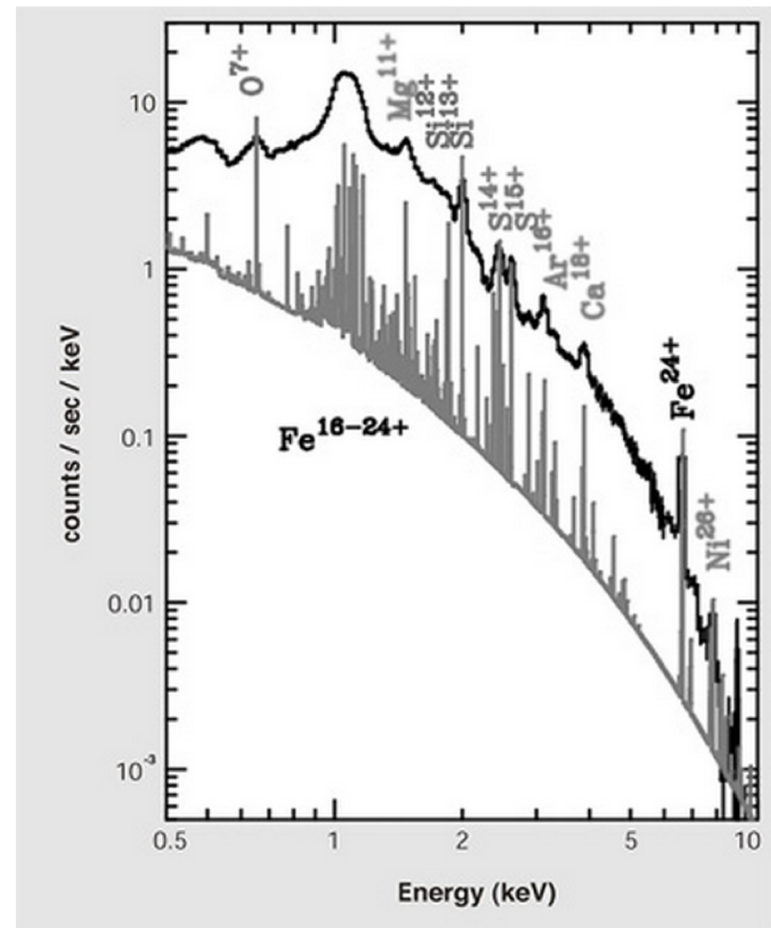


Fig. 1 X-ray spectrum of the Virgo Galaxy Cluster observed by XMM-Newton satellite

# Origin of the intracluster gas

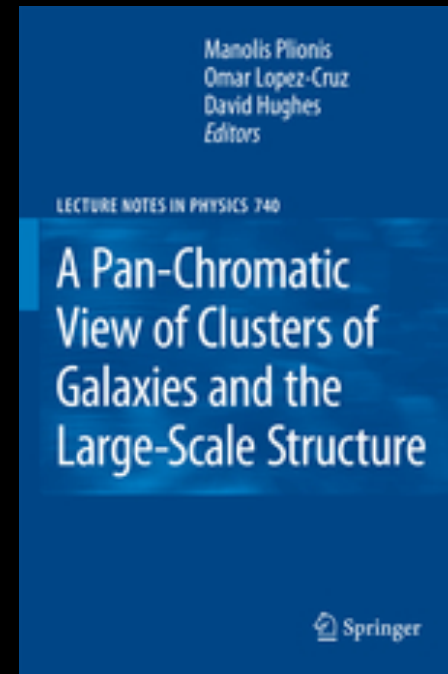
## Two possibilities:

- The intra-cluster gas once resided in galaxies and was later removed:
  - this would explain high metallicity of gas
  - galaxies in the cores of rich clusters are observed to be deficient in HI gas, which suggests that stripping has occurred.
  - but since  $M_{\text{gas}} \gg M_{\text{gal}}$  it is difficult to understand how so much material could have been stripped from galaxies
- The gas is primordial, originating at the time of cluster formation:
  - but  $0.3-0.4Z_{\odot}$ !

# Dynamics of the intracluster gas

The intra-cluster gas can be treated as:

- An ideal fluid
- In hydrostatic equilibrium
- At a uniform temperature



Sarazin C. L.  
Gas Dynamics in  
Clusters of Galaxies

## Why a fluid?

– The mean-free path for an electron to collide with an ion is

$$\lambda_e = \frac{\text{distance - travelled}}{\text{number - of - collisions}} \sim \frac{v_e t}{n \sigma v_e t} \sim \frac{1}{n \sigma}$$

where  $v_e$  = electron speed;  $n$ =number density of ions;  $t$ =time interval and  $\sigma$  = collisional cross-section.

– Strong collisions will occur when kinetic energy of the electron is comparable to potential energy at closest approach,  $b$ ,

$$\frac{1}{2} m_e v_e^2 \sim \frac{q e}{4 \pi \epsilon_0 b}$$

where

$q$ = charge of ion;  $e$ = charge of electron;  $\epsilon_0$  = permmissivity of space.

– The cross-section for strong collisions is thus

$$\sigma = \pi b^2 \sim \frac{q^2 e^2}{4\pi \epsilon_0^2 m_e^2 v_e^4} \quad \lambda_e \sim \frac{1}{n\sigma} \quad (5)$$

– A more realistic treatment, which includes the effects of both nearby and distant collisions increases  $\sigma$  by a factor  $\sim \ln\Lambda$ , where  $\ln\Lambda =$  the Coulomb logarithm (ratio of largest to smallest collision impact parameters  $b_{max}/b_{min}$ )

– Once the gas has reached thermal equilibrium

$$m_e v_e^2 \sim m_{ion} v_{ion}^2 \sim 3k_B T \quad (6)$$

$k_B =$  Boltzmann constant and  $T =$  gas temperature

– Hence

$$\lambda_e \sim \lambda_i \sim 20kpc \left( \frac{T}{10^8 K} \right)^2 \left( \frac{n}{10^{-3} cm^{-3}} \right)^{-1} \quad (7)$$

– Since  $\lambda_e \ll$  size of cluster, the intracluster gas can be treated as a collisional fluid.

## Why hydrostatic equilibrium?

- The intracluster gas will respond to changes at a rate determined by the sound speed.
- The sound speed in an ideal monatomic gas is

$$v_{sound} \sim \sqrt{\frac{5k_B T}{3\mu m_H}} \quad (11)$$

where  $\mu$  = mean molecular weight of gas and  $m_H$  = mass of proton

- The time for a sound wave to cross a cluster of diameter  $d$  is

$$t_{sound} \sim \frac{d}{v_{sound}} \sim 7 \times 10^8 \left(\frac{T}{10^8 K}\right)^{-1/2} \left(\frac{d}{1 Mpc}\right)^{-1} \text{ years} \quad (12)$$

- Because  $t_{sound} \ll t_{cool}$  the gas will be in hydrostatic equilibrium (gas pressure balances gravity). For a spherical mass distribution,

$$t_{cool} \sim 8 \times 10^{10} \text{ yr}$$

$$\frac{1}{\rho_{gas}} \frac{dP}{dr} = -\frac{d\Phi}{dr} = -\frac{GM(r)}{r^2} \quad (13)$$

Because the gas is in hydrostatic equilibrium in the cluster potential well, its distribution maps the cluster's mass distribution.

## Why a single temperature?

– Frequent collisions between electrons and ions exchange energy. This leads to a Maxwellian distribution of particle velocities. Velocities are isotropic.

– The timescale for redistribution of energy between electrons is

$$t_{eq}(e, e) \sim \frac{\lambda_e}{v_e} \sim 3 \times 10^5 \left( \frac{T}{10^8 K} \right)^{3/2} \left( \frac{n}{10^{-3} cm^{-3}} \right)^{-1} \text{ years} \quad (8)$$

– Similarly, the timescale for electrons and ions to reach thermal equilibrium is

$$t_{eq}(e, i) \sim \left( \frac{m_p}{m_e} \right) t_{eq}(e, e) \sim 6 \times 10^8 \left( \frac{T}{10^8 K} \right)^{3/2} \left( \frac{n}{10^{-3} cm^{-3}} \right)^{-1} \text{ years} \quad (9)$$

– X-ray emission by thermal bremsstrahlung cools the gas on a timescale

$$t_{cool} \sim 8 \times 10^{10} \left( \frac{T}{10^8 K} \right)^{1/2} \left( \frac{n}{10^{-3} cm^{-3}} \right)^{-1} \text{ years} \quad (10)$$

– Since  $t_{eq} \ll t_{cool}$ , the intracluster gas can be characterized by a single temperature  $T_{gas}$  for both electrons and ions.

# How much gas is there in clusters?

The observed X-ray surface brightness profiles have a radial distribution

$$\Sigma_X(r) = \Sigma_0 \left[ 1 + \left( \frac{r}{r_C} \right)^2 \right]^{-3/2} \quad (1)$$

Assuming spherical symmetry, constant temperature and X-ray emission proportional to  $\rho(\text{gas})^2$ , then this corresponds to a spatial gas density of

$$\rho_{\text{gas}}(r) = \rho_0 \left[ 1 + \left( \frac{r}{r_C} \right)^2 \right]^{-1} \quad (2)$$

$$\rho_{\text{gas}}(r) \propto r^{-2}, \text{ at large } r \quad (3)$$

This can be integrated to determine the total gas mass  $M_{\text{gas}}$  within distance  $R$  of the cluster center

$$M_{\text{gas}}(< R) = \int_0^R \rho_{\text{gas}}(r) 4\pi r^2 dr \quad (4)$$

Observations indicate that the total gas mass in clusters is usually several times greater than the total galaxy mass

# Cluster Mass estimates: X-ray gas

Assuming that the intracluster gas is in hydrostatic equilibrium in the cluster potential well, the **total** cluster mass can be found:

$$\frac{1}{\rho_{gas}} \frac{dP}{dr} = \frac{d\phi}{dr} = -\frac{GM_{cl}(r)}{r^2} \quad (5)$$

Substituting the ideal gas law,  $P = \rho k_b T / \mu m_H$  and solving for  $M(R)$

$$M_{cl}(< R) = -\frac{k_b T_{gas}}{\mu m_H G} \left( \frac{\delta \ln \rho_{gas}}{\delta \ln r} + \frac{\delta \ln T_{gas}}{\delta \ln r} \right) \quad (6)$$

Note that  $M_{cl}$  depends sensitively on  $T_{gas}$  but weakly on  $\rho_{gas}$ . In principle, radial gradients in  $\rho_{gas}$  and  $T_{gas}$  are observable. In reality, temperature gradients are very difficult to detect.

A simplifying assumption is that the gas is **isothermal**, then

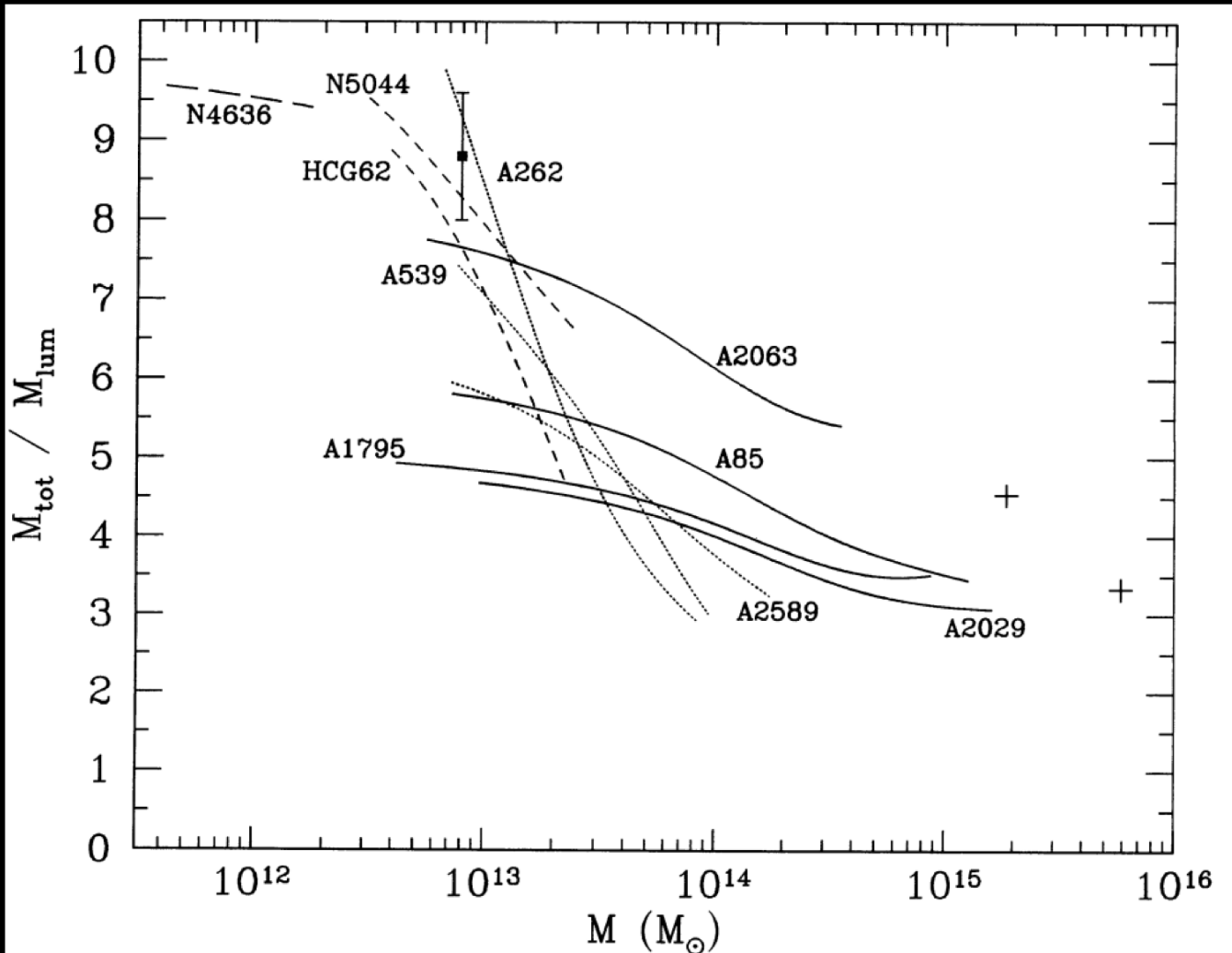
$$\frac{\delta \ln T_{gas}}{\delta \ln r} = 0 \quad (7)$$

$$M(< R) = -\frac{k_b T_{gas}}{\mu m_H G} \left( \frac{\delta \ln \rho_{gas}}{\delta \ln r} \right) \quad (8)$$

The total gas mass in clusters exceeds the total galaxy mass.

Gas contributes as much as 10-20% of the total cluster mass.

	Total mass < 0.5Mpc	gas mass < 0.5Mpc
Abell 85	$2 \cdot 10^{14} M_{\odot}$	$3.4 \cdot 10^{13} M_{\odot}$
Abell 1795	$2.3 \cdot 10^{14} M_{\odot}$	$3.6 \cdot 10^{13} M_{\odot}$
Abell 2255	$3.3 \cdot 10^{14} M_{\odot}$	$3.5 \cdot 10^{13} M_{\odot}$
Abell 2256	$6.3 \cdot 10^{14} M_{\odot}$	$4.1 \cdot 10^{13} M_{\odot}$



Concentration:  
Galaxies > DM > hot gas

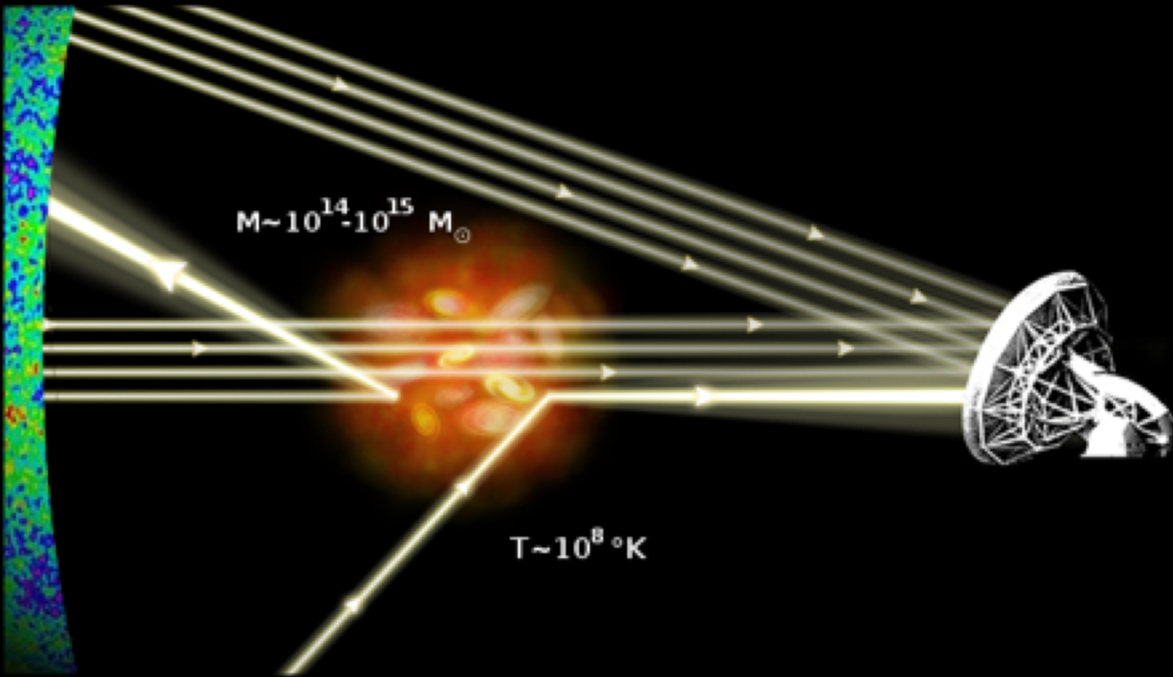
$$\rho_{DM} \propto r^{-2}$$

$$\rho_{gas} \propto r^{-1} \text{ in groups}$$

$$\rho_{gas} \propto r^{-2} \text{ in richest clusters}$$

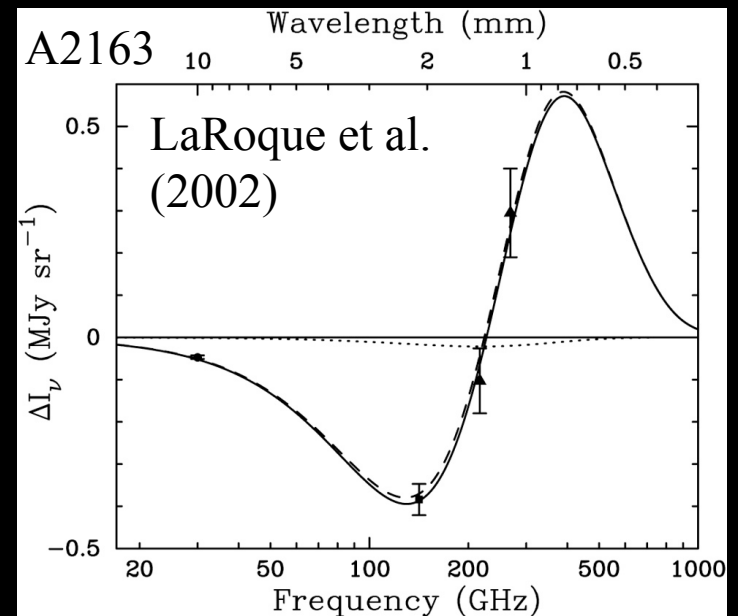
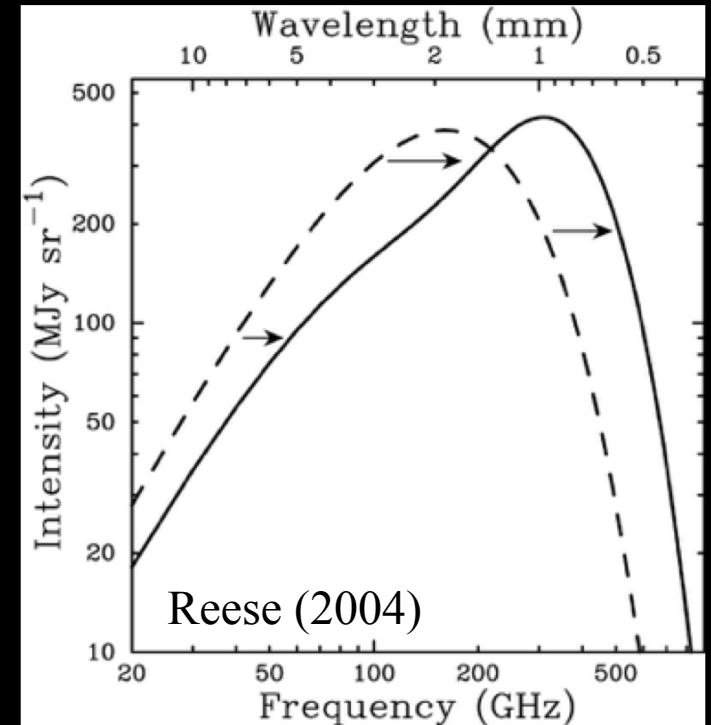
(David, Jones & Forman 1995)

# Sunyaev Zeldovich Effect (SZE, 1970's)



~1% of the CMB photons suffer inverse Compton scattering

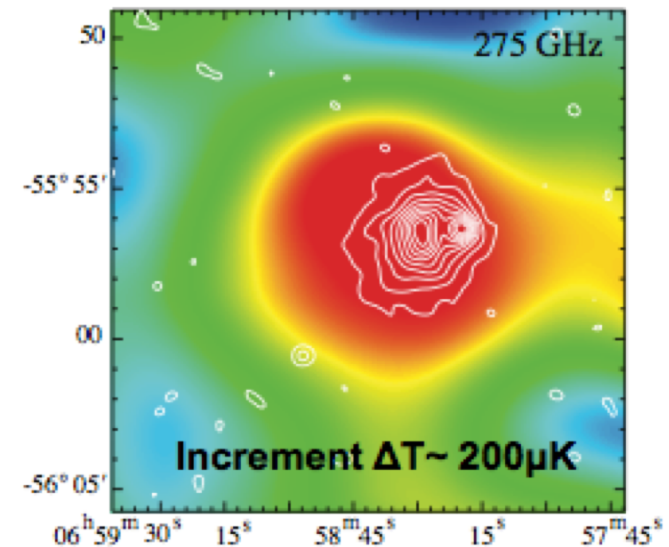
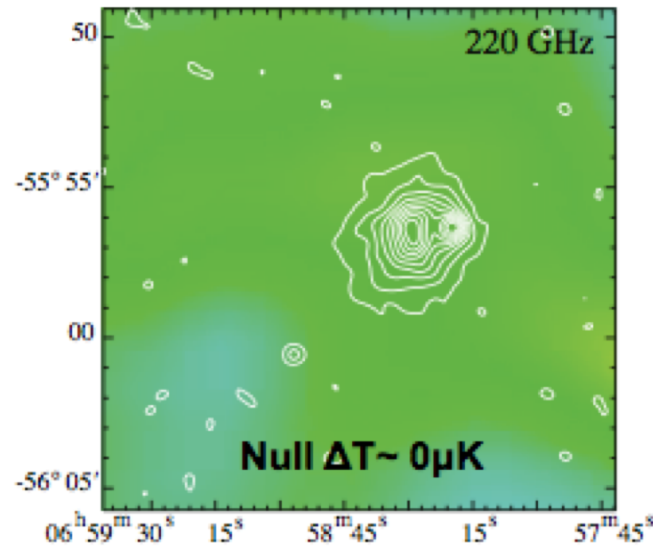
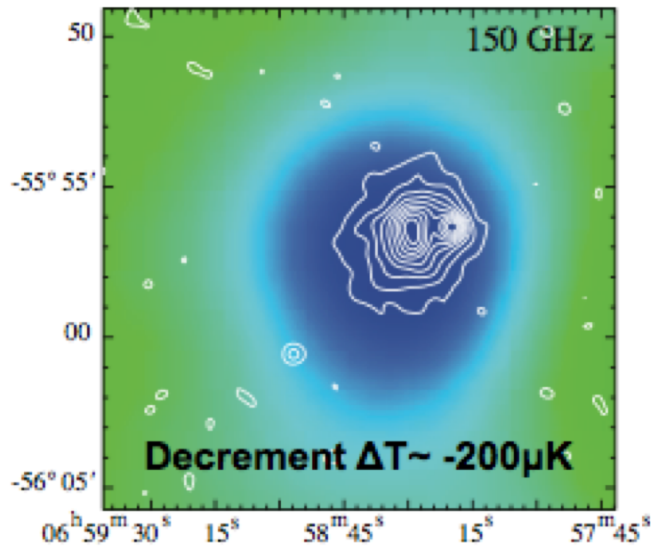
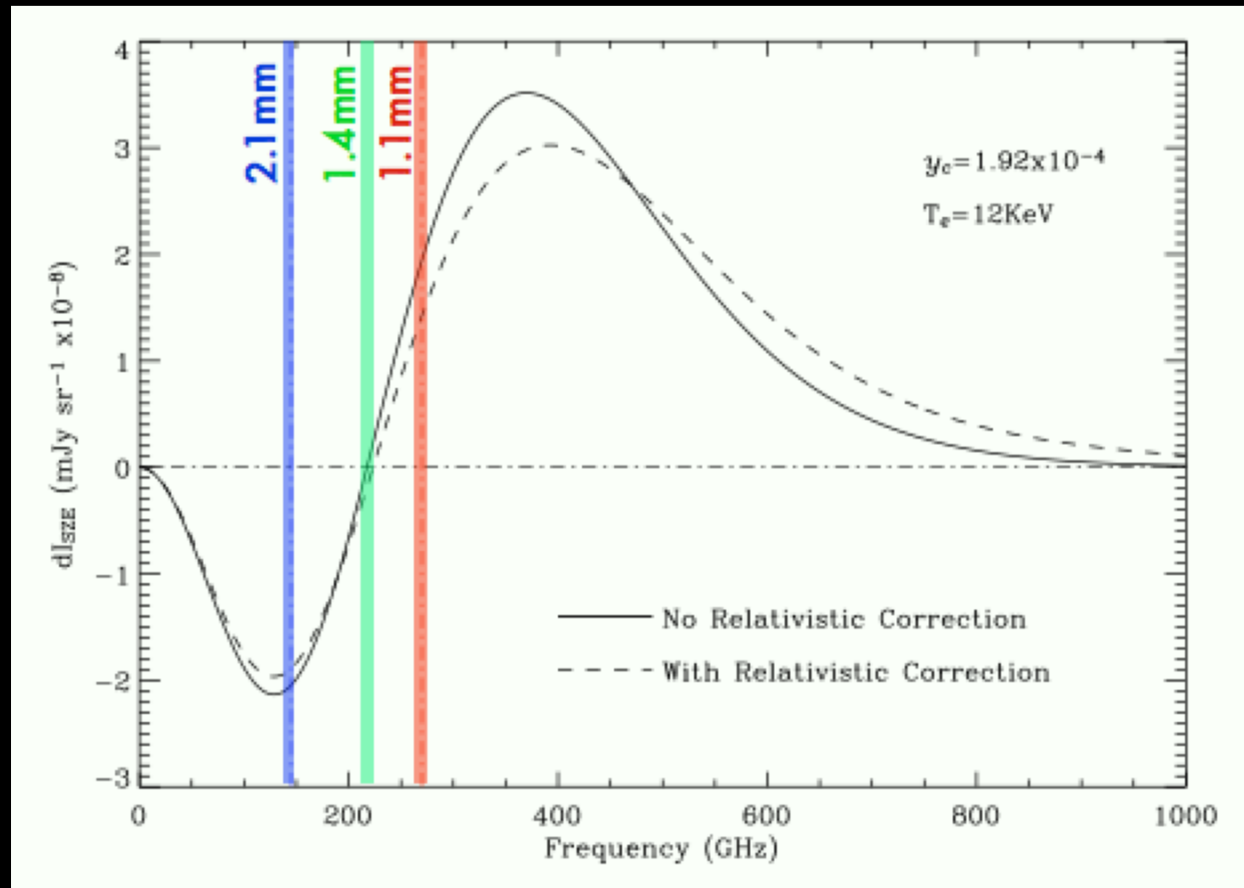
Thermal SZ (tSZ)  
Kinematic SZ (kSZ)



# Thermal SZ

- Unique spectral signature to identify clusters of galaxies.
- Dependent on the total mass of the cluster.
- Redshift independent.
- Mass-limited catalogues.

ACBAR 5' observations of the Bullet cluster at  $z \approx 0.297$  (Gomez et al. 2005)



# Combining the SZE and X-ray obs. to estimate $H_0$

X-ray cooling function

Electron density

Electron temperature

Integrals along the line of sight

X-ray surface brightness

$$S_X \propto \int n_e^2 \Lambda_{T_e} dl = \int n_e^2 \Lambda_{T_e} D_A d\theta$$

SZE

$$\Delta T_{SZE} \propto \int n_e T_e dl = \int n_e T_e D_A d\theta$$

The angular diameter distance can be estimated through a joint analysis of the SZE and X-ray data once a geometrical model for the ICM is adopted to relate  $\theta$  to the angular size of the cluster measured on the plane of the sky.

## Angular diameter distance for a flat cosmology

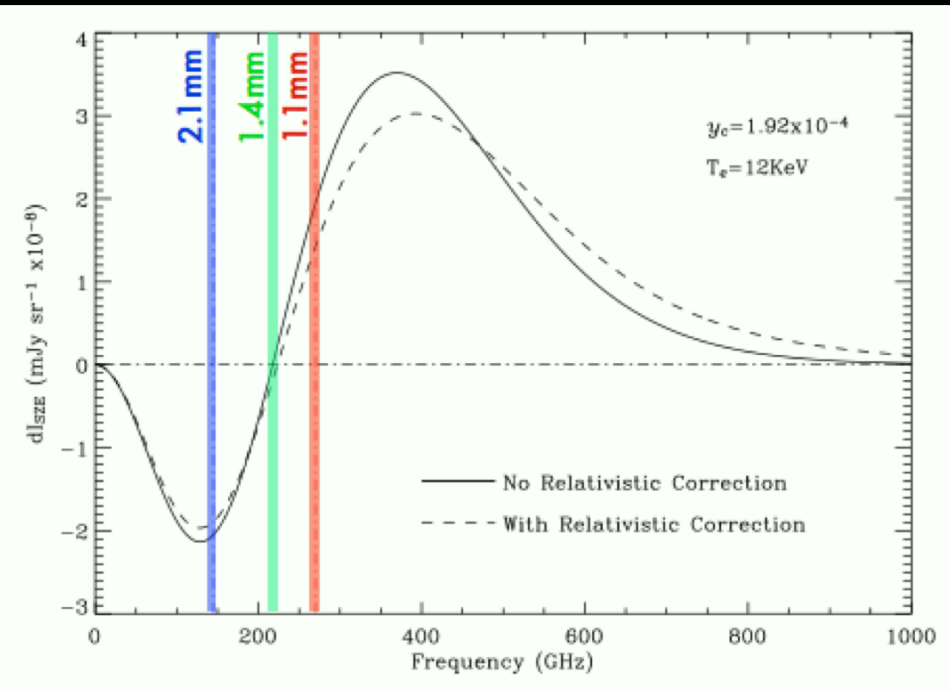
$$D_A(z_s) = \frac{c}{H_0(1+z_s)} \int_0^{z_s} \frac{dz}{E(z)}$$

$$E^2(z) = \Omega_m(1+z)^3 + \Omega_\Lambda$$

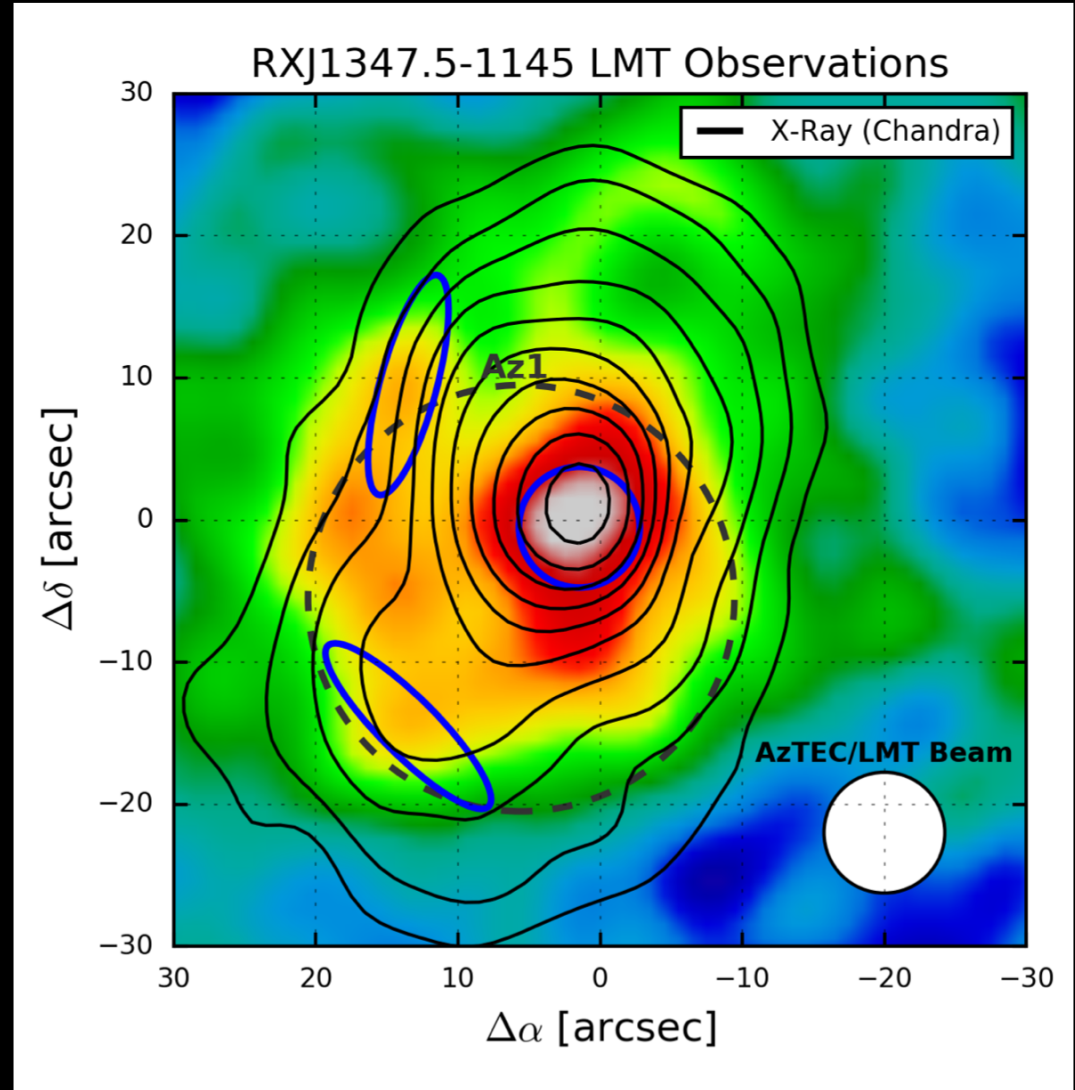
e.g. Bonamente et al. (2006) have combined X-ray Chandra data and OVRO-BIMA SZE observations of 38 massive galaxy clusters with redshifts  $0.14 < z < 0.89$  to estimate  $H_0$ . Under the assumption of a flat Universe with  $\Omega_m = 0.3$  and  $\Omega_\Lambda = 0.7$  they find  $H_0 \sim 77 \text{ km s}^{-1} \text{ Mpc}^{-1}$  using different models.

# SZE with the LMT

- sub-structures and dynamics of the ICM.
- mergers rate as a function of  $z$ .



TolTEC

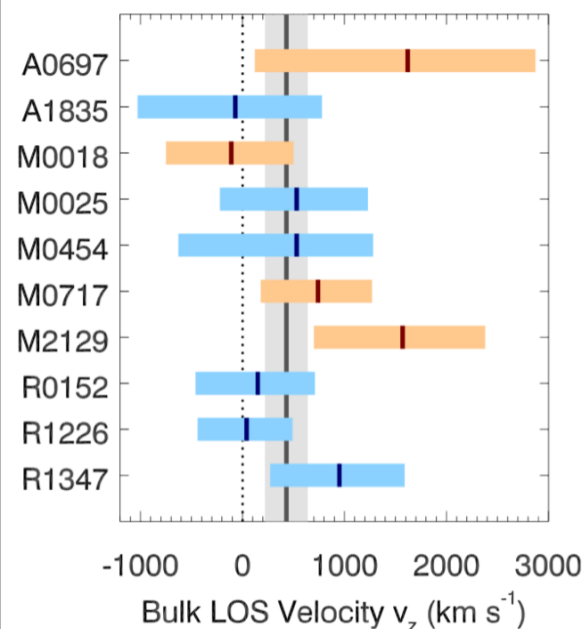
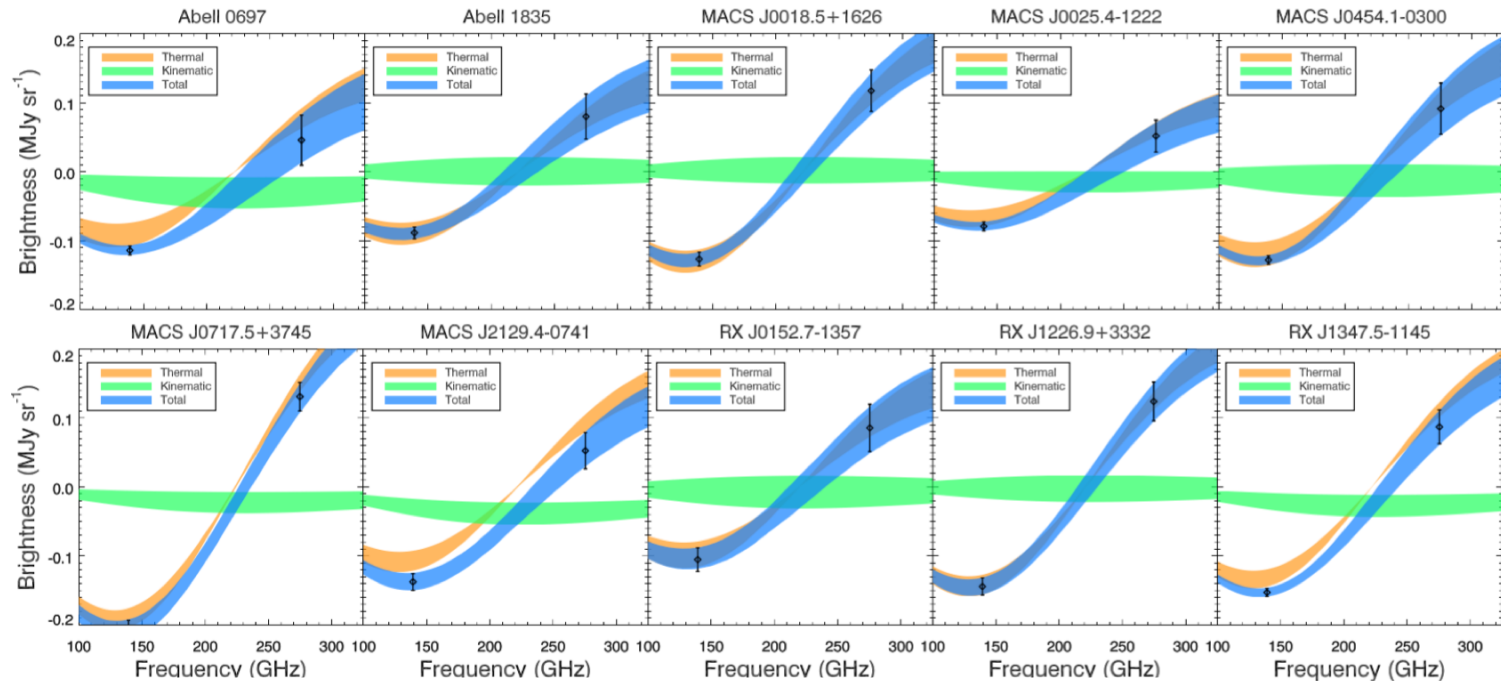


Montaña & Sánchez-Argüelles  
AzTEC 1.1mm

# Kinematic SZE

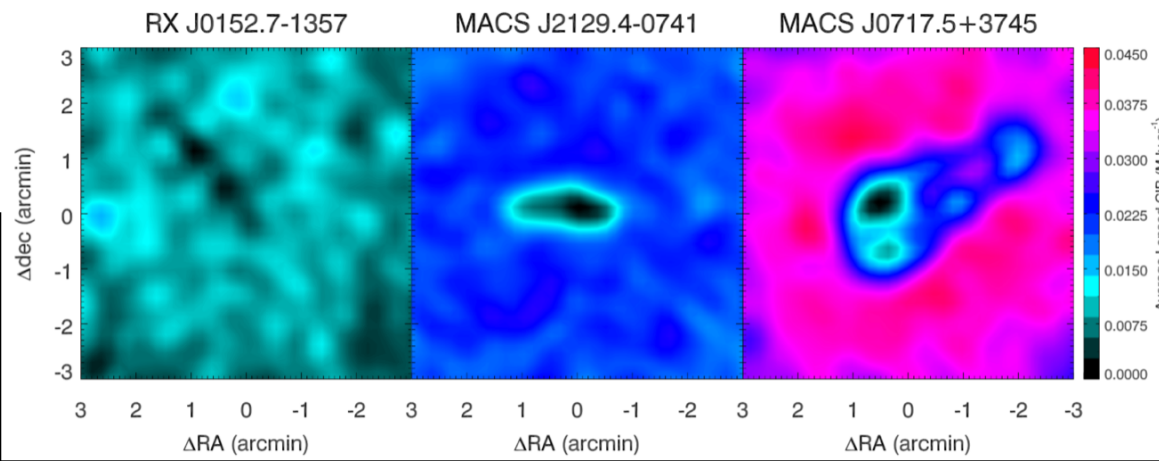
Bolocam

@140/270GHz +  
AzTEC @270GHz  
(+ *Planck*, *Herschel*-  
*SPIRE*, *Chandra*, *HST*)



Name	Temperature (keV)	Optical Depth ( $10^{-3}$ )	LOS Bulk Velocity ( $\text{km s}^{-1}$ )
Abell 0697	$8.99^{+0.53}_{-0.42}$	$4.88^{+0.86}_{-0.99}$	$+1620^{+1250}_{-1500}$
Abell 1835	$7.66^{+0.13}_{-0.13}$	$5.69^{+1.04}_{-1.05}$	$-70^{+850}_{-960}$
MACS J0018.5+1626	$8.30^{+0.49}_{-0.40}$	$7.64^{+0.99}_{-1.01}$	$-110^{+610}_{-640}$
MACS J0025.4-1222	$5.67^{+0.25}_{-0.24}$	$5.83^{+1.05}_{-1.04}$	$+530^{+700}_{-750}$
MACS J0454.1-0300	$8.83^{+0.56}_{-0.50}$	$6.64^{+1.10}_{-1.10}$	$+370^{+910}_{-1000}$
MACS J0717.5+3745	$12.83^{+1.42}_{-1.42}$	$7.55^{+0.92}_{-1.00}$	$+740^{+530}_{-560}$
MACS J2129.4-0741	$8.52^{+1.44}_{-1.14}$	$6.13^{+1.16}_{-1.23}$	$+1570^{+810}_{-870}$
RX J0152.7-1357	$4.72^{+0.56}_{-0.59}$	$9.96^{+2.12}_{-2.24}$	$+150^{+560}_{-610}$
RX J1226.9+3332	$6.84^{+0.75}_{-0.59}$	$10.13^{+1.47}_{-1.36}$	$+40^{+450}_{-480}$
RX J1347.5-1145	$9.47^{+0.37}_{-0.29}$	$6.94^{+0.70}_{-0.71}$	$+950^{+640}_{-680}$

LOS-merger  
relaxed  
LOS-merger  
POS-merger  
POS-merger  
LOS-merger  
LOS-merger  
POS-merger  
POS-merger  
POS-merger



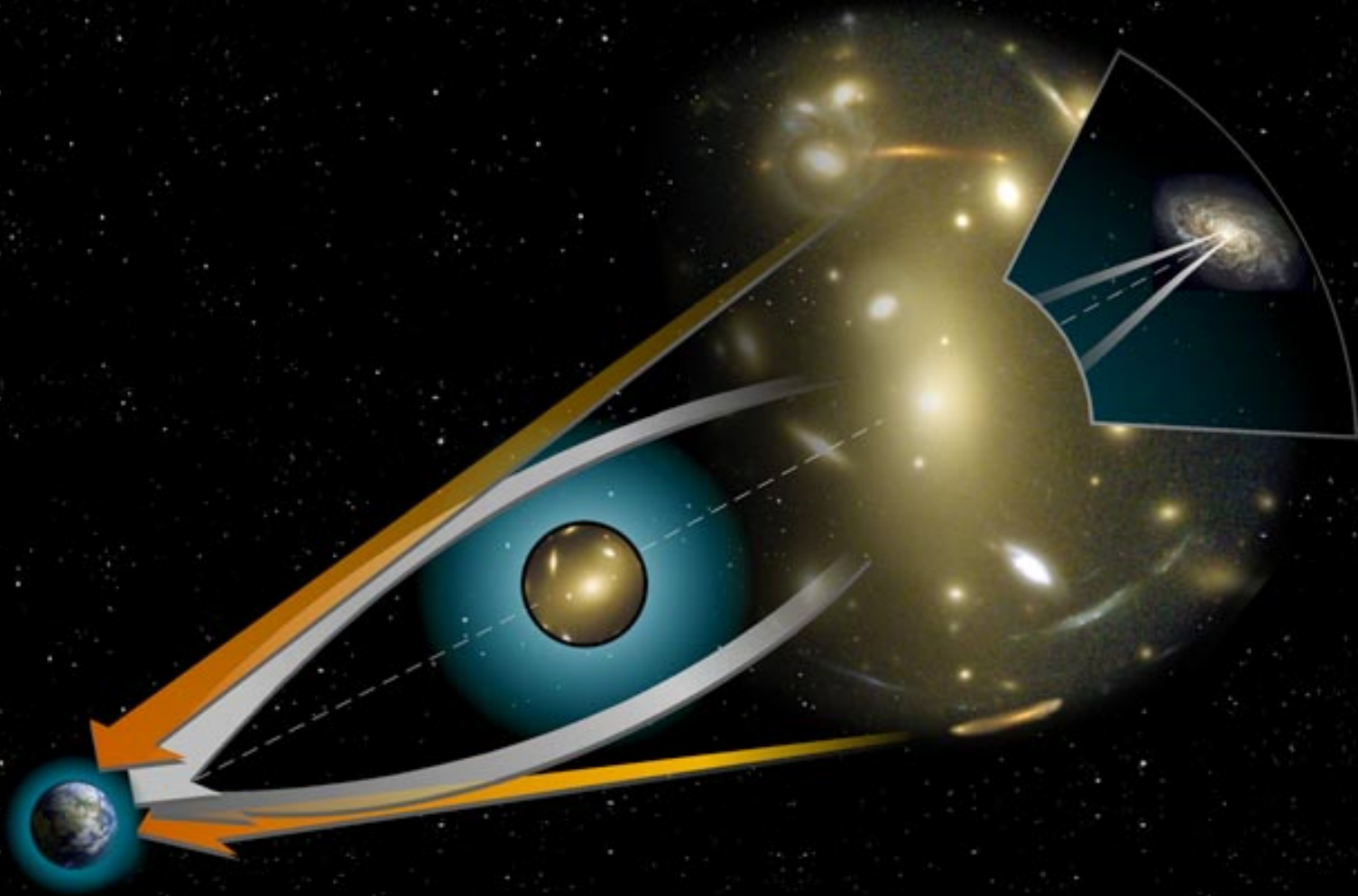
Lensed CIB  
corrections

Sayers et al. (2019)

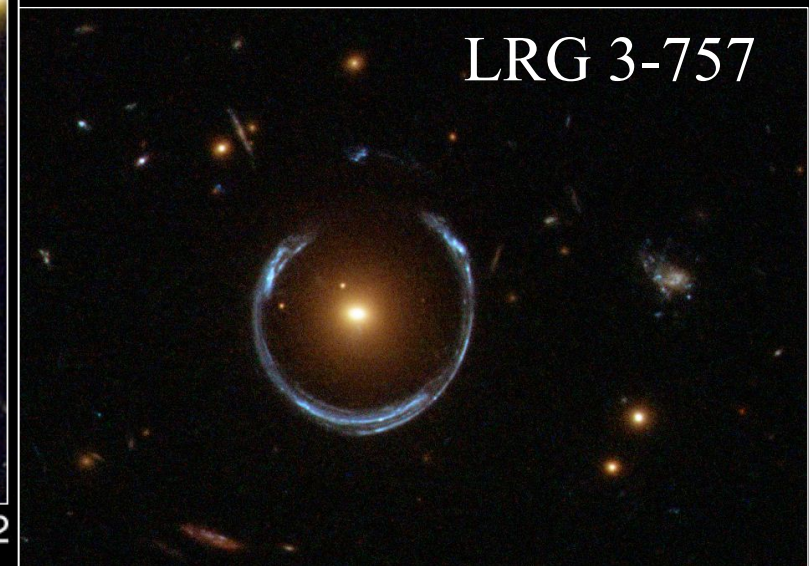
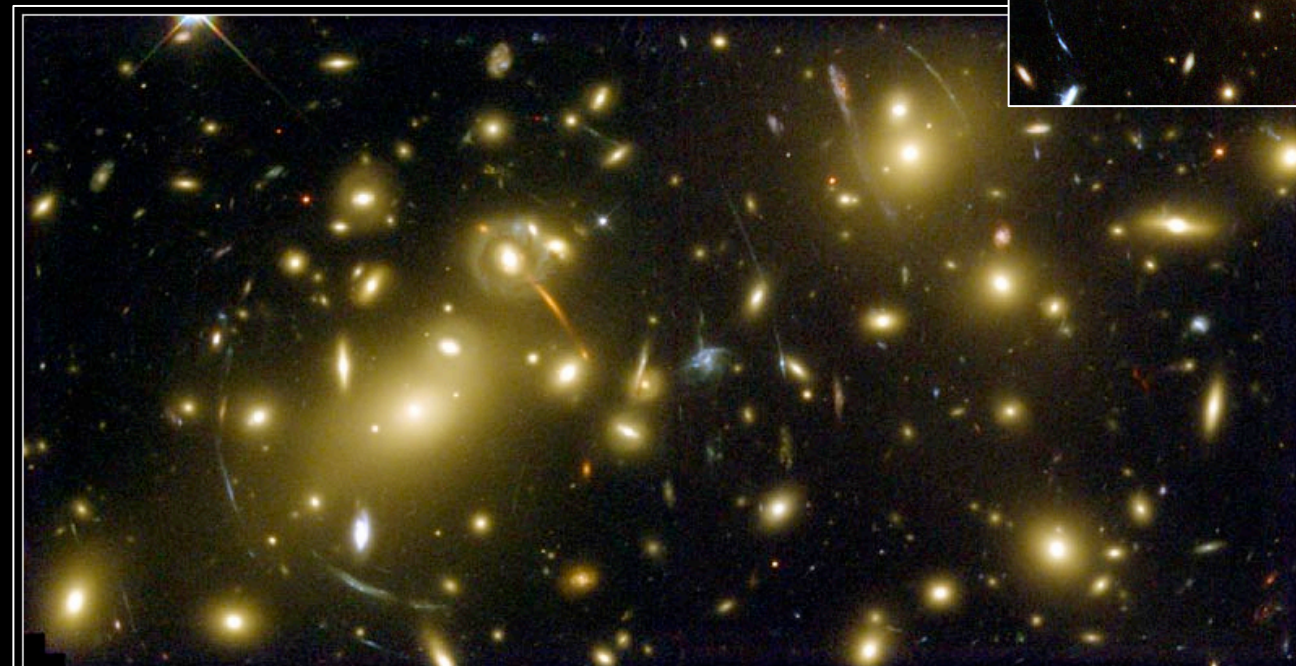
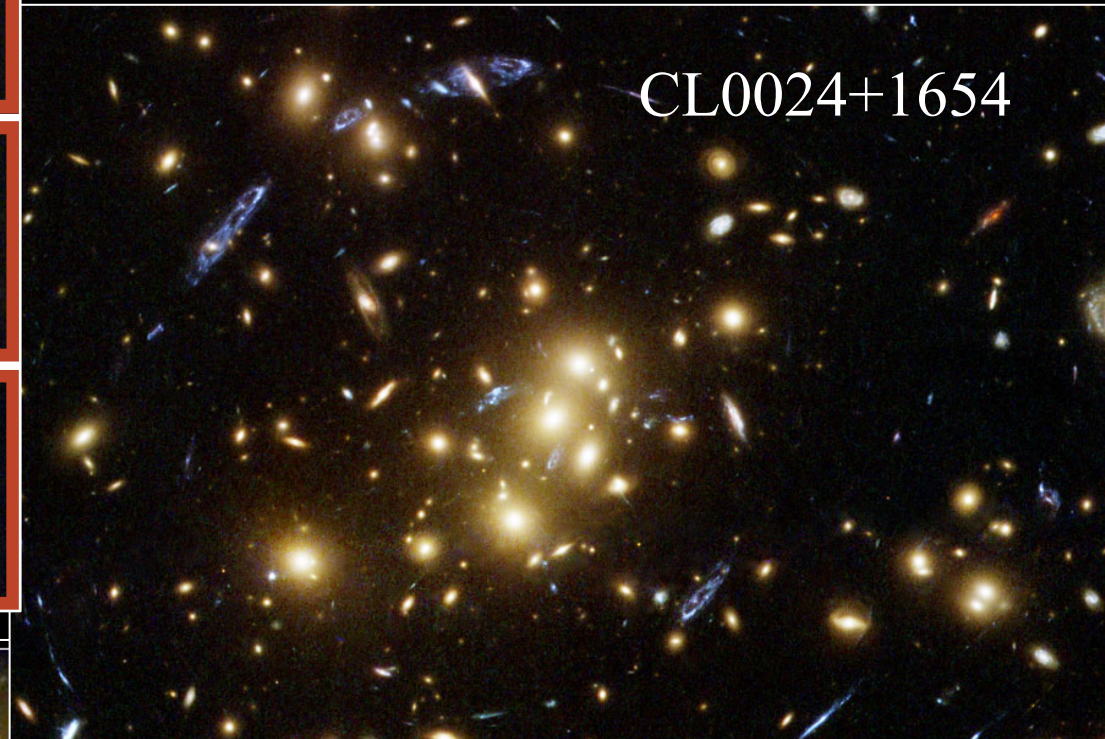
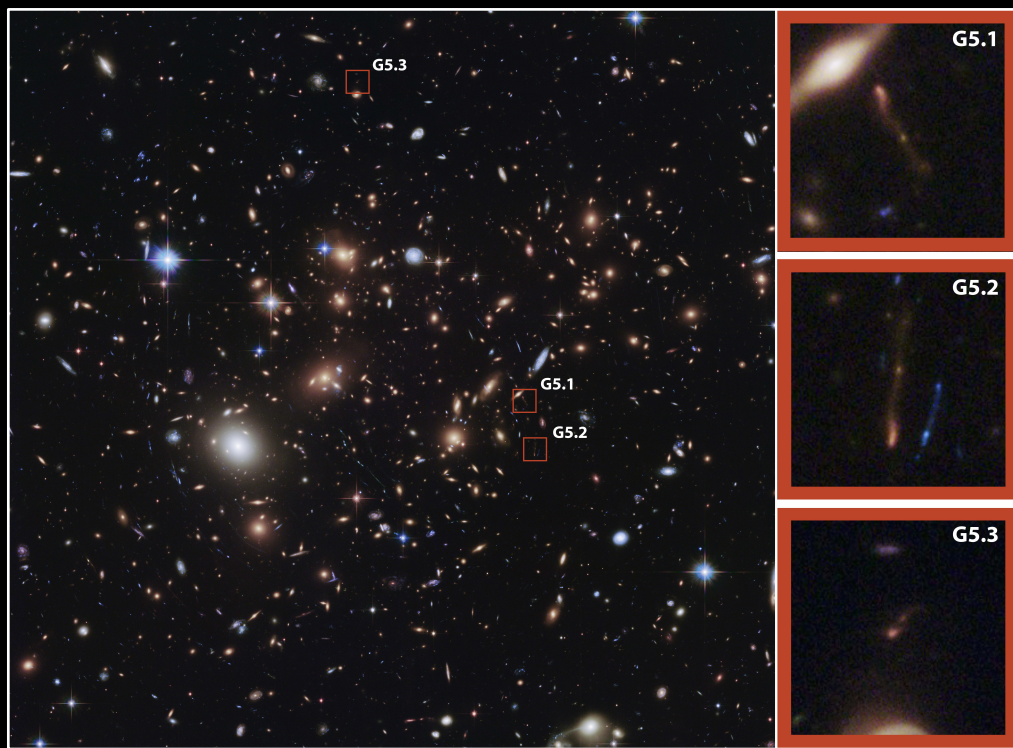
# Summary to remember!

- There is hot ( $10^7 - 10^8$  K) low-density ( $10^{-3} \text{ cm}^{-3}$ ) intra-cluster gas with  $Z \approx 0.3-0.4Z_{\odot}$ .
- The gas mass can be estimated through hydrostatic eq.
- The ICM accounts only for 10-20% of the total cluster mass, and it contains more mass than that locked in galaxies.
- There is a  $L_x - \sigma$  relation: richer clusters are brighter
- X-rays are an efficient way to find clusters, but it suffers from cosmological dimming.
- The SZE is independent of redshift, and can also be used to find clusters and produce mass-limited catalogues

# Gravitational lensing



# Gravitational lensing



**Galaxy Cluster Abell 2218**

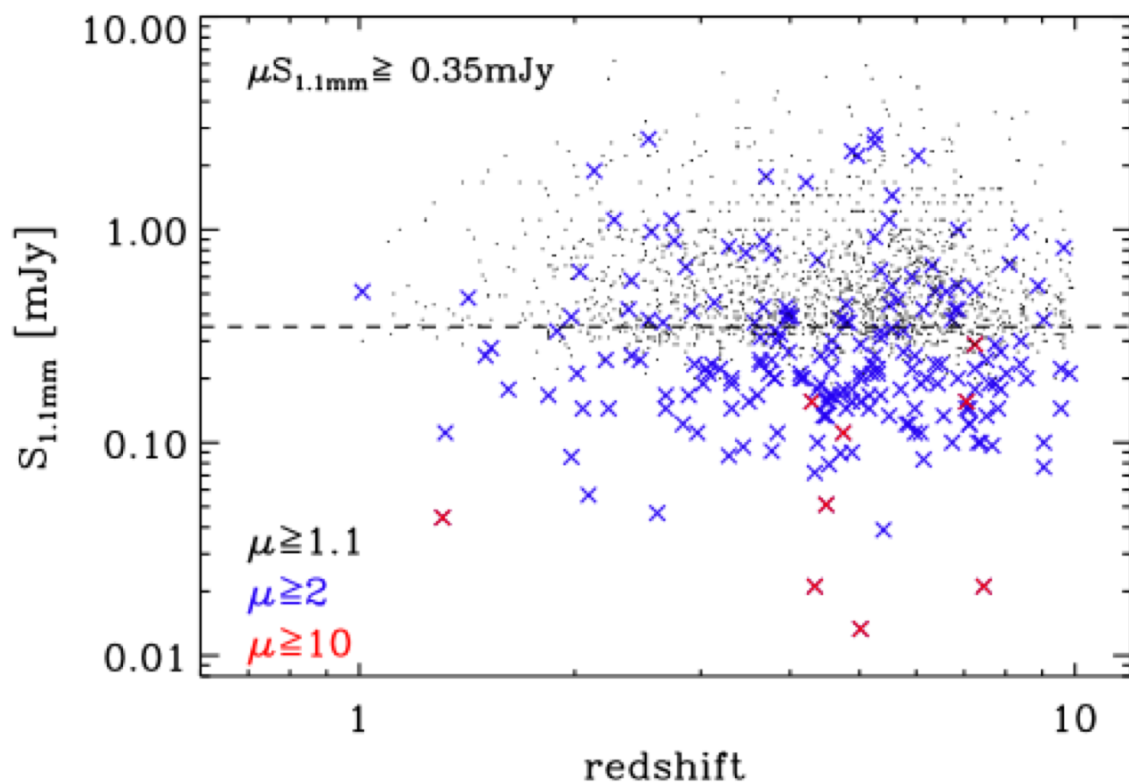
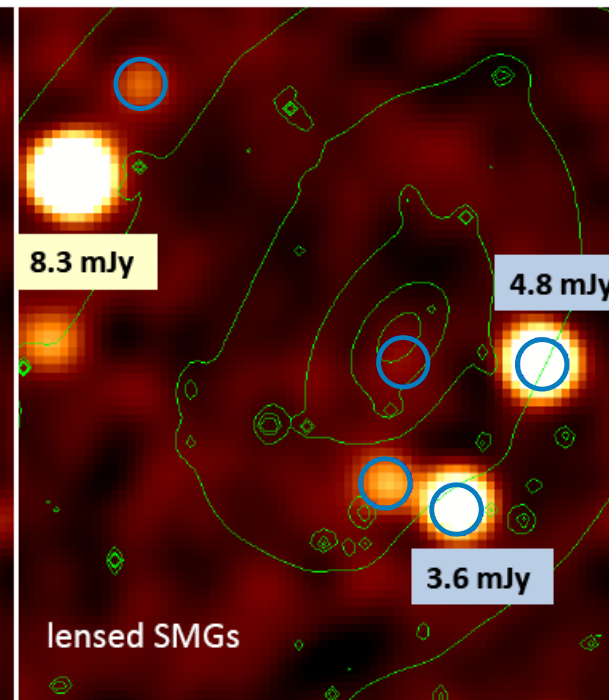
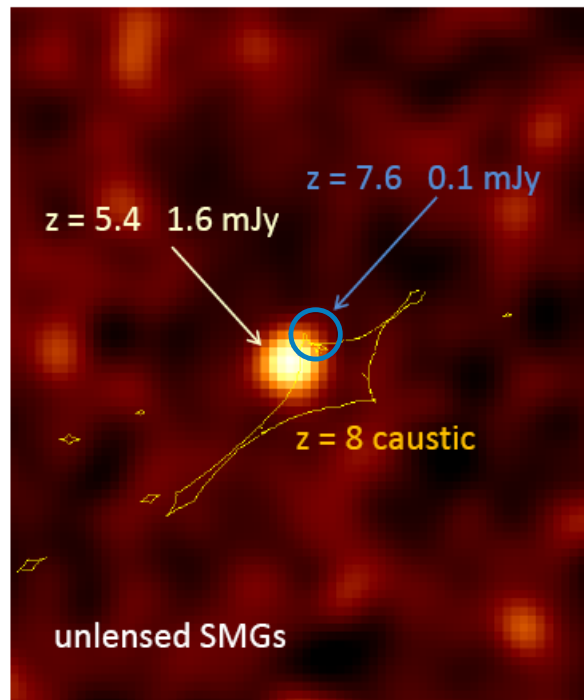
HST • WFPC2

NASA, A. Fruchter and the ERO Team (STScI) • STScI-PRC00-08

# Gravitational lensing

... with the LMT

80 arcsecs



Simulations using LensTool  
Jullo et al. 2007

# Gravitational lensing

... with the LMT

*HST* Frontier Fields

Cluster Name	z
Year 1:	
Abell 2744	0.308
MACSJ0416.1-2403	0.396
Year 2:	
MACSJ0717.5+3745	0.545
MACSJ1149.5+2223	0.543
Year 3:	
Abell S1063 (RXCJ2248.7-4431)	0.348
Abell 370	0.375

Deep optical and NIR

Deep *Spitzer* (3.6 & 4.5 $\mu$ m)

Radio JVLA (3 & / GHz)

*HST* UV ...

Precise lensing models  
from different groups.

Deep 1.1mm AzTEC/LMT (PIs Pope & Montaña)  
directly detect dust-obscured activity in typical galaxies  
constraints on the dust emission at high redshift ( $z > 4$ )  
number-counts below 1mJy, dust-obscured star-formation  
in clusters, high-resolution SZE, etc.  
(Pope et al. 2017)

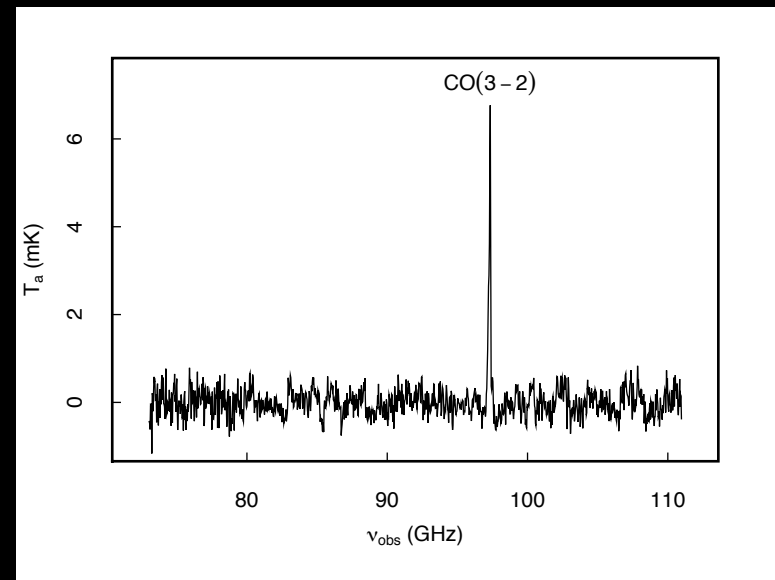
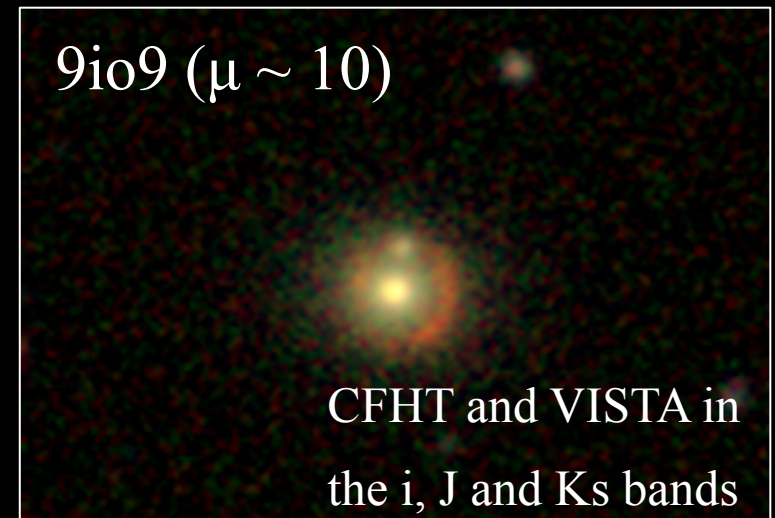


Figure 3. The Redshift Search Receiver spectrum of 9io9 showing the full 38 GHz instantaneous bandwidth spectral coverage in the 3 mm atmospheric window (73–111 GHz). The detected molecular line at 97.312 GHz is  $^{12}\text{CO}(3-2)$  from the lensed background source at a redshift  $z = 2.553$ .

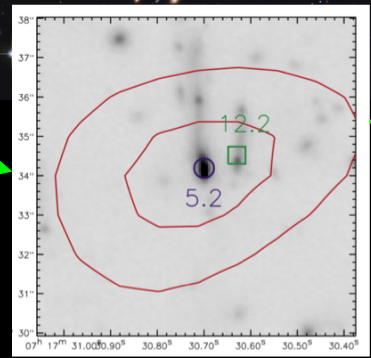
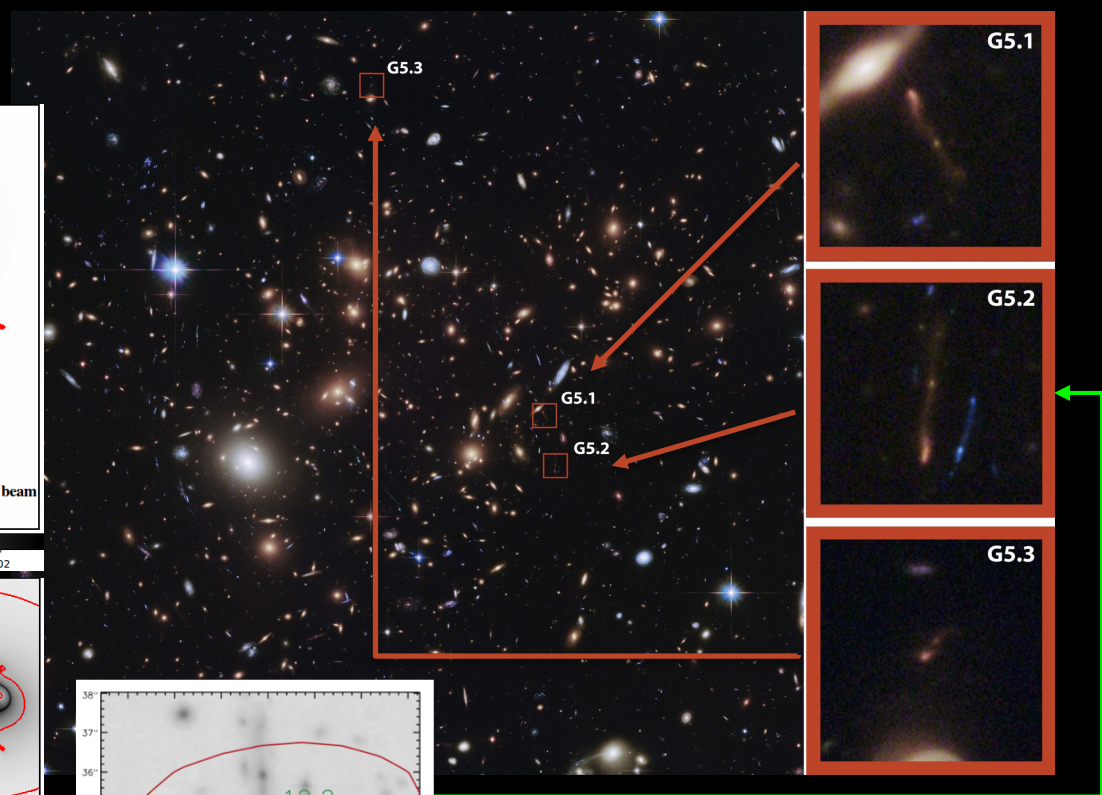
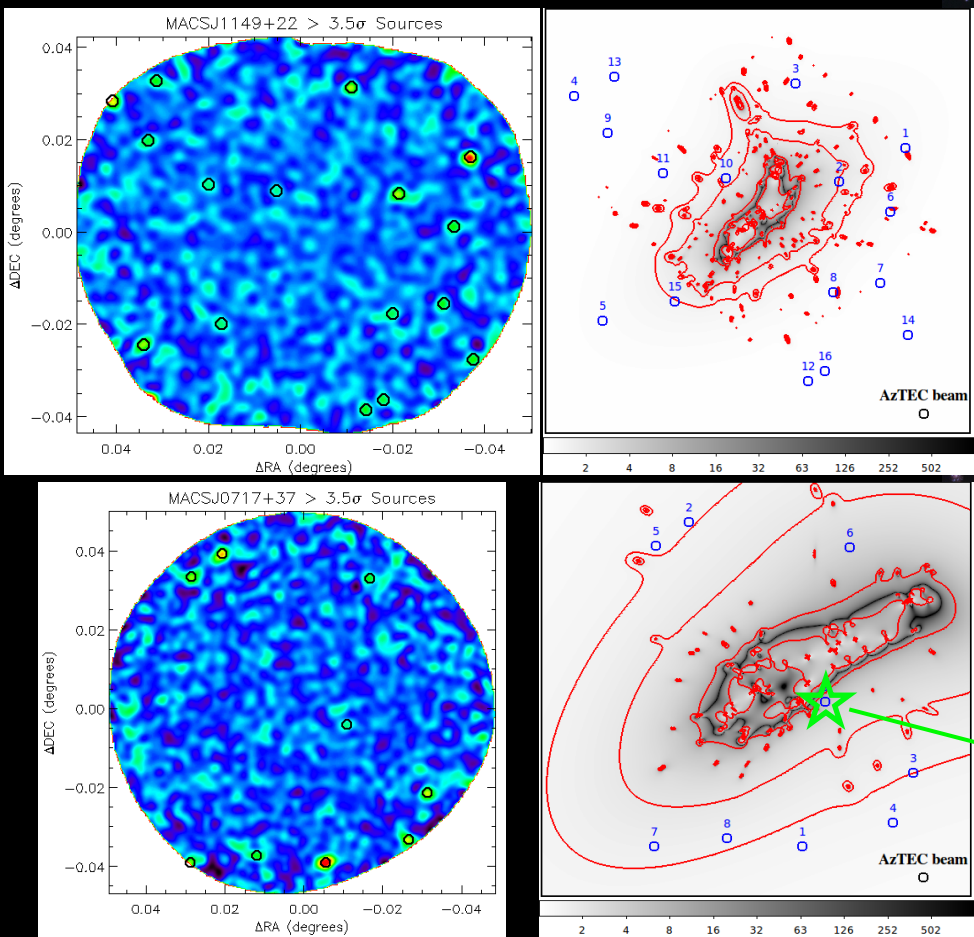
Geach et al. (2015)

Harrington et al. (2016)

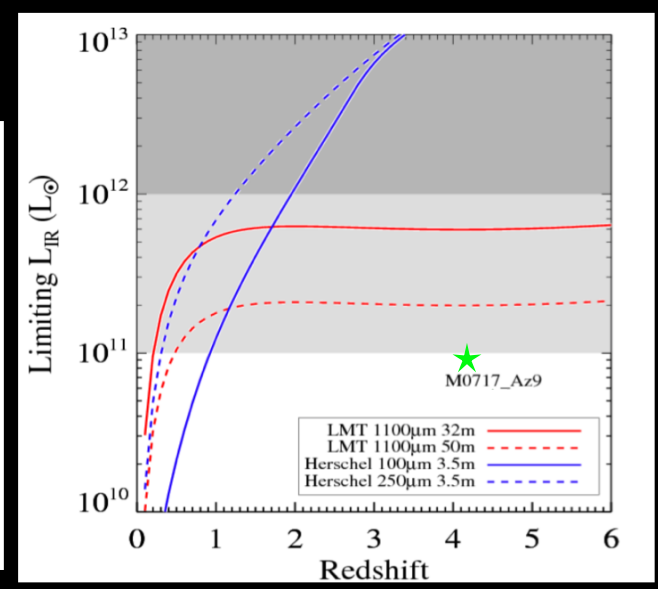
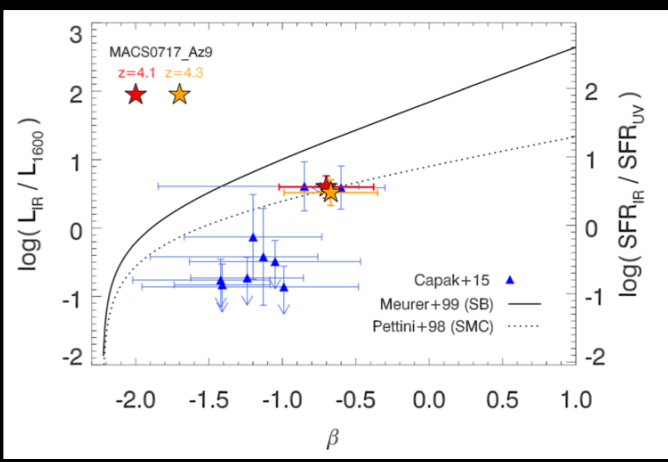
Zavala et al. (2015)

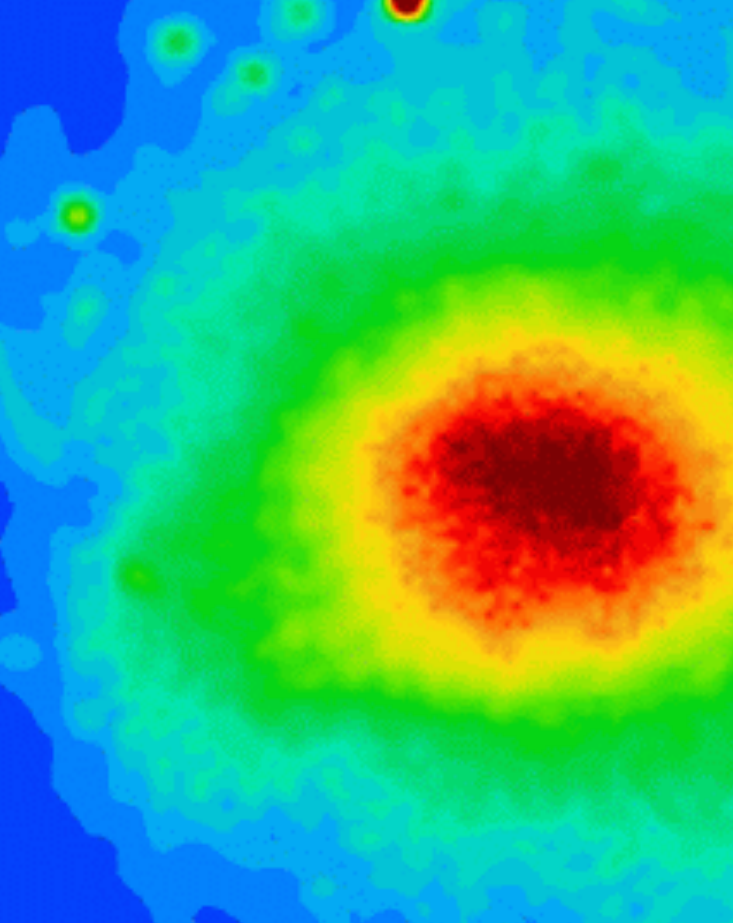
Zavala et al. (2018)

# HST-FF with the LMT



**MACS0717\_Az9 ( $z > 4$  &  $\mu \sim 7.5$ )**  
 $L_{IR} = 9.7 \times 10^{10} L_{\odot}$   
 $SFR_{IR} = 14.6 \pm 4.5 M_{\odot}/yr$   
 $SFR_{UV} = 4.1 \pm 0.3 M_{\odot}/yr$   
 $f_{obs} \sim 75 - 80\%$   
**ALMA [CII]:  $z = 4.27!!!$**   
**Pope et al. (2017)**





Manolis Pliionis  
Omar Lopez-Cruz  
David Hughes  
Editors

LECTURE NOTES IN PHYSICS 740

# A Pan-Chromatic View of Clusters of Galaxies and the Large-Scale Structure

 Springer

